PART I. SYNTHESIS OF NOVEL DOUBLE-ESTER POLYMERIC DRUGS

PART II. AUTOMATED METHODS IN PREFORMULATION DEVELOPMENT

by

EMILY CHILDREY WARE

(Under the Direction of D. Robert Lu)

ABSTRACT

The purpose of part I was to synthesize novel polymeric drug conjugates by combining several orthoesters with N-[2-(hydroxypropyl)-methacrylamide] (HPMA), an analogue for methacrylamide (MA) bound anti-cancer drugs and MA bound targeting moieties, for targetable anti-cancer therapy. HPMA was reacted with various orthoesters in 1:4:2 molar ratios under basic conditions using the Michael addition reaction mechanism. Reaction progress was monitored with thin layer chromatography. No successful addition occurred due to amide delocalization of HPMA competing with enolate ion formation. Acetic anhydride protecting groups were placed on the hydroxyl hydrogen of HPMA to try to prevent this occurrence. HPMA was successfully modified and analyzed via H^1NMR and LCMS, however the Michael addition reaction with orthoesters did not go to completion and byproducts together with leftover reactants made separation and purification difficult.

The purpose of part II was to establish an automated approach to salt selection and preformulation development for a large number of Trazodone salts.

Automated procedures were developed on a Biomek 2000 automation workstation with stacker and plate reader capabilities. Trazodone was dispensed into 96 well plates and an automated method was setup to form 104 Trazodone salts. Salts were observed under a polarized light microscope to determine crystallinity. After stepwise eliminations, the remaining salts were scaled-up and subjected to differential scanning calorimetry (DSC), powder x-ray diffraction (PXRD) and hygroscopic, pH-solubility, density, surface area and particle size analyses. Oils formed in several cases resulting in the preliminary elimination of mesyl and esyl salts and 4 crystallizing solvents. Crystallinity was observed in 34 of the 44 scaled-up Trazodone salts. Analyses indicated a number of new salts, which were comparable in physicochemical parameters to the marketed HCl salt. Among them, the tosylate salt showed its uniqueness for new applications due to low solubility throughout the entire pH range making it a good candidate for a suspension or prolonged action formulation compared to the other salts. In addition, a thermally induced polymorph of the tosylate salt may be present with different properties than the tosylate salt. Automated procedures can be developed to increase the efficiency for pharmaceutical salt selection.

INDEX WORDS: HPMA, Polymeric Drug, Double Ester, Drug Targeting, Automation, High-throughput, Preformulation Development, Salt Selection, Trazodone, Polymorphism

PART I. SYNTHESIS OF NOVEL DOUBLE-ESTER POLYMERIC DRUGS

PART II. AUTOMATED METHODS IN PREFORMULATION DEVELOPMENT

by

EMILY CHILDREY WARE

B.S. in Chemical Engineering, Virginia Tech, 1997

A Dissertation Submitted to the Graduate Faculty of The University of Georgia in Partial Fulfillment of the Requirements for the Degree

DOCTOR OF PHILOSOPHY

ATHENS, GEORGIA

2003

PART I. SYNTHESIS OF NOVEL DOUBLE-ESTER POLYMERIC DRUGS

PART II. AUTOMATED METHODS IN PREFORMULATION DEVELOPMENT

by

EMILY CHILDREY WARE

Major Professor: D. Robert Lu

Committee: J. Price
A. Capomacchia
H. W. Jun
E. W. Taylor

Electronic Version Approved:

Maureen Grasso
Dean of the Graduate School
The University of Georgia
December 2003

ACKNOWLEDGEMENTS

I would like to thank God for His wonderful and challenging creation and leading me down this path of higher education. I thank my family, Mitch, Charlotte and Chris Childrey, for supporting me early in life and giving me the opportunity to attend Virginia Tech where I met my husband, Neal, and obtained my Chemical Engineering degree. Thank you for continuing to support and encourage me. I thank my husband, Neal for his patience and willingness to work with me throughout all the trying times. Thank you for your foresight and tremendous resourcefulness to help me do any and everything that was needed to finish my projects. I want to thank my extended family, Ruby and Connel Ware and Bonnie, Dale, Brock and Sharon Ware, for all their support and encouragement.

I would like to express my sincere appreciation to Dr. D. Robert Lu for allowing me to be a member of his research group. Thank you for all your understanding, encouragement, advice, and guidance. You will be greatly missed and impossible to replace at the University of Georgia.

I thank Dr. Price, Dr. Capomacchia, Dr. Jun, and Dr. Taylor for serving as my committee members and guiding me through difficulties and problems. Thank you for providing the many resources and for being ready and willing whenever I needed you. I also thank Dr. Beach for helping me with the chemistry portion of my projects and providing notes and books for me to find answers.

I thank my labmates Gina Peacock, Richard Sidwell, Mohannad Shawer, Tiffany Adams, Fars Alanazi, Guangliang Pan, Ranajoy Sarkar, and Yan Huang for lively scientific and personal conversations. Thank you for your friendship! I especially thank Dr. H. Li for his help and resourcefulness in synthesis, extraction, and analysis. Without it I might not have gotten through.

I am grateful for the opportunity to earn my Ph.D. with departmental funding as a teaching assistant. For this, I sincerely thank the Pharmaceutical and Biomedical Sciences Department of the College of Pharmacy. Finally, I would like to thank the American Foundation for Pharmaceutical Education (AFPE) for awarding me their financial support in my final year and a half and making me an AFPE Fellow. It has been a great honor.

"The heavens declare the glory of God; and the firmament sheweth his handywork. Day unto day uttereth speech and night unto night sheweth knowledge."
Ps. 19:1-2.

"Through wisdom is an house builded; and by understanding it is established: And by knowledge shall the chambers be filled with all precious and pleasant riches. A wise man is strong; yea a man of knowledge increaseth strength."
Prov. 24:3-5.

TABLE OF CONTENTS

Page

LIST OF TABLES

Page

LIST OF FIGURES

Page

PART I: SYNTHESIS OF NOVEL DOUBLE-ESTER POLYMERIC DRUGS

CHAPTER 1

INTRODUCTION: BACKGROUND AND SIGNIFICANCE

Drug Targeting

The idea of drug targeting or delivering a sufficient amount of drug to a specific site in the body for an appropriate time period, came about over 2000 years ago as described in literary works by Hippocrates [1]. P. Ehrlich expanded this idea in his concept of a magic bullet in the early 1900's [2]. These magic bullets consisted of two parts, a haptophore, which acts as the targeting moiety and binds to the target such as an antibody; and a toxophore, the cytotoxic part or drug. It wasn't until nearly 60 years later that this idea was tested and proven to work in treating tumors in animals using several types of systems [3, 4]. The 1960's and 1970's spawned interest in this area of drug targeting as biochemists and biologists began to figure out the nature of diseases and treatments on the cellular level, especially small drug and macromolecule uptake and trafficking through the cell. Other achievements during this time that helped drug targeting grow into a major area of research were novel synthesis routes for polymers, the establishment of pharmacokinetics, and the evolution of hybridoma and gene technologies [1].

In order to design a successful drug targeting therapy, it is necessary to understand the basic mechanisms underlying cellular uptake and trafficking through the cell. A general overview of the processes governing cellular

structure, function and membrane transport is discussed in appendix A. Low molecular weight drugs can be taken up into the cell by several mechanisms including passive diffusion through the plasma membrane, active transport by receptor proteins on the cell surface, and endocytosis. Unless there is affinity of the drug for a specific cell or receptor, uptake is generally slow and non-specific, and therefore, not targeted to a specific region of the body or cell type. It is possible to introduce a targeting moiety onto drugs to allow specificity and increase the rate of uptake. This modulation of uptake and distribution has been accomplished by conjugating drugs to polymeric carriers, so-called polymeric drugs, which will be discussed in the next section. Most recent efforts in the area of drug targeting using polymeric drugs have been focused on the treatment of tumors in anti-cancer therapy for reasons that will be discussed in a later section; therefore, this chapter will focus only on this aspect and how it relates to the research project.

Polymeric Drugs

The use of polymers in the medical and pharmaceutical fields dates back to the 1940's when Nylon was used as sutures in surgery, and other polymers such as poly[methylmethacrylate] (PMMA), polyesters (PE) and polyvinyl chloride (PVC) were being studied for similar uses [5-7]. With advances in cellular and developmental biology making way for new protein and gene based drug therapy, additional applications for polymers have been developed in the form of implantable devices and tissue engineering. Bioerodible polymers can be

synthesized to control decay rate either over time or when subjected to acidic environments. The versatility of polymers has allowed them to be used in the biotechnology, medicine, food and cosmetic industries in applications such as surgical devices, implants, prosthetics, artificial organs, drug delivery systems, biosensors, bioadhesives, and ocular devices [8]. Several major water-soluble polymers, shown in table 1.1 and initially used as plasma expanders, became the starting point for polymer-drug conjugates or so-called polymeric drugs.

The main mechanism of cellular uptake for polymers and high molecular weight substances is endocytosis [9]. In this process, the cellular plasma membrane forms a cavity or indentation due to an external stimulus, and through normal fluid motion and rearrangement of the membrane, an envelope or endocytic vesicle forms, engulfing the substance, including any surrounding extracellular fluid, into the cavity. Most cells undergo endocytosis on a regular basis and several different types of endocytosis exist based on the specificity and size of the material engulfed [10-12].

Pinocytosis is a process in which both small and large molecules dissolved in the extracellular fluid flow into the formed cavity and are pinched off as vesicles within the cell. Because pinocytosis deals with fluids it is also referred to as fluid-phase pinocytosis, and the internalized vesicle is called an endosome. Much of the time, the dissolved drug or polymeric drug interacts with membrane protein receptors and is basically “caught” in the cavity through specific (receptor-mediated pinocytosis) or non-specific (adsorptive pinocytosis) binding to the receptor when an endosome is formed [12]. The

Table 1.1. Polymers Used as Starting Candidates for Polymeric Drugs [1]

Poly(glutamic acid)
Poly[N-(2-hydroxyethyl)-L-glutamine] (PHEG)
β-Poly(2-hydroxyethyl aspartamide)
β-poly(aspartyl hydrazide)
Dextran
Poly(vinyl alcohol) (PVA)
Polyvinylpyrrolidone (PVP)
Poly[N-(2-hydroxypropyl) methacrylamide] (PHPMA)

endocytosed vesicle containing drug and extracellular fluid fuses with an organelle of the cell called an early endosome, which has an acidic environment. A portion of the material, especially membrane components and receptor proteins, is then selectively recycled back to the membrane or exocytosed while the rest becomes a late endosome containing hydrolases and an even more acidic environment with a pH of around 5-6. The late endosomes move toward the interior of the cell and become lysosomes containing more digestive enzymes that act to degrade the endocytosed material. A schematic of this process is shown in figure 1.1. Due to this progression to lysosomes, many polymeric drugs are designed using specific lysosomal-enzyme degradable spacers so that the drug is released in the lysosomal compartment and can then penetrate through the lysosomal membrane to reach the cytoplasm and potentially the nucleus. This strategy was first used in 1974 to deliver chemotherapeutics to the cell and was called lysosomotropic chemotherapy [13].

Another type of endocytosis involves the uptake of large substances such as solid drug particles, cells, bacteria or viruses. This is called phagocytosis and occurs in a series of steps similar to pinocytosis. Drug particles or other large substances adhere to the cell membrane. The binding usually occurs at a specific site that activates phagocytic mechanisms within the cell. The entire particle along with some extracellular fluid is ingested or engulfed by the membrane forming a detached vesicle or phagosome within the cell. The phagosome then fuses with a lysosome, and the particle and other phagocytosed material is digested while the bilayer materials are recycled.

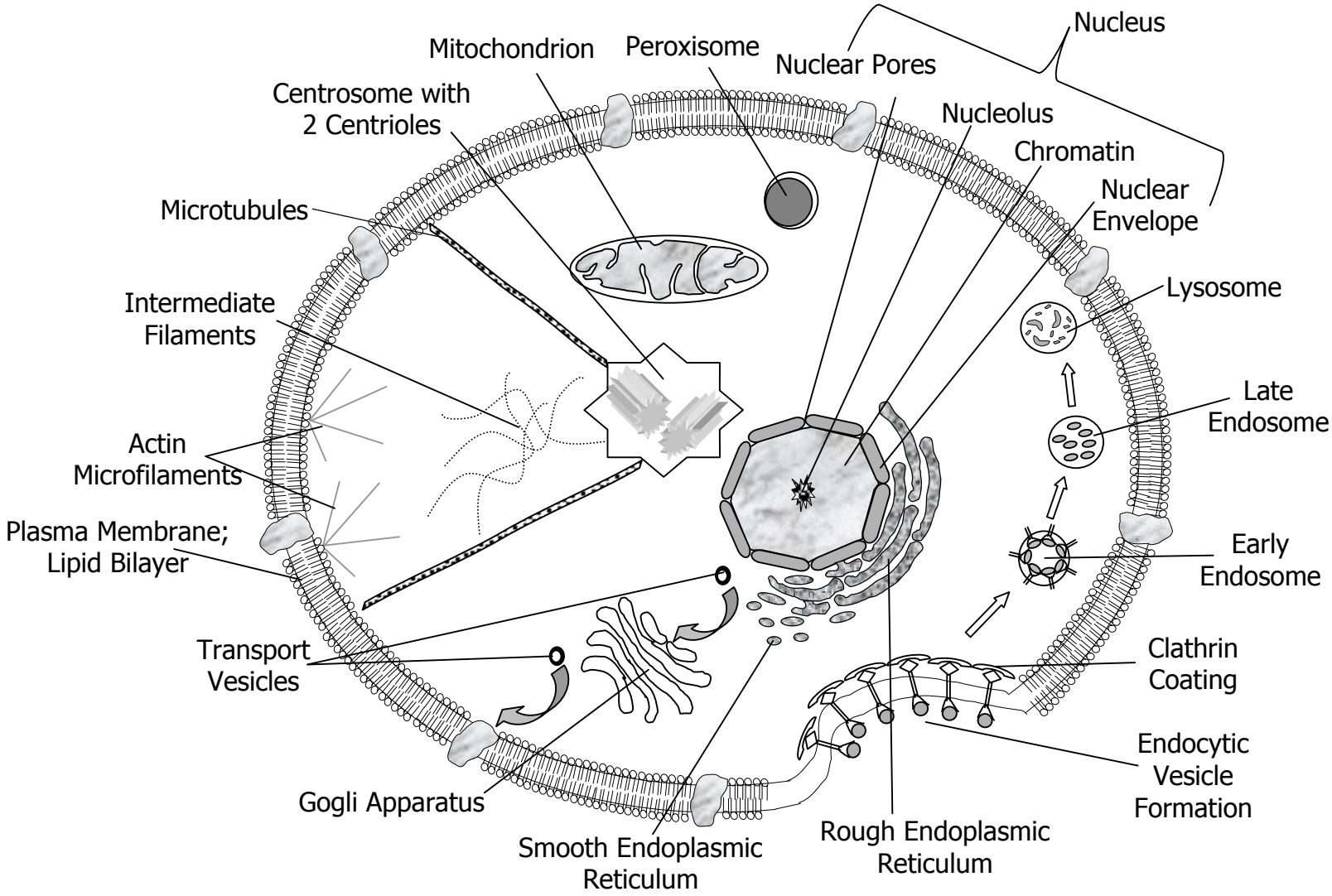

Figure 1.1. Schematic of a Typical Eukaryotic Cell Undergoing Endocytosis

Phagocytosis only occurs in specialized cells called professional phagocytes that exist in specific areas of the body, mainly the reticulo-endothelial system (RES). This includes the liver, bone marrow, and spleen macrophages and circulating blood monocytes. The phagocytes are tremendously important in regulating the body's immune system as they destroy foreign substances and remove particulate antigens. Their importance in drug therapy is limited to those drugs that are delivered in particulate carriers to the cell such as liposomes, erythrocytes, or microspheres. The therapy can be targeted using drug molecules whose site of action is some component of the RES [12].

Receptor-mediated endocytosis is the most versatile type of endocytosis involving a high degree of recognition and specificity. Agonists binding to surface receptors activate the endocytic pathway causing invagination of the bilayer and vesicle formation. The receptors themselves are usually recycled back to the cell surface and the agonist either participates in metabolism or is taken back to the cell surface. The size of material that can be endocytosed via receptor-mediated endocytosis ranges from smaller than 100 Daltons to in excess of a million Daltons, such as a virus particle. Many drug delivery efforts focus on targeting various receptors on the cell surface so that particular biochemical pathways can be exploited. Agonists are typically developed to extend the duration of action via altered metabolic pathways in the lysosomal compartment, or to reduce side effects by specific binding to certain receptors on certain cells. Non-specific adsorptive endocytosis, which occurs significantly for cationic polymers due to electrostatic interactions with negatively charged cell membranes, results in a 10

times faster uptake than normal fluid-phase endocytosis [14]. Receptor-mediated endocytosis is 1000 times faster and highly specific so that cellular specific targeting can be achieved [1]. This shows the importance of drug targeting. If a polymeric drug can be made with targeting moieties to specifically interact with receptors on the cell surface, not only is it taken up much more quickly, it avoids other non-target cells that do not possess the specific receptor thereby decreasing side effects and increasing drug efficacy. In addition, since polymeric drugs use the prodrug approach, typically undergo a different mechanism of uptake than small molecular weight drugs, and are designed to release the active drug only within the target cells, they have the potential to safely and effectively treat diseases where toxicity and multi-drug resistance (MDR) are major obstacles. However, a problem still remains. No matter how many targeting moieties are present specific to a certain cell type or receptor, if the drug or prodrug cannot get into the vicinity of the target, the targeting approach is useless. Because of this problem, there are several important considerations in terms of type and size of drug or prodrug to use, where to target, and disease modalities as discussed below.

One of the main purposes for conjugating drugs to polymers is to obtain a high-molecular weight prodrug that modulates the disposition of the drug in the body. Longer half-life is achieved due to decreased excretion of the conjugate by the kidneys. This biodistribution is affected by size and structure of the polymeric drug. The threshold molecular weight range for glomerular excretion is 40k-70k Daltons for neutral water-soluble polymers [1]. Depending on site of action, if the

polymeric drug is able to circulate in the body for a longer time period, the probability of reaching its target increases, especially if the target is a tumor. This is because capillaries in tumor tissue are quite dense with an enhanced permeability from loose interendothelial junctions allowing for enhanced transport of large molecular weight drugs into the tumor. In addition, tumors have insufficient lymphatic drainage systems leading to poor tissue drainage and accumulation of macromolecules at the tumor site. This effect has been termed the enhanced permeation and retention effect (EPR) and has become one of the main guiding principles in polymeric drug targeting [1, 15, 16]. A similar EPR effect has been noted at inflammation sites due to microbial infections [16] and therefore, targeting of specific drugs to treat infections could be accomplished using this principle.

There is an optimum molecular weight range for polymeric drugs, greater than 70k Daltons to avoid glomerular filtration as already discussed, but the upper size limit depends on several things. As molecular weight increases, permeation through interendothelial junctions decreases and hence it takes longer to accumulate drug at the tumor or inflammation site. More importantly, the larger carriers may be recognized by the reticulo-endothelial system (RES), which scavenges particulates and larger macromolecules from the bloodstream. The cells of the RES are located in the liver, spleen, and lung and have been known to quickly and efficiently eliminate colloidal and vesicular carriers such as liposomes, especially those greater than 40 nm in size. The type of drug conjugated to a certain polymer can also affect biodistribution. A hydrophobic

moiety or a cationic charge introduced as a side chain can cause significant clearance of the polymeric drug through the liver. Kataoka suggests that in general, a hydrophilic polymer that is neutral or slightly anionic with a moderate molecular weight greater than 70k Daltons will have a prolonged circulation [1]. This result also shows promise for treating liver disorders as targets can be designed to specifically accumulate there. Kopecek and Duncan have done significant pioneering work with polymeric drugs based on PHPMA targeting to the liver for treating liver cancer using this principle [17, 18]. Their work is the basis of this research project and will be discussed in the next section.

Anti-Cancer Therapy Using HPMA

As scientific discoveries of new drugs and therapies emerge, nature brings about new diseases or drug resistance and forces scientists to develop novel technologies. Although not new, cancer continues to be a treatment challenge and still has no cure. Much work has been done on developing new treatments and potential cures for cancer, but with little success. In the early 1970's several researchers led by Jindrich Kopecek, began investigating hydrophilic polymers for use as biomedical materials. These would later become novel polymeric drug conjugates for the treatment of liver cancer.

At first, Kopecek experimented with the biocompatibility both in blood and living tissue of N-substituted methacrylic acids, hydrophilic esters of methacrylic acid, and N-substituted acrylamides. The one that was most interesting as a synthetic transfusion solution was poly[N-(2-hydroxypropyl)-methacrylamide]

(PHPMA) [19]. He investigated different solvents, initiators, and copolymers in the radical polymerization of PHPMA to determine the optimum method of preparation. He also looked into potential applications and determined that this polymer could be used in the hardening of steel, photography, and as a blood plasma expander [20], but more importantly as the polymer backbone in novel polymeric drug conjugates [21]. It was at this time with the help of Ruth Duncan that the design of this particular polymeric drug came together. Many experiments followed by numerous publications and a patent lead to several novel PHPMA drug conjugates consisting of enzymatically degradable oligopeptide side chains in specific sequences to promote different degradation rates by lysosomal enzymes (trypsin and chymotrypsin) at the site of action attached to doxorubicin and daunorubicin for treatment of liver cancer. In addition, to utilize the receptor-mediated endocytosis mechanism to increase cellular uptake rate, dangling galactose residues were added as side chains to the polymer backbone [21-26]. The asialoglycoprotein receptor, present in liver parenchymal cells, can specifically recognize galactose residues and efficiently internalize them. Several studies have shown an increase in uptake of polymeric drugs with attached galactose residues. This type of carrier macromolecule has been widely used in liver targeting. Another important fact about the liver that makes it an easy organ to target is its high surface area with a sinusoidal vasculature structure and a lining composed of sieve plates of about 100 nm in diameter. This allows high molecular weight substances to extravasate from the blood into the liver tissue and accumulate there [1, 27-30]. In this way, a dose of

the HPMA bound anti-cancer drug given intravenously, would travel through the bloodstream and accumulate in the liver where enzymes would cleave off the drug, activating it at the cancerous site. The practical results of such an approach are numerous including decreased toxic side effects, less drug necessary for efficacy, lower treatment costs, increased patient compliance and an overall better therapy.

One additional consideration was made addressing the problem of potential accumulation toxicity of the non-biodegradable polymer “shell” at the site of action. Duncan and Kopecek took this into account by crosslinking shorter HPMA polymer chains with degradable oligopeptide crosslinks, which are susceptible to lysosomal hydrolysis, such that when the crosslinks are broken each polymer piece would be small enough to be filtered at the glomerulus. In this manner, the oligopeptide side chains could be tailor-made by manipulating the amino acid sequence to provide enzyme specificity and controllable degradation of the “drug delivery device” itself [26]. Another possibility exists to circumvent this problem. A biodegradable polymer backbone could be employed using the same principle of enzymatically degradable peptide side chains attached to drug and targeting moiety, but the polymer itself can be designed to erode at varying degradation rates according to substituent groups incorporated into the backbone.

Double Ester Strategy

Polyesters have been used for many years in a variety of applications and subjected to different manufacturing techniques, as seen in table 1.2 along with examples of different polyesters. There are numerous advantages associated with polyesters since they are labile to common esterases in the body, degradable in aqueous environments with generally non-toxic byproducts, and they can be synthesized in such a way that their degradation rate can be controlled. However, little work has been done using polyesters in a prodrug type of approach to achieve targeted, specific drug delivery. This may be due to the ease of hydrolysis of many polyesters in aqueous environments indicating the need for more extensive measures in manufacturing and packaging of the products to prevent water vapor incorporation. Also, due to esterases present in a variety of places in the body, some method may need to be employed to protect the polymers from premature degradation whether given orally or intravenously [31, 33-35].

The double ester strategy used by Nycomed has several advantages over typical bioerodible polyesters. It is stable in acidic and neutral environments and degrades by esterases in the body. It is synthesized by condensing two carboxylic acids with $I_2CR_1R_2$ where different R-groups can be incorporated to vary the degradation rate. This is the most important feature of the double ester strategy. The R-groups are called gems and the double esters are also known as gem-dicarboxylic acids. These R-groups or gem linkers can be oligopeptide spacers attached to drug or targeting moieties similar to the PHPMA strategy

Table 1.2. Uses and Manufacturing Techniques Commonly Employed for Polyesters [31, 32]

Purposes	Manufacturing Techniques	Examples
Coatings	Extruded into Filaments	Poly(Lactic Acid) Poly(Glycolic Acid) Copolymers of Above (PLGA) Polydioxanone Poly(Glycolide-co-Trimethylene Carbonate) Poly(Ethylene Carbonate) Poly(Iminocarbonates) Polyhydroxybutyrate Poly(Amino Acids) Poly(Ester Amides) Poly(Ortho Esters) Poly(Anhydrides)
Biodegradable Implants	Spun into Fibers	
Resorbable Applications	Pressed into Shapes	
Delayed Release Drug Delivery Systems	Solvent Film Casts	
Long-Lived Packaging Insert Materials	Doctor-Bladed into Films	
Insecticides and Plant Foods	Coated by Solvent Evaporation	
Detergents	Coated by Fluidized Bed	
Cosmetics	Compression and Transfer Molded	

employed by Kopecek and Duncan or they can be different length organic chains for use as a liposomal or nanoparticle carrier in drug delivery. In this manner the drug can be delivered orally where absorption will occur through the lymphatic system and the rate of drug delivery is controlled by the degradation rate of the polymer vehicle [32, 36]. This research focuses on the development of an intravenously administered anti-cancer compound similar to that of Kopecek and Duncan. The chemical structure of a potential polymer synthesized using the double ester strategy is shown in figure 1.2.

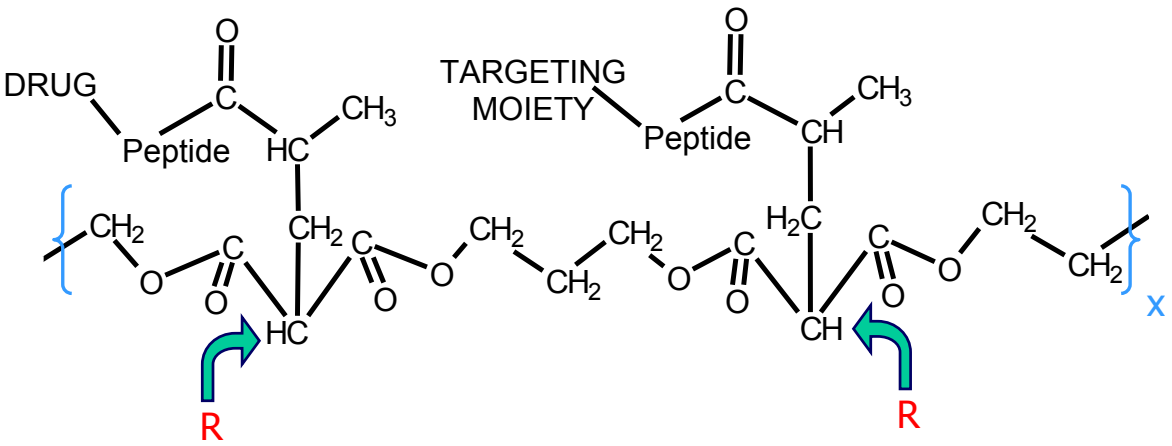

Figure 1.2. General Polymer Structure of the Double Ester Strategy

CHAPTER 2

SYNTHESIS OF NOVEL DOUBLE-ESTER POLYMERIC DRUGS

Experimental Methods

The strategy employed by Kopecek and Duncan was used as a starting point to synthesize HPMA bound targeting moieties and oligopeptide attached drugs. It was decided to try to duplicate Kopecek and Duncan's work in making the monomer attached to peptide spacers and galactose targeting moiety, and the monomer attached to peptide spacers and drug analogue. Then, to polymerize them in order to practice the chemistry and analysis involved before beginning work on the double ester strategy.

Synthesis Steps and Reaction Schemes

All chemicals were ordered from Sigma-Aldrich (St. Louis, MO, USA) and were of analytical grade. The steps in the synthesis of each monomer were obtained from several publications and a patent [19-24] and will be outlined below.

N-[2-(hydroxypropyl)-methacrylamide] (HPMA) monomer is formed from the reaction of 1-amino-2-propanol and methacryloyl chloride (MACl) at –10°C in acetonitrile using a slight excess of 1-amino-2-propanol. The crystalline byproducts of 1-amino-2-propanol hydrochloride are filtered off and the product recrystallized in acetone at -25°C to obtain a pure monomer. The second monomer, N-methacryloylglycylglycine p-nitrophenyl ester (MA-Gly-Gly-ONp), is

the precursor to attach to the drug moiety. It is synthesized using the Schotten-Baumann method of acylation with an acylchloride in an aqueous alkaline media by first reacting glycylglycine with MACl in a one to one molar ratio, purifying the product, and then reacting the product with p-nitrophenol in dimethylformamide (DMF) at -15°C. The same procedure is followed with different amino acid chains to tailor-make the oligopeptide spacers which can be degraded by a particular enzyme. In fact, the glycine leucine tyrosine spacer attached to drug was found to be long enough to allow enzyme attachment in the liver and cleavage without steric hindrance, and it allowed for increased uptake due to an increase in adsorptive endocytosis from increased hydrophobicity over glycylglycine [37].

The third monomer is made in the same way to obtain N-methacryloylglycylglycine galactosamide (MA-Gly-Gly-Gal). The second monomer product MA-Gly-Gly-ONp is reacted with galactosamine hydrochloride, which undergoes an exchange type of reaction to replace p-nitrophenol with galactosamine and gives methacryloylglycylglycine galactosamide (MA-Gly-Gly-Gal) as the product. All three monomers are reacted together in varying molar percentages using a free radical initiator, 2,2'-azodiisobutyronitrile (AIBN), to obtain a PHPMA backbone attached to 2 different side chains. The percentage of ONp groups present in the polymeric precursor is the same percent of drug, which is added in a second exchange type of reaction as the final step to prepare the polymeric drug. Figures 2.1-2.5 show the reaction schemes and detailed steps in the synthesis.

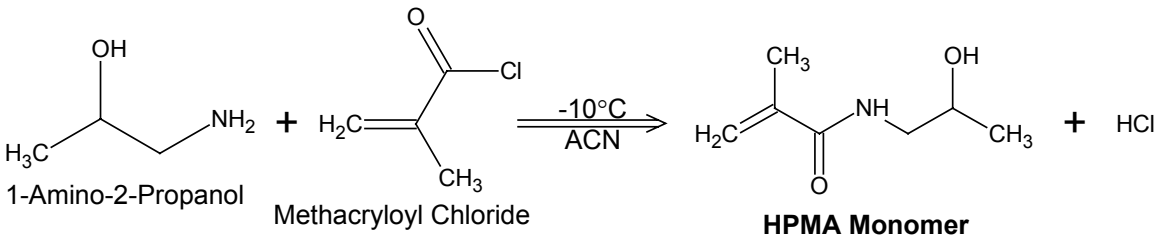

HPMA Monomer Synthesis

1. Prepare 100 mL (or smaller) flask with stir bar, thermometer, dropping funnel, and ice bath (-10°C).
2. Pipette 3.409 mL acetonitrile into flask
3. Weigh 871.212 mg 1-amino-2-propanol in weigh boat
4. Pour into flask and dissolve
5. Cool to -10°C
6. Weigh 606.061 mg methacryloyl chloride (MACl) in weigh boat.
7. Mix with 2.462 mL acetonitrile in small beaker and dissolve
8. Place 7 in “dropping funnel” apparatus (pipette with valve)
9. Vigorously stir 4 while slowly adding dropwise 7 until spent keeping T<-5 °C
10. Continue stirring at 5°C for 30 min
11. Filter off crystals of 1-amino-2-propanol HCl
12. Wash crystals with 5 mL acetonitrile
13. Set crystals to side and label
14. Combine filtrates and evaporate to ½ volume keeping T<=35°C
15. Filter and allow to freely crystallize at -25°C (acetone & dry ice bath)
16. In a small beaker mix 6 mL methanol with 2 mL diethyl ether
17. Slowly add small amount to concentrated filtrate to crystallize 1-amino-2-propanol
18. Filter off and wash crystals with this mix
19. Recrystallize HPMA with acetone from a saturated solution at 25°C and allow to freely crystallize at -25°C, filter crystals and wash
20. Repeat 19 until obtain a clear solution of HPMA in acetone
21. Evaporate to constant weight

Figure 2.1. Synthesis of HPMA Monomer

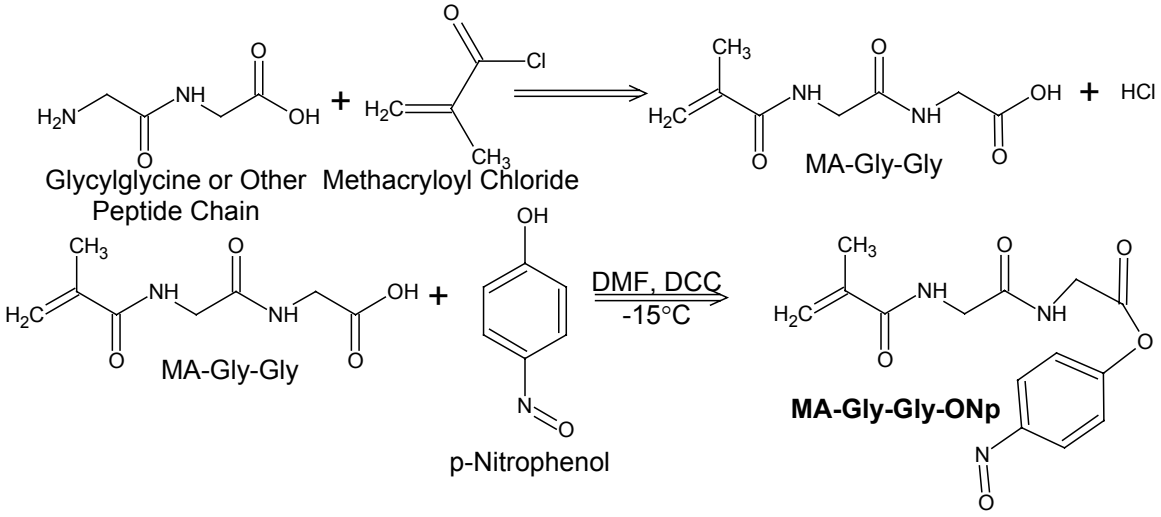

MA-Gly-Gly-ONp Synthesis

1. Prepare 30 ml beaker with stir bar, 2 glass pipettes and an ice bath; also need a pH meter calibrated
2. Weigh 89.93 mg Gly-Gly into weigh boat; pour into beaker
3. Dissolve in 1.0 mL water
4. Add 400 mg NaOH and dissolve with 0.5 mL water, wash with 0.5 mL water
5. Cool to 0°C with ice bath and stirring
6. Prepare 66.13 μL MACl in a pipettor
7. Prepare 400 mg NaOH in 2.0 mL water and suck into a glass pipette
8. Add 6 and 7 to 5 dropwise and simultaneously
9. Continue stirring at room temp. for 1 hour
10. Acidify using HCl to pH=2.0 (obtain crystals?)
11. Recrystallize MA-Gly-Gly using a solvent (DMF) until obtain clear solution

----OBTAIN MA-Gly-Gly----

12. Prepare clean 100 mL beaker with stir bar, thermometer, and salt water bath (-15°C)
13. Mix 123.181 mg of 11 with 1.225 mL DMF and dissolve
14. Cool to –15°C
15. Mix 126.423 mg of DCC (dicyclohexylcarbodiimide) with 0.6127 mL DMF and dissolve
16. Add solution 15 to 13 while stirring
17. Mix 86.082 mg p-nitrophenol with 0.5626 mL DMF and dissolve
18. Add solution 17 to 16 while stirring
19. Stir for 3 hours at –15°C
20. Let stand overnight at 4°C (refrigerator)
21. Remove dicyclohexyl urea crystals by filtration and wash
22. Concentrate filtrates in vacuo to about ¼ volume
23. Add DMF and repeat 19-22 for purification

Figure 2.2. Synthesis of N-Methacryloylglycylglycine p-Nitrophenyl Ester (MA-Gly-Gly-ONp) or Other Peptide Spacer Substituted for Gly-Gly

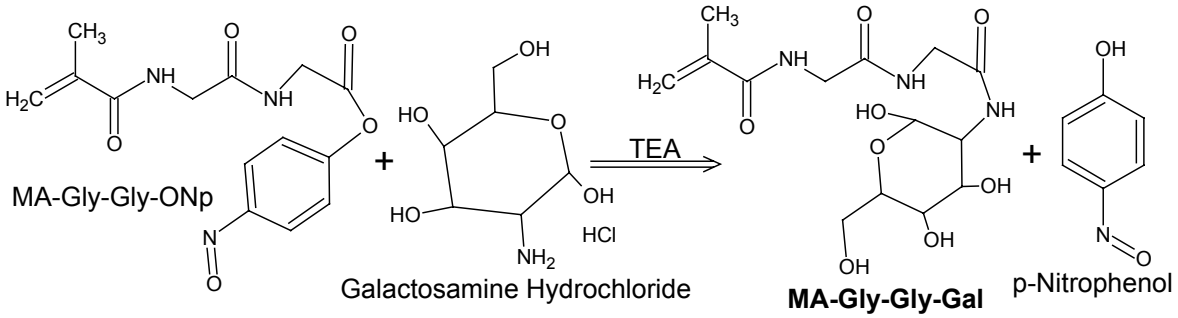

MA-Gly-Gly-Gal Synthesis

1. Prepare 50 ml beaker with stir bar, thermometer, and dropping apparatus
2. Weigh 116.67 mg MA-Gly-Gly-ONp into weigh boat; pour into beaker
3. Mix 93.33 mg galactosamine-HCl to 0.6 mL DMF and dissolve
4. Add solution 3 to 2 and begin stirring
5. Add dropwise while stirring 0.6067 mL triethylamine
6. Stir for 16 hours at 25°C
7. Filter off triethylamine-HCl crystals
8. Evaporate filtrate to a viscous oil
9. Add ethanol and cool; recrystallize with ethanol

Figure 2.3. Synthesis of N-Methacryloylglycylglycine Galactosamide

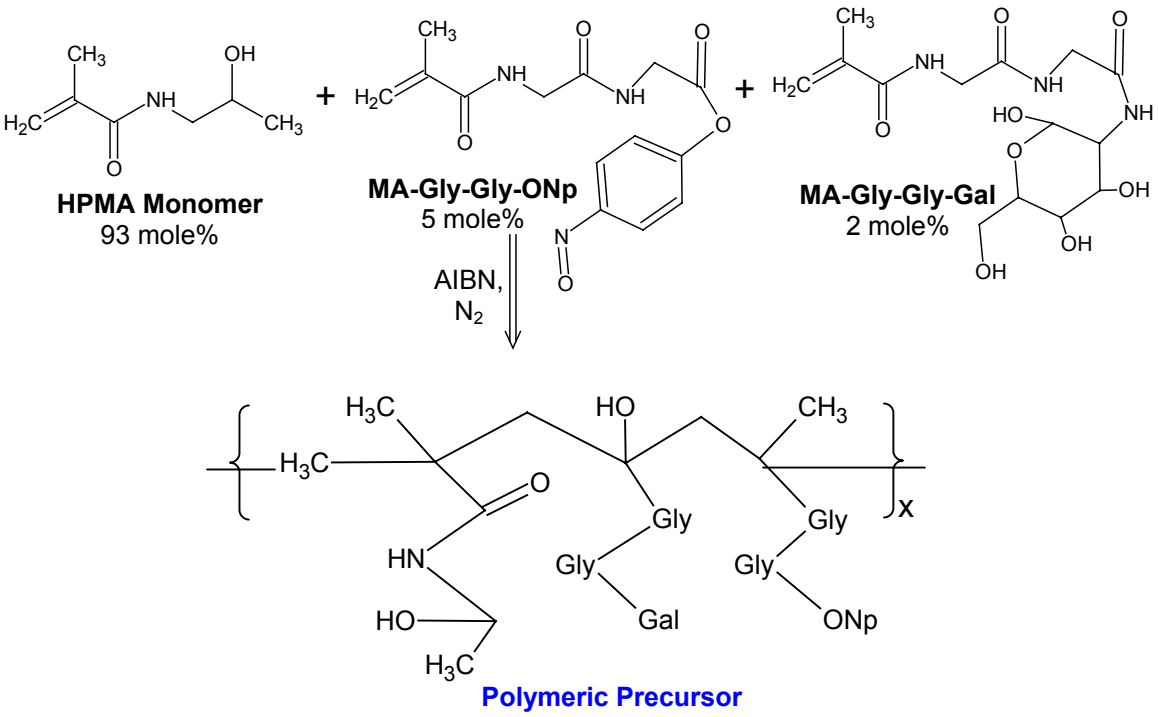

Polymeric Precursor Synthesis

1. Prepare 50 ml beaker and 2 10 mL beakers with stir bar, gather several ampoules together, prepare N_2 tanks with clean tubing, and Bunsen burner to seal ampoules
2. Mix 147.82 mg HPMA with 30 mg MA-Gly-Gly-ONp
3. Dissolve in 0.0277 mL acetone stirring
4. Mix 8.04 mg MA-Gly-Gly-ONp with 0.00111 mL DMSO and add to 3
5. (Recrystallize AIBN from ethanol 5 times for purification---may not be needed)
6. Mix 0.1698 mg to 0.00333 mL acetone and add to (3+4)
7. Pour mixture into ampoules
8. Bubble thru with N_2 and seal
9. Incubate at 50°C for 24 hours
10. Precipitate = polymer
11. Wash polymer with a 20 fold amount of acetone then with diethyl ether
12. Filter and purify (dissolve in methanol, precipitate in acetone)
13. Dry in vacuo to constant weight

Figure 2.4. Synthesis of Polymeric Precursor

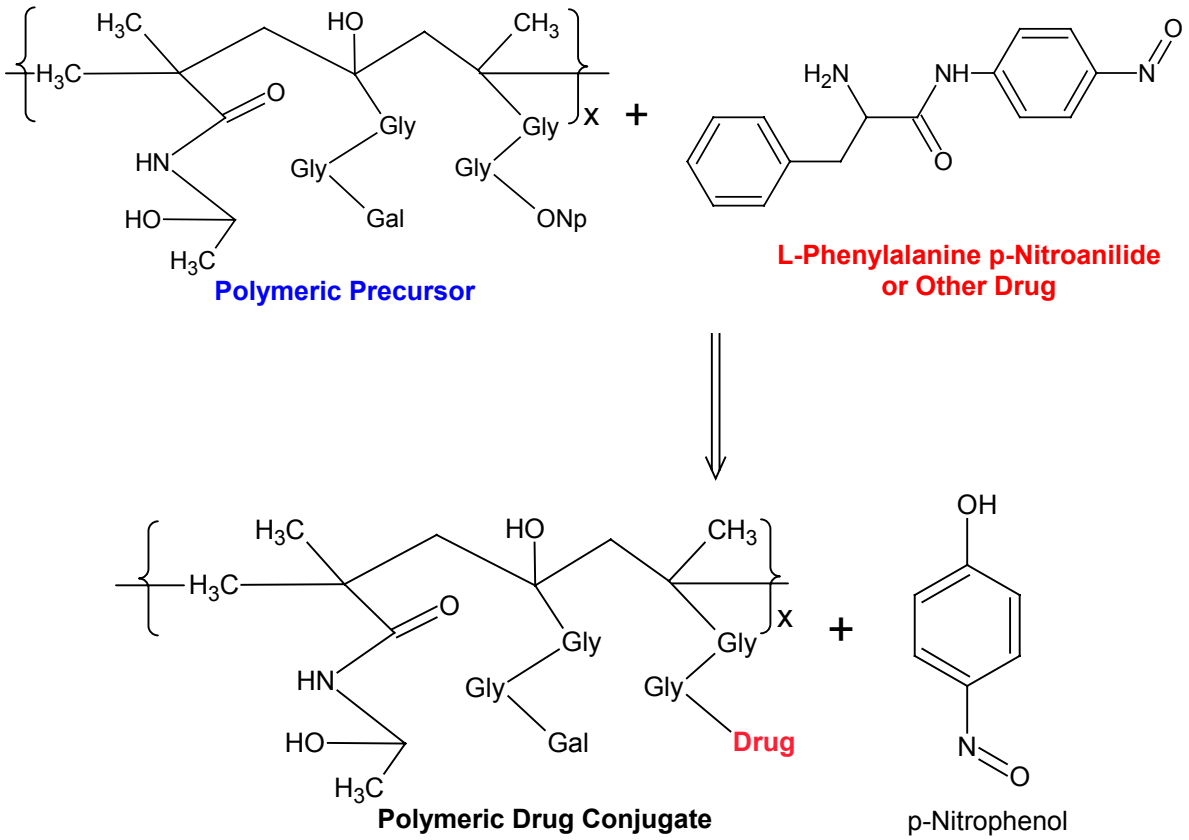

Polymeric Substrate (Drug) Synthesis

1. Prepare 2 10 ml beakers with stir bar or rod
2. Mix 80.0 mg precursor with 0.6 mL DMSO and dissolve
3. Mix 37.6 mg L-phenylalanine p-nitroanilide or other drug with 0.12 mL DMSO, dissolve and add to 2
4. Allow to react for 20 hours at room temperature
5. Aminolyze the remaining ONp's with an excess (50μL) of 1-amino-2-propanol
6. After 4 hours pour into a 20 fold amount of acetone to obtain a precipitate
7. Filter off and wash crystals with acetone, then diethyl ether
8. Dry in vacuo to constant weight

Figure 2.5. Synthesis of Polymeric Drug Conjugate

In beginning these experiments, Dr. H. Li was an excellent mentor. He was a tremendous aid in helping me with the H^1NMR measurements and analysis and in helping me figure out what to do when things did not work out as expected. After several experiments attempting to duplicate Kopecek and Duncan's work, we decided to begin the double ester strategy. Since much of the initial determinations as to how to add oligopeptide side chains attached to drug and targeting moieties had been achieved using HPMA, it was theorized to use very short polymer chains incorporating the three monomers, chemically add carboxylic acid groups at the terminal ends of each HPMA polymer chain, then use I_2CH_2 and eventually $I_2CR_1R_2$ to polymerize the carboxyls and make a polyester. A schematic of this method is shown in figure 2.6. To terminate chain growth during free radical polymerization in order to obtain short polymer chains, the reaction mixture would be immersed into liquid nitrogen and then poured into an excess of acetone. Adding the COOH's to each end of each polymer chain was more difficult to figure out, but it was thought that it could be possible by adding a terminating agent ending in carboxyl groups which would stop the polymerization while adding these groups.

Another idea to initiate the double ester strategy was to react a monomer typically used to make polyorthoesters that also has potential for degradation control (modifiable side chains) with the HPMA monomers. This strategy uses a Michael addition reaction through enolate ion formation shown in figure 2.7. Several orthoesters including trimethyl orthoformate (TMOF), trimethyl orthoacetate (TMOA), and dimethyl malonate (DMM) were used with several

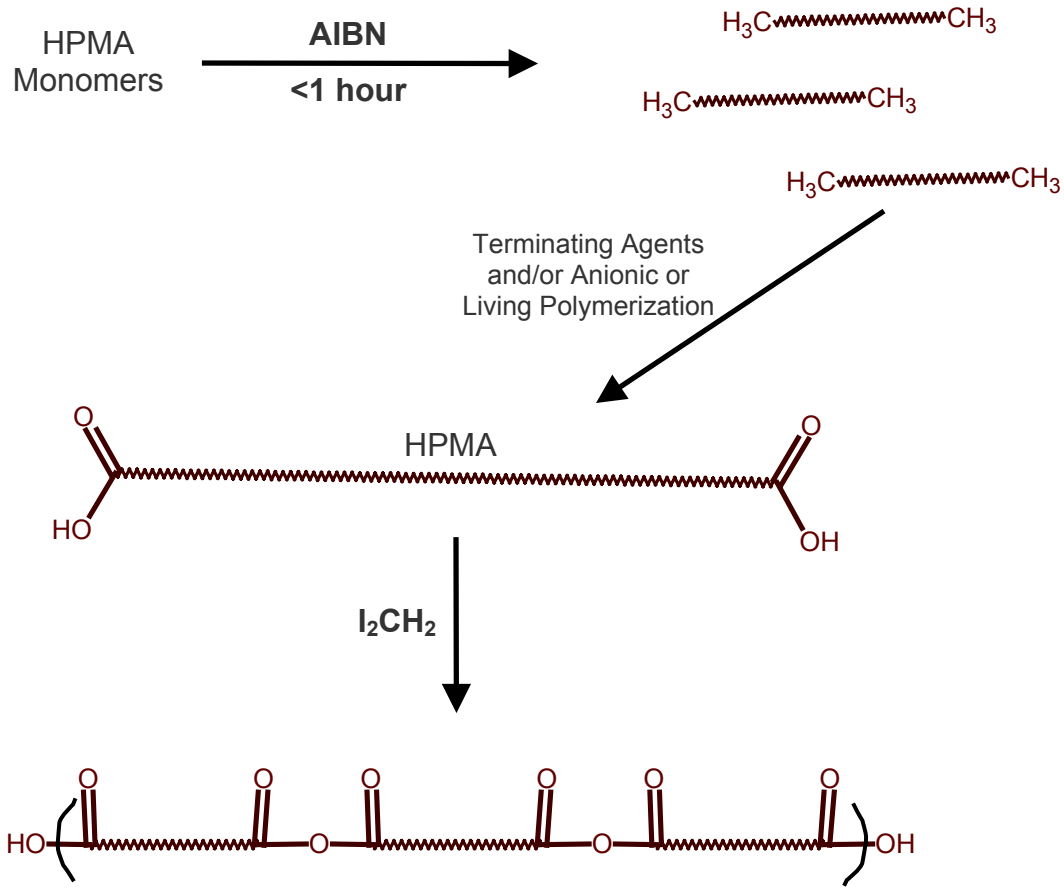

1. Make 3 HPMA Monomers According to Kopecek and Duncan
2. Polymerize the monomers for a short time period to obtain various short chain polymers
3. Add COOH's groups on the terminal ends of all polymer chains
4. Use I_2CH_2 or $I_2CR_1R_2$ to polymerize the COOH's into a polyester

Figure 2.6. Double Ester Strategy Utilizing the HPMA Monomers with Oligopeptide Side Chains Attached to Drug and Targeting Moieties

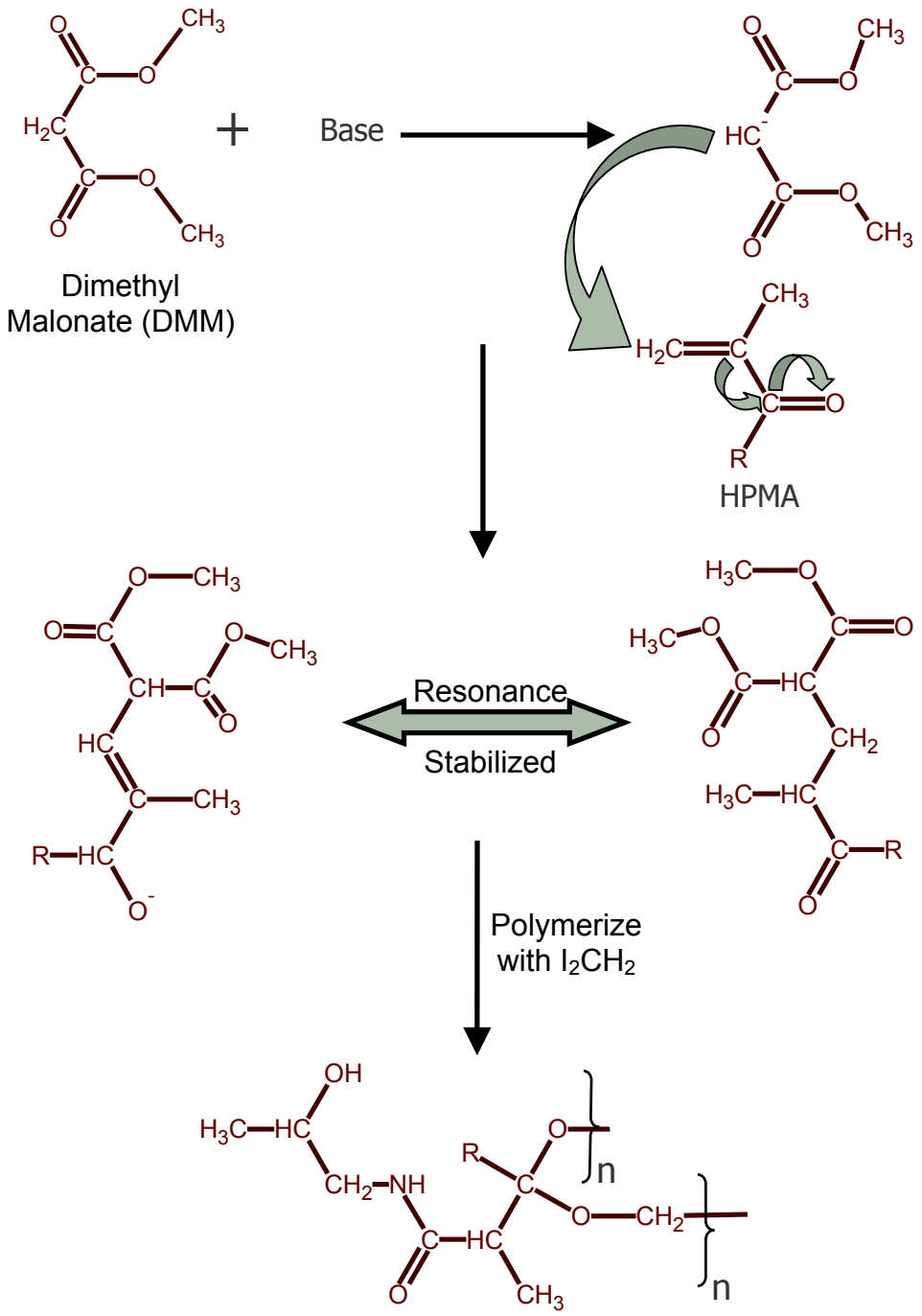

Figure 2.7. Michael Addition Reaction Through Enolate Ion Formation

bases including sodium tertbutoxide (NatBuO), butyl lithium (BuLi), and lithium diisopropylamide (LDA) to react with HPMA. A typical reaction scheme is detailed in figure 2.8 with reaction setup shown in figure 2.9.

Thin Layer Chromatography (TLC)

Reaction progression was monitored using TLC. UV indicating TLC plates, 250 μm silica gel [Whatman, Clifton, NJ, USA] were used and were spotted using fine glass capillaries made by heating glass pipettes under a Bunsen burner and pulling the melting glass into fine tubes. Plates were developed in 2" X 2" glass TLC chambers using different solvents and solvent mixtures including 1:9 methanol:ethyl acetate, 1:1 ethyl acetate:petroleum ether, and 1:1 petroleum ether:dichloromethane depending on what chemicals were present on the plate. To view the spots, the plates were exposed to long and short wavelength UV light, an iodine chamber and bromothymol dye solution.

Proton Nuclear Magnetic Resonance Spectrometry (H^1NMR)

Nuclear magnetic resonance spectra were recorded on a Bruker 400 AMX spectrometer at 400 MHz using tetramethylsilane (TMS) as the internal standard. All solids analyzed were dissolved in deuterated chloroform ($CDCl_3$) or methanol (CD_3OD) and placed in 5 mm o.d. X 178 mm length round bottom glass NMR tubes for measurement.

Fourier Transform Infrared Spectroscopy (FTIR)

Infrared spectra were collected using a BioRad FTS-60A spectrometer equipped with a wide band liquid nitrogen cooled HgCdTe detector model HCT-100 (IR Associates, Inc.) at 2 cm^{-1} resolution. This equipment was located in Dr.

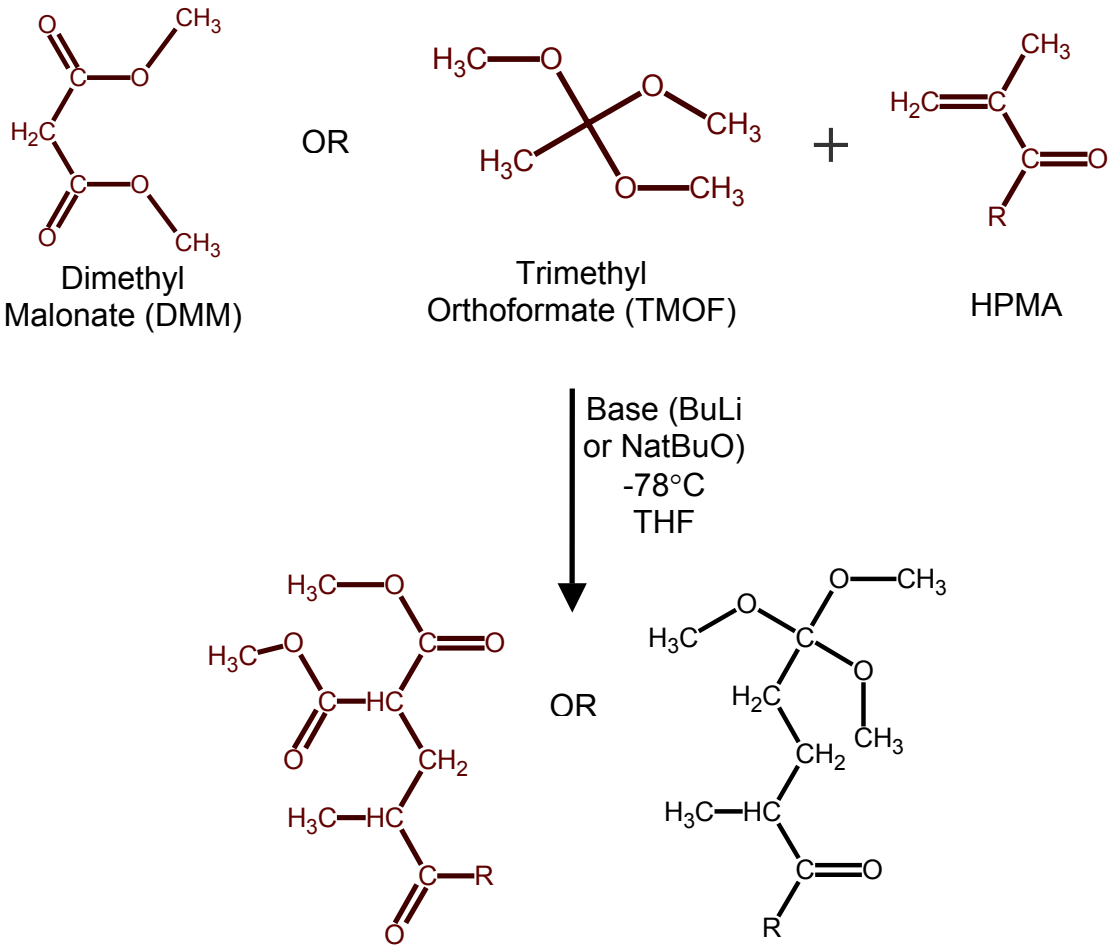

1. Trimethylorthoformate (TMOF), trimethylorthoacetate (TMOA) and dimethyl malonate (DMM) were dried using molecular sieves overnight. All glassware and stir bars were heated under Bunsen burner to remove as much water as possible.
2. A round bottom flask was setup in the apparatus as shown in figure 2.9 with a septum placed over the top; it was evacuated under vacuum then purged with dry N_2.
3. Dry TMOF or DMM was added via glass syringe into the round bottom flask; the syringe was washed twice with THF and then an excess of THF was placed into the round bottom flask.
4. The flask was cooled to –78°C for 5 minutes using an acetone in dry ice bath; it was evacuated under vacuum then purged with dry N_2 again.
5. Either butyl lithium (BuLi) or sodium tertbutoxide (NatBuO) base was placed in the flask and allowed to react for 35 minutes.
6. HPMA monomer dissolved in THF was added in a 2:1 up to 5:1 molar ratio of HPMA to orthoester to the flask while purging with N_2.
7. The flask was placed back in the –78°C bath for 1 hour and reaction progression was monitored via TLC.
8. After 1 hour, flask was allowed to warm to room temperature and left overnight.
9. Reaction was quenched with aqueous ammonium chloride.
10. Liquid products were evaporated to obtain solid precipitates and analyzed.

Figure 2.8. Typical Reaction Scheme for Reacting Orthoesters with HPMA

Figure 2.9. Dry Nitrogen Purge and Evacuation Setup for Orthoester HPMA Reaction

Dluhy's lab in the chemistry building. Samples were prepared by mixing the solids with potassium bromide and pressing into a pellet.

Column Chromatography and Liquid Liquid Extraction (LLE)

Several products required separation from solvent, excess reactants or byproducts. This was accomplished using liquid liquid extraction (LLE) for removal of pyridine solvent and column chromatography to separate byproducts and reactants. The LLE procedure was performed using ethyl acetate containing product and an aqueous cupric sulfate solution to draw out pyridine from the product into the aqueous layer. The pyridine was considered to be gone when no more blue color remained in the ethyl acetate layer. This layer was then washed with distilled water and a saturated sodium chloride solution. It was swished over anhydrous sodium sulfate powder to remove any traces of water. The remaining ethyl acetate containing product was poured into a silica gel column and ejected under vacuum with ethyl acetate, petroleum ether, dichloromethane and/or methanol in varying ratios to separate products and reactants, which were collected in 16 X 125 mm glass test tubes. The solvent in each tube was evaporated and the remaining residue was analyzed via H^1NMR.

Liquid Chromatography and Mass Spectroscopy (LCMS)

LCMS was performed by a third party in the mass spectroscopy facility in the University of Georgia chemistry building.

Results and Discussion

There were several overall objectives for this project. The first was to learn chemical synthesis, separation and analysis procedures especially those involved in polymeric drug conjugates. Second was to utilize the work of Kopecek and Duncan on HPMA monomers as a starting point in developing a novel polymeric drug, and third was to combine this strategy with the gem-dicarboxylic acid or double ester strategy in hopes of synthesizing a novel biodegradable polyester with oligopeptide linked drugs and targeting moieties. Due to my novice experience level, several professors and post docs helped me when problems were encountered by suggesting different routes of synthesis either by changing reactants, bases, or solvents.

Several initial experiments were attempted to synthesize the HPMA monomer by reacting methacryloyl chloride (MACl) with 1-amino-2-propanol. This first reactant was highly reactive with water and polymerized in the presence of water. Therefore, care had to be taken to dry all solvents and glassware. However, it was discovered that the HPMA monomer could be ordered instead of having to make it and separate it from potential byproducts and leftover reactants. This saved much time. If HPMA could be added successfully into the polyester backbone, then MA-oligopeptide-drug or targeting moiety should also be able to be added in much the same way. The H^1NMR and FTIR of HPMA from PolySciences are shown in figure 2.10 and 2.11, respectively.

The initial idea involving adding COOH groups at the terminal ends of PHPMA seemed quite difficult and no straightforward approach was found to

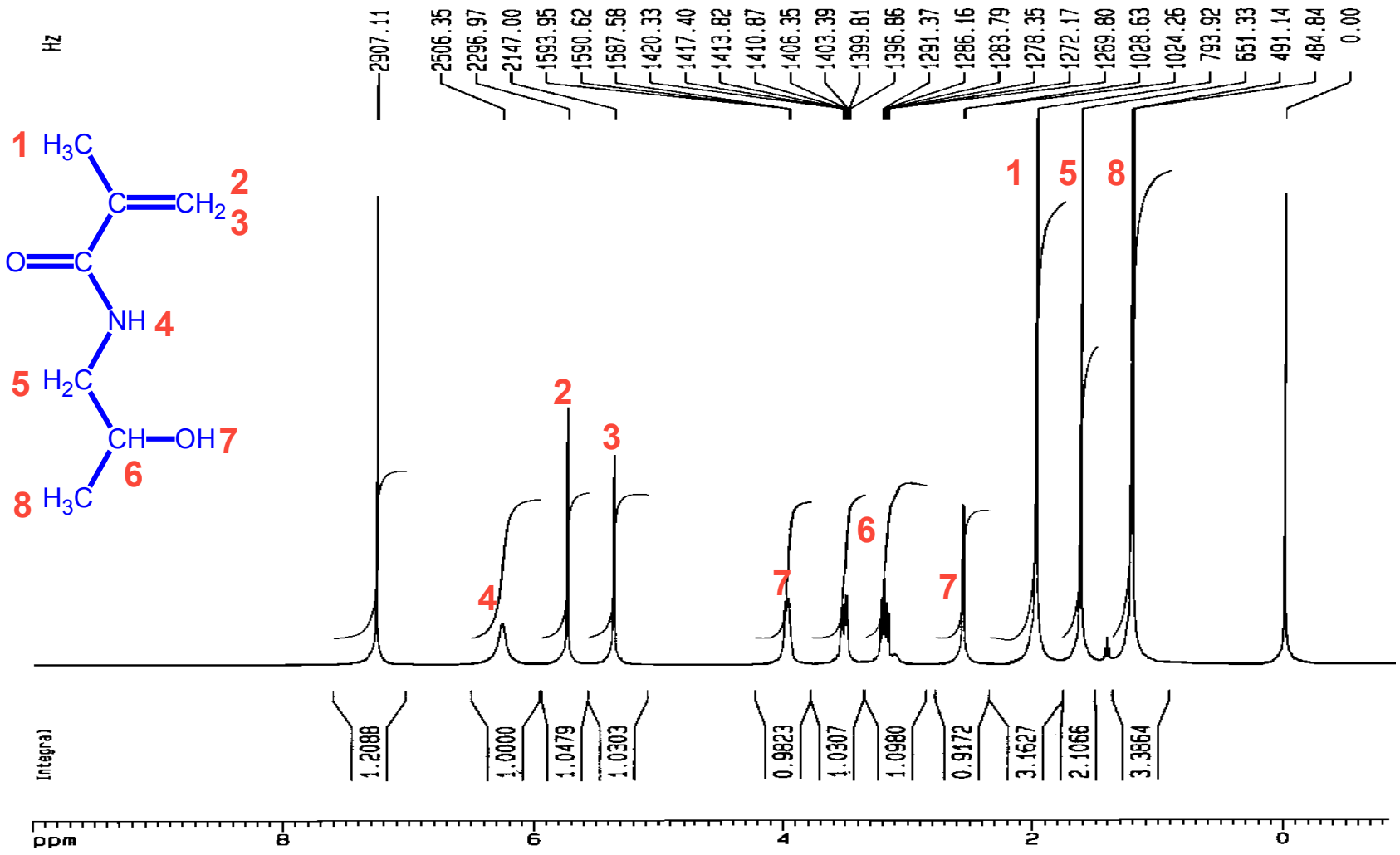

Figure 2.10. H[1]NMR of HPMA, 99% Pure, from PolySciences with Peaks Labeled According to Chemical Structure

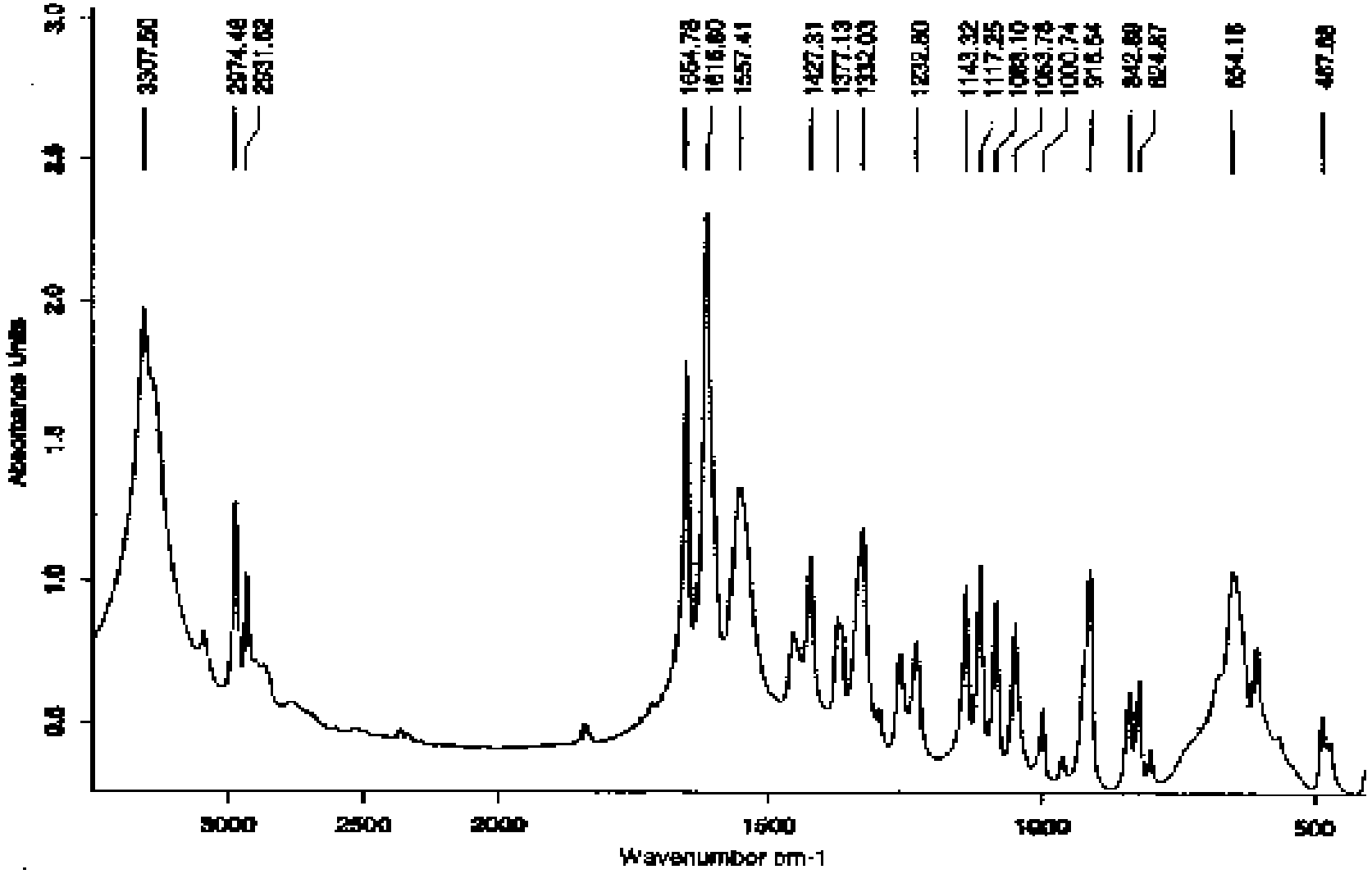

Figure 2.11. FTIR of HPMA, 99% Pure, from PolySciences in KBr Pellet

achieve this. Therefore, a better plan was adopted to react HPMA with various orthoesters under strong base using the Michael addition reaction. Three orthoesters were used: dimethyl malonate (DMM), trimethylorthoformate (TMOF) and trimethylorthoacetate (TMOA) in several reactions with two different bases: sodium tertbutoxide (NatBuO) and butyl lithium (BuLi). Reactions with HPMA were carried out at -78°C, 0°C, and room temperature using THF or dry ether with 1:2:4 molar ratios of HPMA:orthoester:base. In each case, little reaction progress was noted when viewed via TLC, or all of the product was hydrolyzed back to reactants accidentally upon addition of aqueous ammonium chloride used to quench the base and end the reaction. In addition, separation of the products, byproducts, and reactants was quite difficult using column chromatography. The most promising result from this series of reactions was that using TMOA and BuLi at room temperature; however, upon purification of the expected product and analysis via H^1NMR shown in figure 2.12, there was quite a resemblance to the original HPMA reactant indicating no reaction likely occurred. This may be due to accessibility of the amine and hydroxyl hydrogens of HPMA preventing enolate ion formation due to competition with amide delocalization and hindering reaction progression. Dr. Beach offered several possible solutions, the most viable of which was to add protecting groups at one or both of these positions on HPMA and react the modified HPMA with the orthoesters.

The hydroxyl group on HPMA was protected first using acetic anhydride (AA) via pyridine. This reaction took place quickly with all HPMA becoming

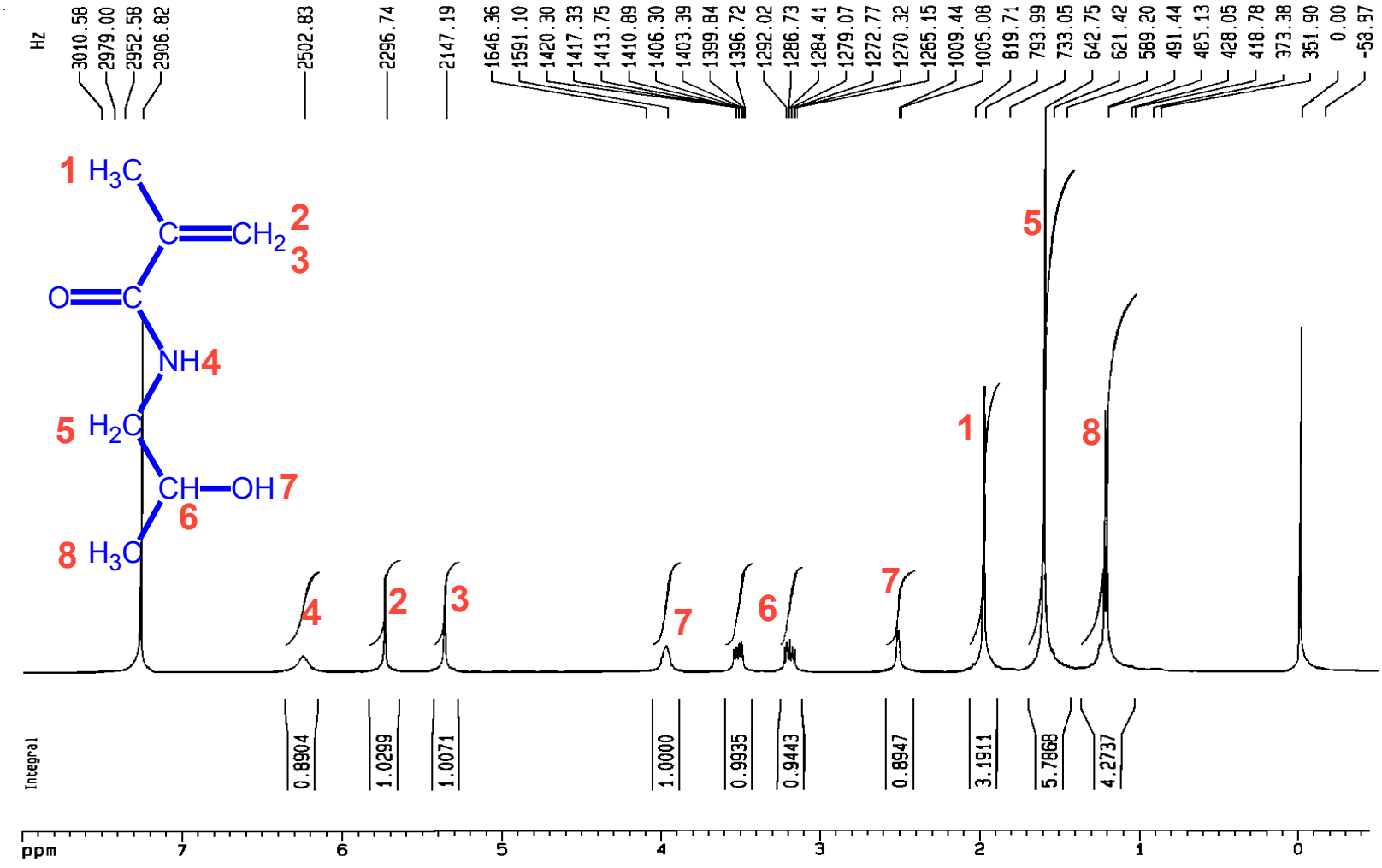

Figure 2.12. H[1]NMR of Reaction Between TMOA and HPMA via BuLi at Room Temperature in a 1:2:4 molar ratio of HPMA:TMOA:BuLi

modified (mHPMA) by the AA within 1.5 hours. A LLE procedure as described in the methods section was performed to remove pyridine, and separation was done on a silica gel column using 100% petroleum ether followed by 25/75% ethyl acetate/petroleum ether, 50/50% ethyl acetate/petroleum ether, 75/25% ethyl acetate/petroleum ether, 100% ethyl acetate, and 100% methanol to elute various fractions of the different products. Figure 2.13 shows the TLC plate indicating all HPMA reacted, and figure 2.14 is the H^1NMR of the AA modified HPMA showing a chemical structure of the product. Additionally, LCMS was performed on this product to obtain an m/z of 185.25 corresponding to the molecular weight of the expected product.

The AA mHPMA was reacted with DMM in a series of experiments in the presence of BuLi or NatBuO at room temperature using several solvent systems: dry ether, THF, dichloromethane (DCM), and ethyl acetate. Little success was noted and conversion of mHPMA to HPMA occurred rapidly. This time the problem was theorized to be the bases were insufficiently strong to ionize DMM to allow the Michael addition to occur to any extent, and the temperature may have been too high such that under the basic conditions mHPMA rapidly converted to HPMA. Therefore, a stronger base, lithium diisopropylamine (LDA), was used and the temperature was reduced to -78°C. This time the ionization of the orthoester was monitored for 45 minutes and TLC'd before adding mHPMA. The TLC plate shown in figure 2.15 appears to indicate that all DMM was ionized successfully by LDA. Upon addition of mHPMA in THF and allowing it to react overnight, a new spot is present as seen on the TLC plate in figure 2.16 and

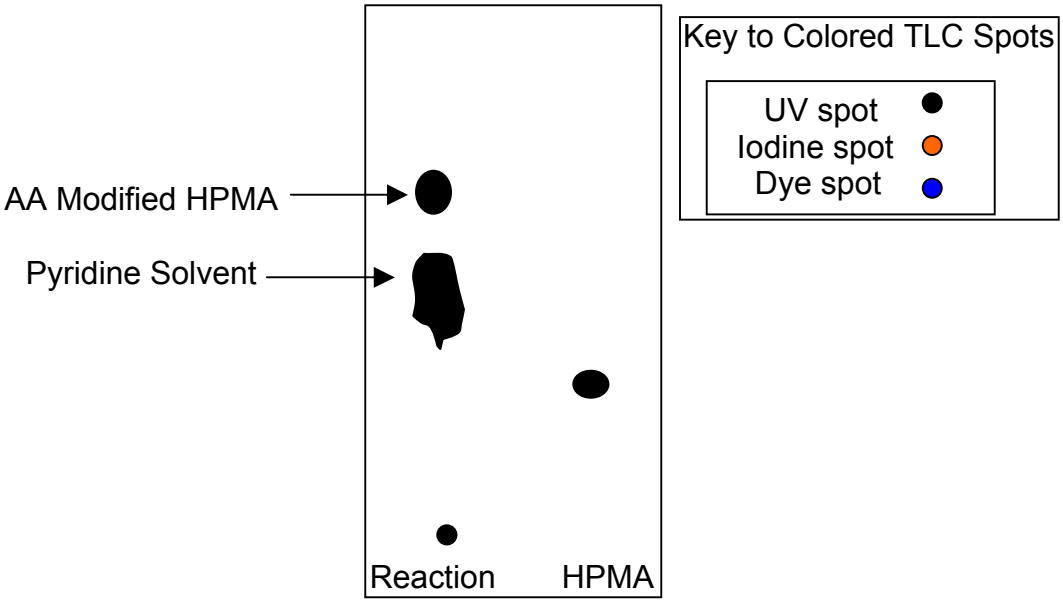

Figure 2.13. Schematic of the TLC Representing AA Modified HPMA Compared to HPMA Reactant; Mobile Phase was 50/50 Ethyl Acetate/Petroleum Ether

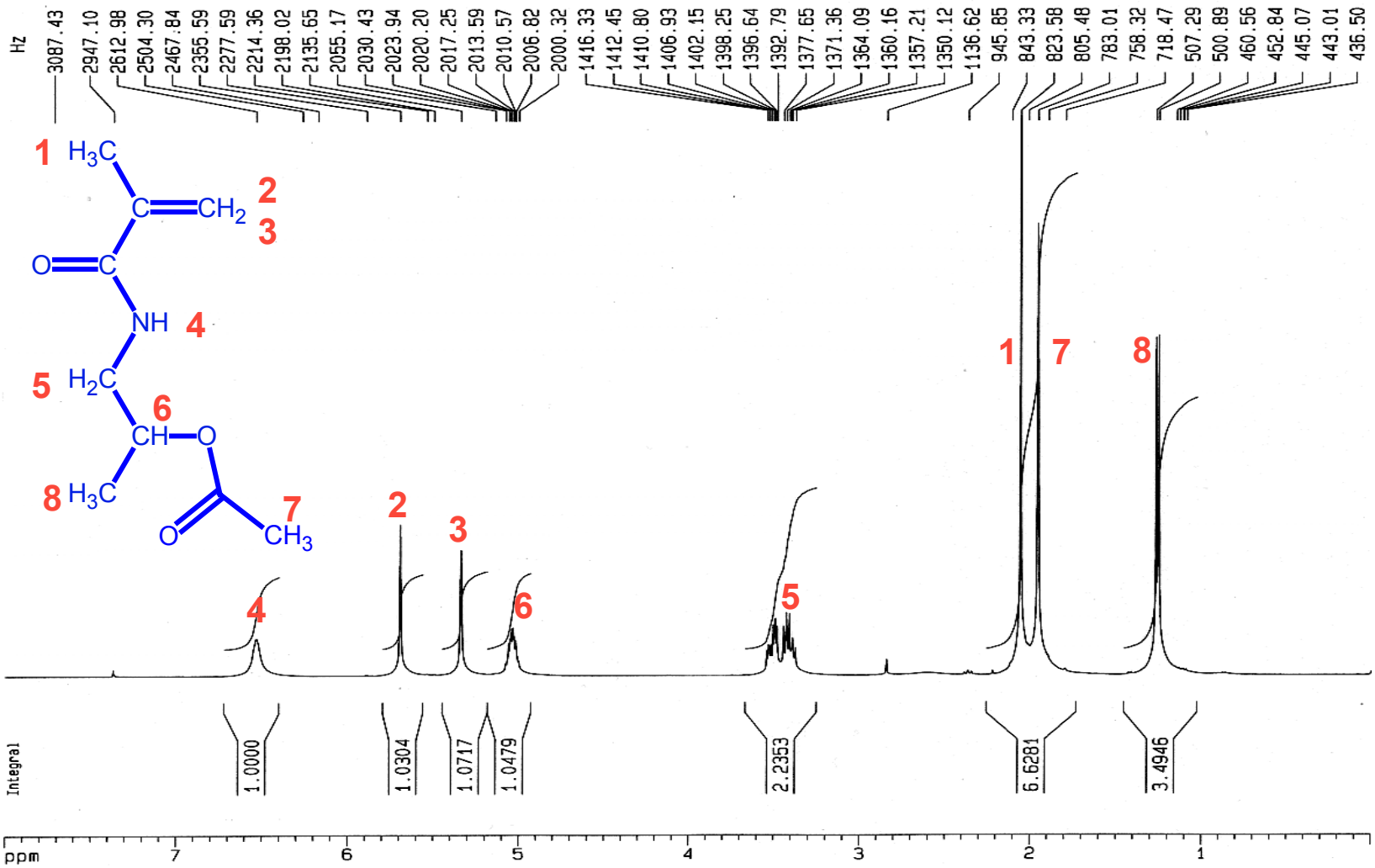

Figure 2.14. H^1NMR of AA Modified HPMA and the Chemical Structure of the Product

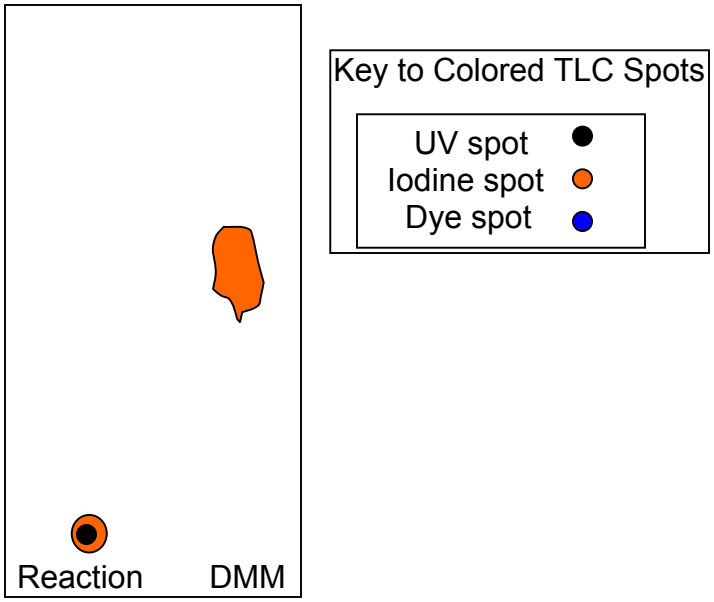

Figure 2.15. Schematic of TLC Plate of Ionization of DMM with LDA; Mobile Phase was 50/50 Ethyl Acetate/Petroleum Ether

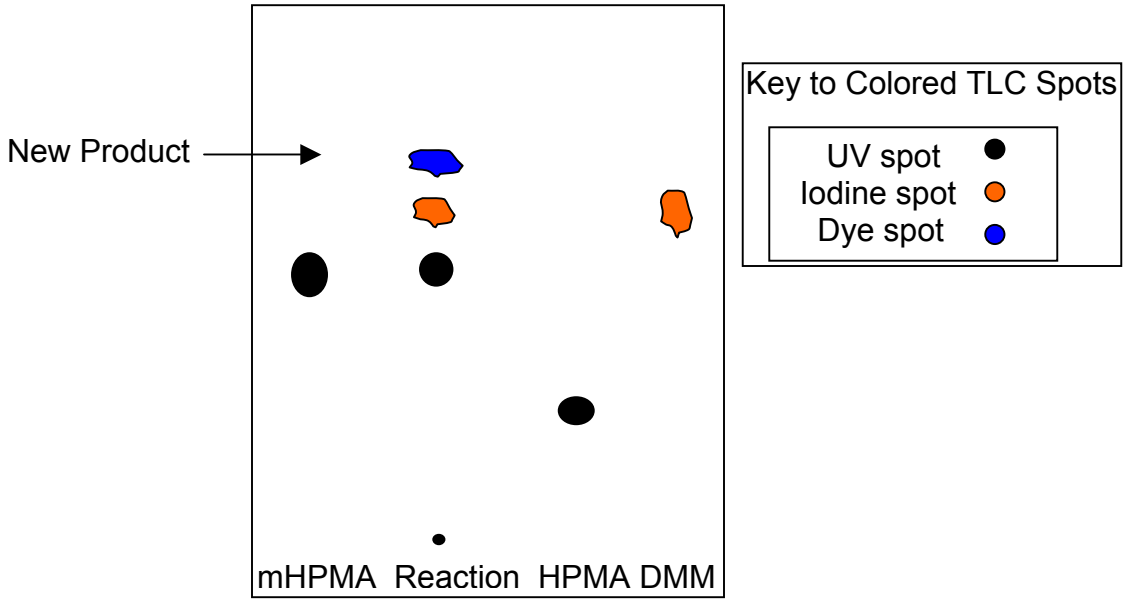

Figure 2.16. Schematic of TLC Plate of Reaction of Ionized DMM with mHPMA in THF Compared to Reactants; Mobile Phase was 50/50 Ethyl Acetate /Petroleum Ether

conversion of mHPMA to HPMA was prevented due to low reaction temperature. This reaction was left over the weekend (about 48 more hours) and all reactants were still present indicating reaction progression is extremely slow. There may still be competition of the enolate ion formation from amide delocalization of the amine nitrogen present on mHPMA hindering reaction progression. A couple of new synthesis approaches were suggested involving either protecting the amine hydrogen of mHPMA with trimethylsilyl chloride (TMS Cl) or using something other than HPMA that can be modified with side chains to obtain peptide spacers attached to drug and targeting moieties. The latter approach was chosen.

Two chemicals were used, benzyl methacrylate (BMA) and methacrylonitrile (MACN), to replace HPMA in the Michael addition reaction. In both of these cases it was thought that 1-amino-2-propanol could be reacted with the new chemicals to form HPMA after adding them to the orthoester. In this way, it would be a kind of two-step approach of adding HPMA to the orthoester and avoiding the problem of amide delocalization hindering enolate ion formation. Two reactions were carried out involving both new chemicals and reacting them with DMM and NatBuO at room temperature in a dry ethanol solvent system. Both reactions appeared to have given a new product indicated by a TLC spot slightly above the DMM reactant spot; however, separation of products was extremely difficult using column chromatography. At this point many months had been spent simply trying to synthesize and purify one monomer successfully. No work had been done yet on polymerization or characterization of high molecular weight products or on formulation potential. It was decided that this project could

take much longer and no definite product may result. In addition, the first objective of the project had been fulfilled in that I learned some lab synthesis and analysis procedures. I did not want my entire PhD project to be only chemical synthesis, purification and analysis; therefore, this project was discontinued.

Summary, Conclusions, and Future Direction

Although many experiments over the course of this project seemed to produce insufficient product yield or very difficult to separate products, byproducts and reactants, much useful knowledge was gained as to potential future synthesis routes. This area of polymeric drug conjugates is relatively new and has great potential. If a polymeric drug can be made with targeting moieties to specifically interact with receptors on the cell surface, not only is it taken up much more quickly, it avoids other non-target cells that do not possess the specific receptor thereby decreasing side effects and increasing drug efficacy. In addition, since polymeric drugs use the prodrug approach, typically undergo a different mechanism of uptake than small molecular weight drugs, and are designed to release the active drug only within the target cells, they have the potential to safely and effectively treat diseases where toxicity and multi-drug resistance (MDR) are major obstacles.

Kopecek and Duncan were forerunners to HPMA polymeric drug conjugate anti-cancer therapy. They designed HPMA monomers with enzymatically degradable oligopeptide side chains attached to targeting moieties and drugs to specifically treat liver cancer. One potential problem with HPMA

polymers is accumulation toxicity due to their non-biodegradable nature. However, if polyesters capable of controlled degradation are combined with HPMA monomers attached to drugs and targeting moieties, a novel therapy with great potential results. Many experiments were performed to attempt to achieve this type of polymeric drug as summarized in table 2.1.

A large portion of the problems encountered dealt with low reaction conversion. This means that a product was formed, but not all reactants were consumed such that separation and purification would be quite difficult just to analyze the product, which may not even be the desired product; and the yield may be extremely poor. In addition, HPMA monomer seems to be quite stable even under basic conditions due to resonance stabilization from amide delocalization. This prevented the Michael addition of HPMA to the ionized orthoester. Acetic anhydride modification of HPMA was successful, but still did not seem to prevent amide delocalization upon addition of base. There were two potential solutions to this problem. Protection of the amine hydrogen of HPMA with TMS Cl was not tried and could potentially solve this problem. Replacing HPMA with different chemicals in a two-step HPMA addition approach seemed to give promising results except byproducts resulted making separation and purification extremely difficult. This project has excellent potential in the area of polymeric drugs if better synthesis and purification strategies can be developed. To ensure a balance between chemical synthesis and other areas of pharmaceutics and obtain proper training for my future in industry, it was decided to discontinue this project.

Table 2.1. Summary of Synthesis Routes, Problems Encountered, and Solutions Implemented

Reactants	Conditions	Problems	Solutions
HPMA + TMOF	BuLi, -78°C, THF, N_2 Purge	HPMA amide delocalization in competition with enolate ion formation	Protect one or both accessible H's
HPMA + TMOA	BuLi or NatBuO; -78°C or Room temp.; THF, N_2 Purge		
HPMA + DMM	BuLi or NatBuO; -78°C, 0°C or Room temp.; ether, N_2 Purge		
HPMA + AA	Room temp., pyridine; LLE to remove pyridine and column chromatography for purification	None	Continue
mHPMA + DMM	BuLi or NatBuO; Room temp.; ether, N_2 Purge	Conversion of mHPMA to HPMA Little to no reaction conversion	Try lower temperature
mHPMA + DMM	BuLi or NatBuO; -78°C; pyridine, N_2 Purge	Little to no reaction conversion	Check Ionization of DMM with Stronger Base
DMM	LDA; Room temp.; pyridine, N_2 Purge	None (Ionization occurred)	Continue
mHPMA + DMM	LDA; -78°C up to 50°C; pyridine, N_2 Purge	Extremely slow reaction conversion	Replace HPMA with other chemicals
BMA + DMM	NatBuO; Room temp.; dry ethanol	Very difficult to separate and purify	Change projects
MACN + DMM	NatBuO; Room temp.; dry ethanol		

PART II: AUTOMATION IN PREFORMULATION DEVELOPMENT

CHAPTER 3

INTRODUCTION: BACKGROUND AND SIGNIFICANCE

Automation and High-Throughput Screening

The concept of automation, making a process or data acquisition for a process automatic, has been around for decades. In practice, many different fields have utilized automated strategies to make processes faster and more efficient. In the late 1940's and early 1950's, agriculturists developed automatic recording apparati to record onion bulb development [38], ceramic scientists invented automatic devices for testing refractories [39], and early recording equipment was devised to obtain IR spectra from spectrophotometers [40]. Around 1955, the term "high-throughput" was beginning to be used to describe fast, highly efficient processing of numerous items, especially in the field of microbiology involving cell counting and plate assays [41]. Throughout the 1960's and 1970's, high-throughput methods were used for manufacturing processes such as grinding [42] and microfabrication [43], and in computer data simulations. It was not until the late 1970's that high-throughput became an important technique in the chemical and pharmaceutical industries in HPLC method development [44].

In the last two decades, high-throughput screening (HTS) and automated method development have gained much attention with over 7,000 articles published on these topics since 1980. In the pharmaceutical industry, most

recent publications on these topics have only focused on the drug discovery process [45-50]. However, since time restrictions and product deadlines can result in potential delays with a cost of as much as $1 million/day of revenue reduction in the first year [51], more effort should be exerted on other areas of pharmaceutical research and development. The need for automated, highly efficient steps in every part of a drug development program has become evident. High-throughput drug screening and selection assays have already proven invaluable to many pharmaceutical companies by allowing them to rapidly and efficiently scan numerous compounds from tens of thousands of plants, microorganisms and insects in an effort to find an optimum drug candidate or "lead" compound for a specific application [52]. The drug discovery area demands coordinated efforts from many different fields of study including pharmacology, chemistry, biology, biochemistry, among others. One author suggests that the future of HTS will no longer be random searching for compounds, but computer defined drug design for a specific biological target [53]. Much of the knowledge gained from this well-researched area of drug discovery could be transferred to other areas of pharmaceutical research and development, such as preformulation development.

Drug discovery is only the first step to developing a pharmaceutical product. Many tests for physicochemical parameters on the newly found compound as well as testing during preformulation to formulation development must be done in order to obtain a final marketable product. Several automated, high-throughput methods to aid in the efficiency of this process have been

developed over recent years. Most have been designed for greater than 10 compounds per instrument per day (high-throughput), with low drug usage per experiment. Ideally, they would also take into account minimum sample preparation, data measurements and calculations, and a fast elimination and reporting approach providing high quality products [51].

Automated HTS HPLC methods are typically and routinely developed, usually during the drug discovery process so that a compound can be detected. There are numerous examples of HPLC methods developed for each drug that has gone through drug discovery as a “lead” compound [44, 54-56]. Other methods for pharmaceutical profiling have been developed and implemented by various companies and academia. One HTS method that has been used for several years is the automated dissolution tests through either a flow cell or automated dissolution workstation. The workstation is capable of running up to 8 samples using 4 different media with an option to utilize on-line UV analysis. This allows analysis of 8 samples in a 24 hour period compared to 6 samples per week according to the old development approach of Barr laboratories, Inc. [57].

A third important parameter of interest early in the developmental stages of a pharmaceutical product is solubility. Since many drugs are intended to be formulated into orally administered dosage forms, solubility is a key property in determining where absorption might occur in the gastrointestinal tract. Several automated solubility and pH-solubility tests have been developed both for kinetic and thermodynamic equilibrium solubility testing. Thermodynamic methods have typically been very time consuming, as they require solid compound to be added

to aqueous medium and equilibrated up to 72 hours before measuring solution concentration. Although these methods overcome crystal lattice forces, they are not as amenable to the drug discovery process as kinetic methods. Kinetic methods employ DMSO dissolved drug directly from combinatorial chemists with dilution into aqueous media. These methods give a larger solubility value than actual due to the presence of DMSO which is excellent at solubilizing many compounds [51]. Each HTS solubility method will be discussed below.

An automatic titrating instrument called “pSol” can automatically provide an FDA approved thermodynamic pH-solubility profile consuming only 100 μg of compound and analyzing up to 8 compounds per day. A second thermodynamic HTS method, capable of analyzing 59 samples per day, employs 1 mg of compound dissolved in small volumes of pH-adjusted, buffered aqueous media. The samples are placed in an HPLC autosampler block, stirred for 24 hours and analyzed via HPLC automatically [51]. A quick, high-throughput kinetic approach involves utilizing 96 well plates or other low volume containers, adding DMSO dissolved drugs to buffered aqueous solutions, and measuring concentration with a UV plate reader [58]. Two other kinetic methods measure solution turbidity of a drug precipitating from solution. One method involves stepwise addition and light scattering UV analysis of a DMSO dissolved drug to aqueous buffer until precipitation occurs [59, 60]. The second approach utilizes a robot and 96 well plates to serially dilute a DMSO drug solution, and nephelometry and forward light scattering is employed to detect the appearance of turbidity [61, 62]. While

the UV turbidity method is only capable of about 45 samples per day, nephelometry can analyze up to 300 per day.

Several other types of automated, high-throughput methods have been developed to test important parameters such as permeability, lipophilicity, and pK_a. Permeability is a critical property for drug absorption as is pK_a and lipophilicity. Generally, a drug has difficulty being absorbed into the bloodstream if it is in its ionized form or cannot permeate through or be carried through the lipid bilayers of the cells. The lipophilicity of a compound can have a major impact on a drug's solubility and permeability as well as physiological distribution, binding, and metabolism [51].

One of quickest HTS permeability tests capable of analyzing 300 compounds per day is the artificial membrane permeability assay. It uses an artificial membrane on a polymer filter sandwiched between two aqueous chambers, resembling a Caco-2 cell widely used in *in vitro* permeability estimations. The drug solution is placed in one chamber and a blank aqueous buffer in the other; after an allotted time of around 15 hours, the receiving chamber is quantitated for sample concentration. High-throughput is achieved using 96 well plates filled with blank buffer and filter plates containing the drug solution. Rapid concentration is measured on a UV plate reader after the allotted equilibration time [63].

Both reversed phase HPLC and micellar electrokinetic chromatography provide fast, efficient analysis for lipophilicity resulting in 120 compounds per day throughput. The methods allow indirect determination of the octanol water

partition coefficient by measuring retention either in a lipophilic HPLC column [64, 65] or a capillary electrophoresis unit [66].

Spectral gradient analysis is perhaps the fastest high-throughput method for obtaining the pK_a of a compound capable of analyzing upwards of 240 samples per day. This method uses a changing pH gradient obtained by constantly varying acid to base ratios to measure the UV absorption change of a compound at the different pH values. A commercial instrument for this type of analysis has been developed to deliver the compounds in 96 well plates as DMSO solutions directly from the drug discovery group to allow high throughput [67].

With analytical testing equipment becoming more sophisticated and specialized, more automated and high-throughput methods continue to be developed. However, the focus still remains on the drug discovery stage of development. Many of these automated methods can and should be employed elsewhere in product development. Additionally, many of the concepts involved in these HTS methods can easily be transferred to other areas of pharmaceutical research and development such as preformulation to formulation development. This will allow for more application possibilities, optimum products for specific treatments and an overall faster, more efficient development program.

Preformulation Development and Salt Selection

Preformulation is a relatively new concept that began in the early 1960's. It has become recognized as one of the more important phases of product

development and is to some extent a prerequisite for investigative new drug (IND) applications for drug patentability [68]. One author has defined preformulation development as, “The application of biopharmaceutical principles to the physicochemical parameters of a drug with the goal of designing an optimum delivery system” [69]. It is a testing phase after drug discovery and before formulation work begins; an initial learning phase about a drug so that a stable, safe and efficacious product can be brought to market. To design an optimum delivery system really depends on a number of factors including type of dosage form desired, route of administration, target consumer, indication, and properties of the drug itself. In general, the ideal or optimum delivery system whether it be a free acid, base or salt, should be chemically stable, non-hygroscopic, and be easy to process into the desired dosage form [69]. Since the preformulation stage immediately follows drug discovery, only a minute amount of compound is typically available and a careful step by step testing regimen must be designed to conserve the most usable quantities of drug in obtaining only the data that is immediately relevant. According to one author, the preformulation scientist is responsible for providing information on drug solubility; what salt forms are to be used; the presence of solvates, hydrates or polymorphs; hygroscopicity; pK_a; pH-solubility profile; micromeritics such as particle size distribution and crystal habit; compatibility with other compounds; and what dissolution parameters to use [68]. It should be noted that the small drug quantity available poses a tremendous challenge that must be worked around in order to obtain all the required data for the formulation scientists. That

is why a carefully planned and executed strategy of experimentation is a necessity, and it is quite useful to undertake a stepwise elimination and scale-up as experiments progress. In fact, many pharmaceutical preformulation programs are designed to systematically analyze and eliminate drug or drug salt candidates in a multi-step process. Two of the most important parameters, which may be provided at least as a rough estimate by the drug discovery group, are the intrinsic solubility and dissociation constant or pK_a [70]. These values will give an idea as to feasibility and need for making a salt form of the drug. Again the intended application plays a major role in determining if a salt form should be attempted, but in general there are several purposes that salts are typically made as outlined in table 3.1 [71]. If the intended route of administration is a tablet or capsule and the drug has a low solubility of less than 1 mg/mL, a more soluble salt may be necessary to prevent absorption problems [72]. However, low solubility could be an advantage for a suspension type formulation or to prolong the release or dissolution of drug from a dosage form.

After deciding whether or not a salt form of the drug would be beneficial, the next step is to find a suitable counterion. Table 3.2 shows the counterions typically involved in making pharmaceutical salts and the frequency with which each are used. Since 75% of drugs are basic with only 20% acidic and 5% ionic [70], a major portion of this project deals only with basic drugs, and the discussion to follow will be for basic drugs and their salts.

The hydrochloride salt, which is frequently used instead of free base drug in many pharmaceutical products, offers several advantages over other salt

Table 3.1. General Reasons a Drug May be Formulated into a Salt Form

Purpose of Choosing a Salt
Enhance Aqueous Solubility
Achieve Appropriate Stability
Modify PK Properties
Optimize Manufacturing Properties
Decrease Aqueous Solubility for Suspensions, Taste-Masking or Sustained Release Products

Table 3.2. Counterions Typically Used to Synthesize Pharmaceutical Salts and the Frequency With Which They are Used

Basic Drugs		Acidic Drugs	
Counterion	**% Frequency**	**Counterion**	**% Frequency**
Hydrochloride	43.0	Sodium	62.0
Alternatives	30.2	Potassium	10.8
Sulfate	7.5	Calcium	10.5
Tartrate	3.5	Alternatives	8.8
Phosphate	3.2	Zinc	3.0
Maleate & Citrate	3.0	Lithium	1.6
Mesylate	2.0	Magnesium	1.3
Acetate	1.3	Diethanolamine	1.0
Tosylate, Napsylate, Besylate, Salicylate, Lactate, Benzoate, and Succinate	<1.0	Aluminum & Choline	<1.0

forms. It has a low counterion pK_a allowing it to form a salt with even the weakest bases. Once a salt is formed, recrystallization is usually very straightforward with many different organic solvents. For these reasons it is usually the first choice for basic drugs [73]; however, it may not be the optimum candidate in most cases. Several disadvantages also exist for the hydrochloride salt since it is quite corrosive to manufacturing equipment, dissolution results in a low pH that could damage the lining of the GIT (gastrointestinal tract) in the case of oral dosage forms, and it tends to be more hygroscopic leading to stability problems. It is necessary to evaluate each salt according to the intended application. This means trying many different combinations of counterions and crystallizing solvents in an attempt to find an easily manufactured stable product. This can be very time consuming and costly. Preformulation scientists at Aventis Pharma have developed semi-micro techniques utilizing microtiter plates in order to quickly and efficiently produce salts. These experiments involve manually placing drug solutions into wells, adding a different counterion to each column of the plate and adding different crystallizing solvents to each row of the plate [71]. Automation of salt formation, scale-up and analysis procedures can be a valuable tool for this early phase of preformulation development. In addition, it will result in time and money savings, and it may lead to additional application opportunities never before imagined.

Once the salts have been made, a selection strategy involving a multi-tiered approach of testing followed by elimination and scale-up is performed. Scientists at Bristol Myers Squibb have developed such an approach. The least

time-consuming experiments that would allow a “go or no go” decision are performed first, followed by more time-consuming or labor-intensive experiments as the salt candidates are sequentially eliminated [74]. Several authors have varying ideas as to the most important parameters to determine and the order in which to test for them. Table 3.3 shows 3 authors’ approach to a structured preformulation drug characterization program. It is difficult if not impossible to design such a structured program that will apply to any and every situation since much of the information gathered will answer specific questions about a certain drug or salt intended for a specific application. Nevertheless, several properties stand out as most important to each program. They are thermal and crystalline properties, hygroscopicity, and solubility. The thermal and crystalline properties include melting point and detection of any polymorphs or solvates and hydrates, also called pseudo-polymorphs. The importance of finding these polymorphs or pseudo-polymorphs early in product development will be discussed in the next section.

Polymorphism

Polymorphism is the ability of a compound to exist as two or more crystalline phases that have different arrangements of molecules in the crystal lattice. It comes from the Greek, “poly” meaning many and “morph” meaning forms. The first appearance of the word was in a dictionary in 1656 referring to the diversity of fashion, and it wasn’t used in the scientific arena until the early 1820’s to describe different crystal structures of the same compound. As the microscope became more sophisticated and gained wider use, this tool played a

Table 3.3. Comparison of 3 Authors' Approach to a Structured Preformulation Development Program

Wells [70]		Bastin [71]		Morris [74]	
Test	**Purpose**	**Test**	**Purpose**	**Test**	**PurposePP**

major role in the study and characterization of polymorphic solids. Scientists learned how to form different polymorphs by using different solvents or seeding with a certain polymorphic form. They also found particular characteristics that were distinctly different among polymorphs of the same compound. These are depicted in table 3.4 [75] and helped enable scientists to begin developing tests and procedures to distinguish among the different polymorphs.

With the emergence of chemical crystallography in the 1870's, the concept of polymorphism was expanded to describe different types. Monotropic describes an irreversible transition from one form to another, and enantiotropic describes a transition from one form to another that is reversible. Upon heating, a transition to the more stable form, which is usually the higher melting one, can occur [76, 77]. In addition, the metastable forms tend to be more soluble and will eventually transition to the stable form, albeit it may take years to occur [78].

Another type of polymorphism that is known to exist is termed pseudopolymorphism by some scientists. This type involves molecules of solvent or water, in the case of hydrates, present in the crystal lattice. If they are bound tightly, they may be an integral part of the crystal structure, which upon desolvation causes a collapse of the original crystal lattice and formation of new one. This terminology is still debated upon by chemists since some view the presence of water or solvent in the crystal lattice to be a different compound and hence, not a polymorph of the same compound [79]. This phenomenological view of polymorphism changed in the early 1900's as x-ray crystallography become one of the main methods to characterize solids. It wasn't until the

Table 3.4. Characteristic Distinctions Among Polymorphs of the Same Chemical Composition [75]

Polymorph Characteristics
Different Melting Points and Vapor Densities
Distinct Transition Found for Low-Temp. Form (A) to High Temp. Form (B)
Form B is Metastable Below This Transition
Form A Cannot Exist Above This Transition
Below This Transition, Form B Converts to Form A Upon Contact with Form A or Seeding by Mechanical Shock or Scratching
Heat is Absorbed During Transition from Form A to Form B

1960's that polymorphism gained importance in the pharmaceutical industry [80]. Over the past few decades, polymorphism has been recognized as a common occurrence. McCrone suggested in 1965 [80]:

> It is at least this author's opinion that every compound has different polymorphic forms known for a given compound proportional to the time and money spent in research on that compound.

Several other well-known scientists have said [81], "polymorphism is an inherent property of the solid state and that it fails to appear only under special conditions", and [82]:

> [polymorphism] is now believed to be characteristic of all substances, its actual non-occurrence arising from the fact that a polymorphic transition lies above the melting point of the substance or in the area of yet unattainable values of external equilibrium factors or other conditions providing for the transition.

Polymorphism is a critical parameter in the pharmaceutical field. It influences almost every stage of manufacture and storage of drugs. Differences can exist in nearly every physicochemical property of the solid state including molar volume, color, density, solubility, refractive index, heat capacity, conductivity, stability, hygroscopicity, compatibility, dissolution rate, crystal habit, crystal hardness, reactivity, and melting and sublimation. Major concerns have been noted in therapeutic efficacy, toxicity and bioavailability of pharmaceutical polymorphs [70].

Despite these numerous apparent disadvantages, polymorphism can provide a means for additional patentability of more market viable products. One polymorphic form may be more stable, more easily manufactured, and more bioavailable than another previously patented form. If it is not obvious that the first form will lead to the second, a patent may be granted offering significant economic advantages. However, tremendous controversy abounds in the patentability of pharmaceutical polymorphs, and courts decide the outcomes on a case-by-case basis. Generic companies fight to be first to market for a generic form of high profile drug either before or as soon as it comes off patent. In some cases, the innovator company finds a way, such a polymorphism, to keep a major portion of the market share, while trying to prevent a generic firm from manufacturing the drug without infringing on their patent exclusivity. The generic company can file an abbreviated new drug application (ANDA) to the FDA in order to try to facilitate marketing their product, and the innovator company will sue the generic firm for patent infringement. The courts decide whether the generic firm is truly infringing or if the innovators patent is invalid [75]. This sequence of events occurs more and more frequently as additional generic firms pop up and better drugs are discovered to treat emerging diseases.

CHAPTER 4

EXPERIMENTAL METHODS

Drug Selection

From the conception of this second project, several objectives were outlined as important goals to accomplish. First was to utilize some of the newest high-tech equipment recently purchased within the department to perform automated methods for salt selection and preformulation development. Pharmaceutical companies do not necessarily find the optimum salt candidate for a specific application in their preformulation development programs, but instead just the easiest and fastest to form product. By performing these experiments, knowledge about what it takes to develop an automated method for salt selection, the screening and scale-up processes, and the physicochemical testing necessary to make a decision on the final product would be obtained. The initial application was planned to be some sort of prolonged or sustained release product for oral administration to treat a chronic disease. Due to my continued interest in polymers, it was hoped that a study could be implemented on excipient interactions with hydroxypropyl methylcellulose (HPMC) compared to release properties of the dosage form. HPMC is one of the main excipients used in controlled and sustained release oral dosage forms; and therefore, it would be best to choose a drug that did not already have this excipient in the marketed formulation. In order to spark interest with local pharmaceutical companies, the

patent expiration date was also looked at, in case the project found a very interesting active product ingredient (API) with patent potential. One last goal was to study crystal properties of the salts formed and attempt to identify any potential polymorphs, solvates or hydrates through a combination of thermal and x-ray powder diffraction techniques.

Ideally a new drug would be best for project novelty and publication purposes, but this was not available at the time the project began. A current lab mate, Ranajoy Sarkar, found a list on the internet of all currently marketed over-the-counter (OTC) and prescription (RX) drug products with their patent and exclusivity data. API's with patents and exclusivities that had just recently ended or that would end within a few years were initially chosen. In the end, this was the least important criterion for the final drug selections since a new polymorph or a new salt of a previously marketed drug is patentable especially if the application or dosage form is different than the original product. Several websites were referenced to obtain more information on each drug's indication, solubility, dosing regimen, half-life, dosage form, excipients present in the dosage form, and price and availability [83-97]. It was necessary for the API to be marketed in salt form for oral administration. This would mean that the drug is able to form a salt, has already been approved by the FDA for use as an oral API, and possesses some oral bioavailability.

Water solubility was another seemingly important criterion in the initial phases of drug selection. Since one initial objective was to obtain a drug that might be used in a sustained or prolonged release product, a poorly water-

soluble drug seems to be a good choice. However, this need not be the case as some salts of highly soluble free drugs can be nearly insoluble, thereby achieving decreased solubility in salt formation for prolonged or sustained release purposes. Therefore, it was later decided that a better plan of action was to choose API's with a range of solubilities and make this criterion of low priority.

A chronic disease indication with a regimen of several doses per day was necessary. Usually this also meant that HPMC, either as an excipient or coating, was not present in the formulation since HPMC is used in sustained release products that would be taken as a once-a-day medication. In treating a chronic disease, a prolonged action type dosage form, which might only need to be taken once-a-day or less, created by changing the salt form of the API would be beneficial as long as the drug's half-life did not limit the usefulness of such a product. Using these criteria, ten drugs were chosen as good initial candidates for this project as shown in table 4.1. The final criteria used to select one drug to begin method development were price and availability.

The cheapest, most readily available drug was Allopurinol, and it was supplied in free acid form such that no extraction or initial preparation was required before salt formation could begin. The chemical structure of this drug is shown in figure 4.1 [98]. It is a moderately strong acid with a molecular weight of 136.11 Daltons, melting point of 383°C, used for the treatment of gout, and currently marketed as the sodium salt. A few "practice" experiments were performed on this drug to attempt to form salts using different molar ratios of bases in test tubes. It was later decided that this drug was not representative of

Table 4.1. Final Ten Drugs Initially Selected to Begin Automated Salt Selection and Preformulation Development Project

Drug Salt	Indication	Water Soluble?	Dosage Form	Dosing Regimen	Availability & Price	Patent Expiration
Hydrocodone Bitartrate	Pain	Moderate	500-650 mg Tablets	1-2 every 4-6 hours	Fisher #AT018063 1 mg/mL = $25.00	12/2004
Abacavir Sulfate	Anti-HIV		100-300 mg Tablets	1 twice a day	GSK (Samhir Mehta) {Potentially free}	12/2009
Trazodone HCl	Anti-Depressant	Sparingly	50, 100, 150, 300 mg Tablets	150 mg in divided doses	Fisher #ICN19151805 5 g = $46.05	3/1999
Prazosin HCl	Anti-Hypertensive	Slightly	1, 2, 5 mg Capsules	1 every 2-3 times a day	Fisher #ICN15378280 100 mg = $93.70	9/2003
Pergolide Mesylate	Parkinson's		0.5, 0.25, 1 mg Tablets	Once a day	Fisher #ICN19417625 25 mg = $45.25	10/2009
Amiodarone HCl	Anti-Arrhythmic	Slightly	200 mg Tablets	1 every 4-8 times a day	Fisher #ICN15353583 1 g = $76.50	8/2003
Allopurinol Na	Gout	Moderate	100 mg Tablets	1 every 2-3 times a day	Fisher #ICN19015025 5 g = $28.90	5/2003
Midodrine HCl	Orthostatic Hypotension	Soluble	2.5, 5 mg Tablets	2 every 3 times a day	Fisher #ICN15571783 250 mg = $57.25	9/2001

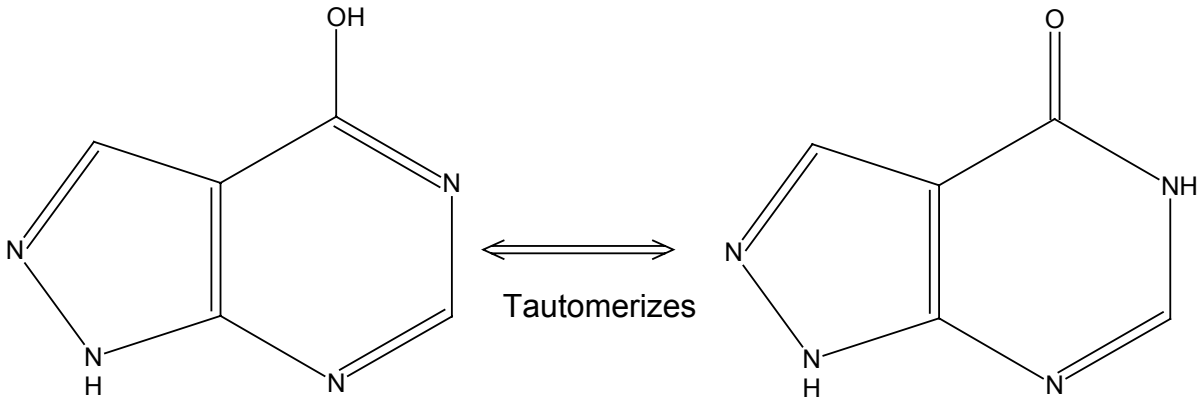

Figure 4.1. Chemical Structure of Allopurinol in Free Acid Form with One of the Possible Tautomers Shown

the majority of pharmaceutical API's since 75% of them are bases; therefore, trazodone was used for automated method development instead. This drug was supplied as the hydrochloride salt and extraction to free base form was required. The chemical structure of this drug is shown in figure 4.2 [98]. It is a weak base with a molecular weight of 408.32 Daltons and a melting point of 237°C. Trazodone is currently marketed as the hydrochloride salt under several brand names. It is known as Desyrel, Trazon, and Trialodine in the U.S. with a former controlled release tablet marketed as Molipaxin CR in the U.K. [85, 99]. It is indicated in the treatment of depression, and to reduce the symptoms of agoraphobia, insomnia, essential tremor, repetitive screaming and some pain syndromes . The mechanism of action is not well understood, but in animals it works to increase the available serotonin levels in the brain by selectively inhibiting re-uptake at the brain synaptosomes [83, 85, 97]. Trazodone is chemically and pharmacologically unrelated to other currently marketed antidepressants. Several studies have shown it to be a superior antidepressant and anti-insomniac in the elderly with few side effects [97]. Due to typically low patient compliance with divided doses especially in the elderly, a sustained or prolonged release product may be beneficial. The significance of this therapy will help prevent depression, which leads to suicide, the eighth leading cause of death in the U.S. alone [100].

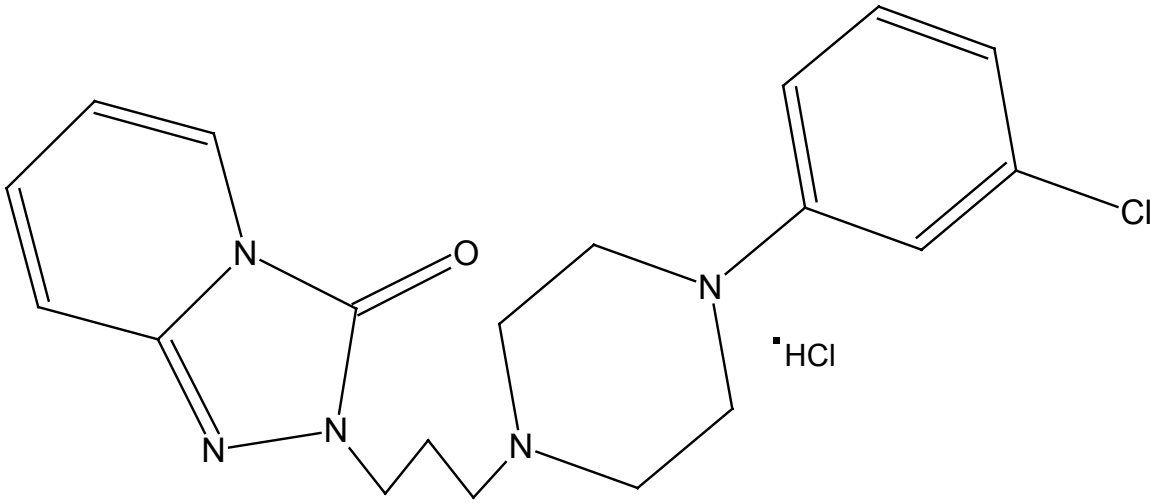

Figure 4.2. Chemical Structure of Trazodone Hydrochloride

Drug Extraction

Since Trazodone was supplied as the hydrochloride salt, extraction to free base was required before salt selection could begin. Dr. Beach offered a general liquid/liquid extraction (LLE) procedure that worked very nicely with this drug from the very beginning. The first step was to dissolve the HCl salt in distilled deionized water, which had to be heated since this salt is only slightly soluble in water, and add it to a separatory funnel. Sodium hydroxide (NaOH) solution was then added dropwise to raise the pH to around 13 so that all of the salt was converted to free base form. This caused a white precipitate of NaCl that had formed from the HCl reacting with NaOH. The free base was insoluble in the brine and formed a yellow oily layer. Chloroform was added to the separatory funnel. The free base was extracted into the chloroform layer and extraction was repeated until no more free base remained in the separatory funnel. This was monitored via thin layer chromatography (TLC) by simply placing a drop of each successive chloroform extraction layer onto a UV indicating TLC plate. The less intense the spot as observed under UV light, the lower the concentration of free base present until no visible spot remained. This is depicted in figure 4.3. It took about 10 extractions with chloroform to remove all of the free base. The collected chloroform layers containing free base were washed with a saturated brine solution to remove any excess NaOH, and then dried over anhydrous sodium sulfate to remove traces of water. The chloroform-dissolved drug was transferred to a round bottom flask and evaporated using a Rotovap. A yellow oily substance remained requiring a “salting-out” process using petroleum ether.

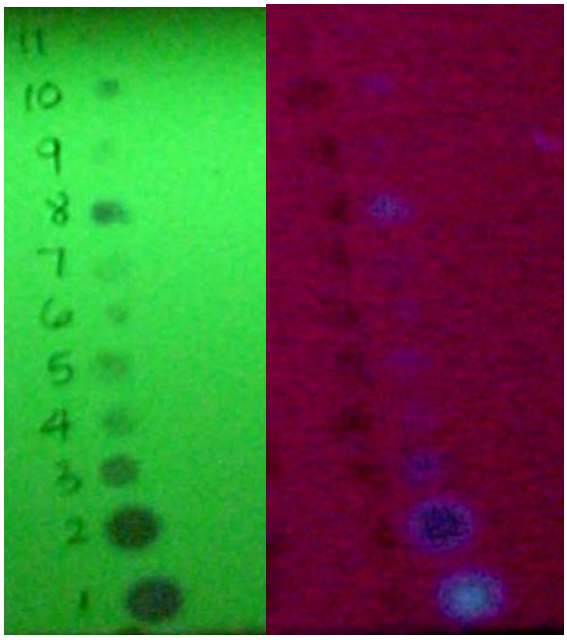

Figure 4.3. TLC Plate Under UV Light Showing the Progression of LLE Procedure of Trazodone Free Base

The petroleum ether was added to the flask under a hood and swirled until an off-white precipitate formed. This precipitate is the Trazodone free base product, and due to some instability at room temperature, it must be stored in a sealed container in the refrigerator until use. Typical yield from this procedure is 90-100%. To verify that free base was formed, differential scanning calorimetry (DSC) was performed against the supplied Trazodone HCl. The DSC thermogram, which shows a large difference in melting points between the free base and HCl salt, is shown in figure 4.4. Since there are no other peaks visible in the thermogram of the free base, this indicates a pure product.

Automated Method Development

One of the main objectives and part of the novelty of this research was to utilize the new, high-tech robotic equipment recently purchased within the department. The Beckman Coulter Biomek 2000 workstation was originally designed for the high-throughput screening of new drug candidates synthesized through combinatorial chemistry. The setup of this system in the college of pharmacy is depicted in figure 4.5. Its capabilities include automated liquid handling, moving labware around the worksurface or onto a stacker carousel, and a plate reader for fluorescence and UV-Vis spectrophotometry. The operations of the Biomek 2000 workstation can be programmed to automatically perform pre-determined experimental steps, allowing precise and efficient operations. The use of such diversified robots for pharmaceutical preformulation development has not been widely reported. Implementation of such a machine

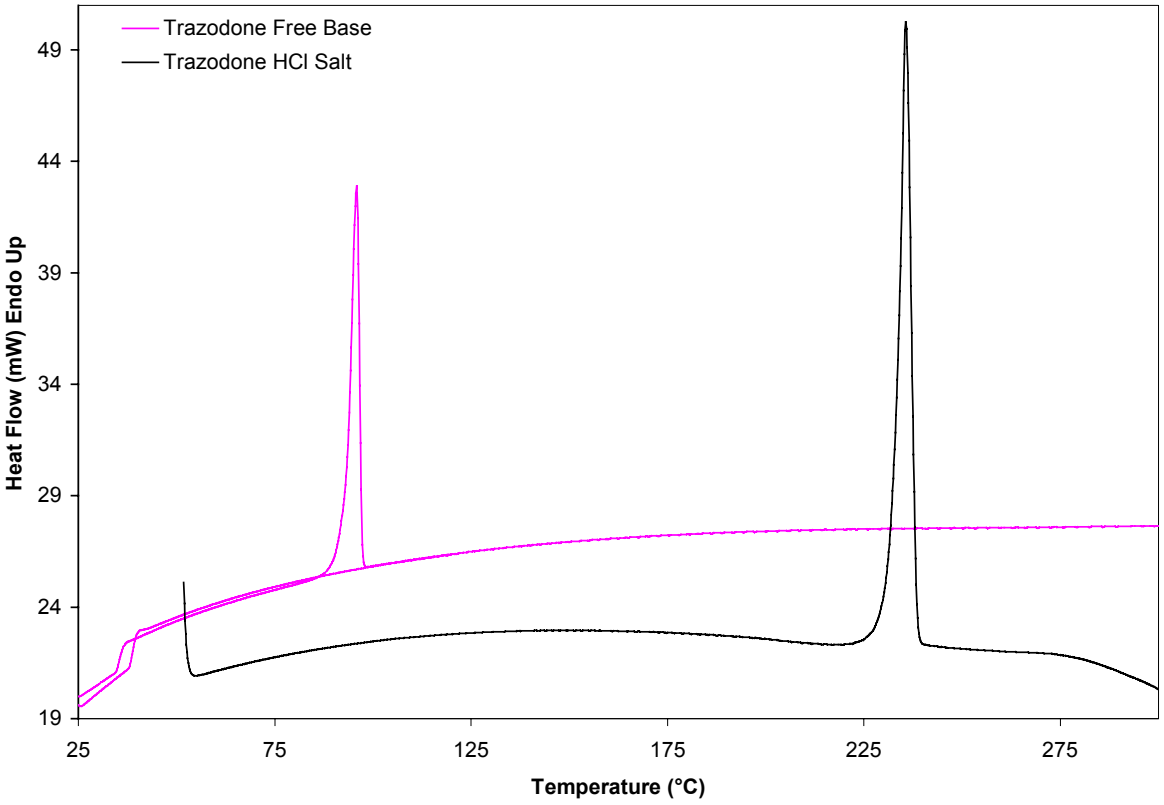

Figure 4.4. DSC Thermogram Verifying Pure Free Base Formation Compared to the Supplied Trazodone HCl Salt

Figure 4.5. The Beckman Coulter Biomek 2000 Automated Liquid Handling System Setup in the College of Pharmacy

may not only enhance experimental efficiency, but will also significantly reduce experimental error, meeting cGMP requirements. The software supplied with the Biomek provides a graphical user interface (GUI) that is intuitive and relatively easy to use. The main challenge for this project was to figure out which 96 well plates and other labware to use that would be automatically recognized by the Biomek so that extra programming would not be required. All supplies were ordered through Beckman Coulter or VWR. The methods of Bastin, *et.al.* [71] involving semi-micro techniques with microtiter plates, changing counterions with column, and changing solvents with row were used as a starting point to develop the automated salt formation method. A list of commonly employed pharmaceutical counterions [71] with their pK_a values [70] was used to determine which anions to choose to form a salt with the weakly basic trazodone. A general rule of thumb, according to Wells, is in order to form a salt, the pK_a of the counterion should be at least 3 units different than the pK_a of the drug [70]. This is not an absolute necessity because it is still quite possible to form a salt from the reaction of a weak acid with a weak base.

A variety of acids were chosen including hydrochloric as a control, sulfuric, nitric, phosphoric, methane sulfonic, ethane sulfonic, p-toluene sulfonic, acetic, propionic, glutamic, aspartic, citric, tartaric, glycolic, decanoic (also called capric), trans-oleic (also called elaidic), stearic, and pamoic acids. Since the Biomek 2000 is only capable of liquid handling tasks, several things were considered leading to the elimination of a few acids. Trazodone in free base form is soluble in several organic solvents including chloroform and acetone. Due to the health

hazard associated with chloroform, acetone was chosen as the solvent to dissolve the free base and as many acids as possible. Nitric acid reacts with acetone leading to a potential explosion hazard and it was therefore eliminated. Glutamic and aspartic acids would not readily dissolve in acetone and the glycolic acid on hand seemed to have an unknown contaminant. Stearic acid is very similar to elaidic acid and a new bottle of elaidic had recently been ordered leading to the elimination of stearic acid. It was decided that the remaining 13 anions were sufficient to begin salt selection, and the next step was to decide what crystallizing solvents to use. Since there are only 8 rows per 96 well plate and a limited supply of free base, 8 solvents were chosen in a range of polarities. These were methanol, ethanol, isopropanol, tetrahydrofuran (THF), ethyl acetate, acetone, chloroform, and propylene glycol (PPG).

After having selected the counterions and solvents to use in the automated method, the next step was to program the robot to perform the tasks and setup a trial run. The tools purchased for the Biomek 2000 are a single channel pipettor, multi-channel pipettor, gripper tool, and multi-channel wash tool. There is also a 4-station stacker carousel capable of storing extra tips, plates, lids, or reservoirs. The worksurface of the Biomek is capable of holding up to 9 plates, tip racks, reservoirs or other labware needed to carry out a specific experiment. In the event that more than 9 items are required to complete an experiment, the stacker carousel together with the gripper tool can be used to clear used labware from and place new labware onto the worksurface. The automated salt formation method, with a setup as shown in figure 4.6, only

Figure 4.6. Automated Trazodone Salt Formation Setup of Labware on the Worksurface of the Biomek 2000 Workstation

required 8 spaces on the worksurface. Each space is labeled according to row A or B and column 1-6 to make it easy to identify where labware and tools are located.

Programming the robot is accomplished through a GUI provided in the computer software. By clicking the mouse first on an action (e.g. pipetting) located in the function palette/labware bar, then on one of the four tools, next on the labware to pipette from and finally on the labware to pipette to, a GUI pops up so that parameters can be entered. The parameters include volume to pipette, what portion of the reservoirs to use to pipette from, what portion of the plate to pipette to and so forth. Other options such as dispense tips into waste container, change tips after use, liquid level sensing, or mixing upon pickup or delivery can also be specified here. Messages and pauses can be incorporated to let the user know when to remove a plate for solvent evaporation, for instance. The text version of the automated salt formation programs is shown in figure 4.7 and will be explained below. Two separate programs had to be created since the wash step should be performed at least 12 hours after the salt formation program to give enough time for salts to form and precipitate, and solvents to evaporate. Figure 4.8 depicts each step of the method as the robot fills plates with drug solution, places solvents in each row of the plates, and fills the columns with different counterions.

A one to one molar ratio of drug to counterion was used. This was necessary to avoid excess reactants present in the final product and prevent an extra separation step in the process. Trazodone was in limited supply, so it was

Bioworks Editor Filename: Salt Formation 96

Initial Configuration
System: Pause Until Cancelled, Message
//First drug is put in every well of the plate
Pipette 100.00 μL from B5 to B2 using MP200—Repeat—P250
Pipette 100.00 μL from B5 to B3 using MP200—Repeat—P250
//Then solvents are put in rows, one row for each solvent
Pipette 200.00 μL from B6 to B2 using P200L—P250
Pipette 200.00 μL from B6 to B2 using P200L—P250
Pipette 200.00 μL from B6 to B2 using P200L—P250
Pipette 200.00 μL from B6 to B2 using P200L—P250
Pipette 200.00 μL from B6 to B2 using P200L—P250
Pipette 200.00 μL from B6 to B2 using P200L—P250
Pipette 200.00 μL from B6 to B2 using P200L—P250
Pipette 200.00 μL from B6 to B2 using P200L—P250
Pipette 200.00 μL from B6 to B3 using P200L—P250
Pipette 200.00 μL from B6 to B3 using P200L—P250
Pipette 200.00 μL from B6 to B3 using P200L—P250
Pipette 200.00 μL from B6 to B3 using P200L—P250
Pipette 200.00 μL from B6 to B3 using P200L—P250
Pipette 200.00 μL from B6 to B3 using P200L—P250
Pipette 200.00 μL from B6 to B3 using P200L—P250
Pipette 200.00 μL from B6 to B3 using P200L—P250
//Next anions are put in columns, one column for each anion
Pipette 15.00 μL from A4 to B2 using MP200—P250
Pipette 15.00 μL from B4 to B2 using MP200—P250
Pipette 18.00 μL from B4 to B3 using MP200—P250
END

Bioworks Editor Filename: Salt Wash 96

Initial Configuration
//Wells will be aspirated and washed with pet. ether to remove any leftover liquids
Purge Wash8 using 1.00 mL Port 1
Aspirate B2 for 5.00 seconds using Wash8
Wash B2 using Wash8, 0.250 mL Port 1
Wash B3 using Wash8, 0.250 mL Port 1
END

Figure 4.7. Text Version of the Automated Salt Formation Programs

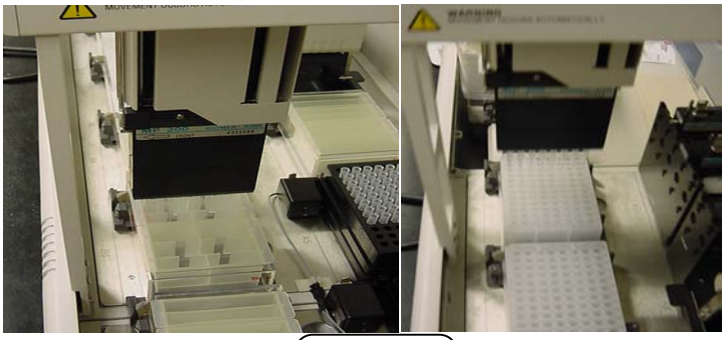

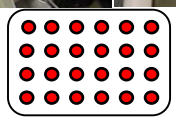

Fill Plates with Drug Solution

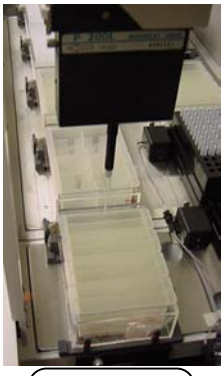

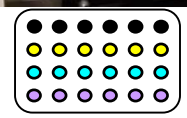

Change Solvents by Row

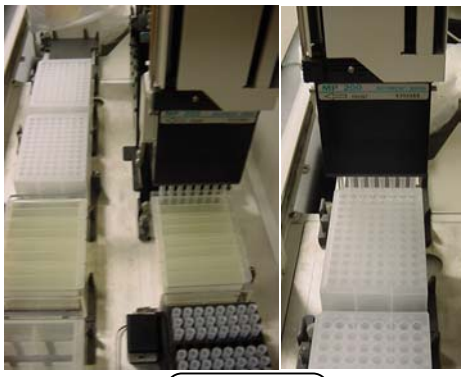

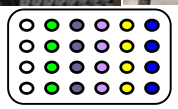

Change Counterions by Column

Figure 4.8. Step-by-Step Depiction of Automated Salt Formation Performed by the Biomek 2000 Robot

decided that 5 mg per well in 104 wells would be enough for an initial salt screening. Seventeen milliliters of acetone was used to dissolve 0.85 g of Trazodone for a concentration of 50 mg/mL.

The first step of the “Salt Formation 96” method is simply a pause with a message to the user to remove all lids from the pipette tip racks before beginning. The user must click the cancel button to continue with the method. This step could also be automated using the gripper tool to pick up the lids and place them in another location, such as the waste container. Steps 2 and 3 of this method utilize the MP200 or multi-channel pipettor tool to pick up drug solution from the 75 mL ½ module reservoir at position B5 on the worksurface and deliver it to the two 96 well plates located at positions B2 and B3. The MP200 tool is only capable of aspirating and delivering up to 200 μL, and the P250 pipette tips can hold up to 250 μL. Before aspiration at the drug reservoir, the robot was programmed to mix for 3 cycles at 150 μL per tip, 10% aspirate height and 25% dispense height above the bottom of the reservoir. It would then aspirate 200 μL, and dispense at 50% height 100 μL to two different columns of the plates (hence repeat) until all 12 columns of the first plate and the first column of the second plate were filled. At 50 mg/mL free base concentration, a delivery of 100 μL deposits 5 mg of free base per well. The robot would not change or discard tips until these steps were completed and every well of the plates contained drug. This conserved the pipette tips.

Each line in green is a comment line designed to help the user more easily view which steps of the method perform certain functions. All of the pipetting

steps under the second comment line deliver 200 μL of a solvent located in 19 mL ¼ module reservoirs divided by length at position B6 to the rows of the two 96 well plates using the P200L single channel pipetting tool fitted with P250 pipette tips. Aspiration occurs at 50% height followed by a tip touch at the source labware (solvent reservoirs). The dispense height was set to 70% so that each tip would not become contaminated with drug solution, which resided in the bottom of the wells. At the end of each row, the robot would discard the used tip and switch to a new one so as to avoid cross contamination among the solvents.

The anion solutions were prepared so that a 1:1 molar ratio would occur at 15 μL of acid dissolved in acetone, except for the last anion. Elaidic acid was not as soluble as the other acids and the solution was slightly more dilute. For this reason 18 μL of this acid solution gave the necessary 1:1 molar ratio. Delivery of the anions, which were located in 19 mL ¼ module reservoirs divided by length at positions A4 and B4, to each column of the plates took place in the final three steps of the method. Before aspirating at a height of 50%, the solutions were mixed for 3 cycles at 150 μL per tip, 10% aspiration height and 50% dispense height. The multi-channel tool MP200 fitted with P250 pipette tips was used “to contain” the 15 or 18 μL of acid solution. This “to contain” option was very important during this step since upon dispensing at 80% height, the robot would then mix at the destination labware (96 well plates) for 3 cycles at 200 μL per tip, 10% aspirate height, and 50% dispense height. If “to deliver” had been chosen instead, a small amount of excess counterion would have been delivered to the every well and would potentially be present in the final product.

Upon completion of the “Salt Formation 96” method, the 96 well plates were taken to a fume hood and left for 12 hours for the reactions to run and solvents to evaporate. After the 12 hour period, the plates were put back onto the worksurface of the Biomek and the “Salt Wash 96” method was performed. The Wash8, an eight channel wash tool, was initially purged with 1.00 mL per channel of buffer 1, which was petroleum ether, from port 1. The washing apparatus purchased for the Biomek is capable of handling 6 different buffers or solvents utilizing 6 different ports. The second step of the method aspirated every well of the 96 well plates at a height of 25% for 5 seconds to remove any liquids present. It then washed each well with petroleum ether for 2 cycles consisting of a 0.250 mL dispense per channel at the slowest rate setting of 1 and height of 25% followed by a 5 second aspiration at a height of 10%. The slow dispense rate was necessary to prevent products from being washed up onto the sides of the wells where they may be aspirated. In every other instance the highest rate setting of 10 was used.

After method completion, the plates were viewed under microscope and polarizing light microscope to determine crystallinity of the salts formed. The methods involved in the salt screening and each of the physicochemical testing procedures will be described in the next section.

Salt Screening and Physicochemical Testing Procedures

Salt Screening

The screening of 104 potential salts through the combination of 13 counterions and 8 crystallizing solvents took place in a three-stage process. The first stage involved deciding which combinations of counterions and solvents gave solid crystalline drug products. The solid drug products from this first stage were scaled up to 25 mg quantities for the second stage and analysed via DSC, PXRD, and hygroscopic stability to determine which conditions gave a new, pure drug salt versus mixtures of products and reactants. In the final stage of screening, the remaining salts were scaled up to gram quantities and tested for particle size, pH-solubility, density, and surface area. These salts were compared to the marketed hydrochloride salt and free base. One salt was chosen as the best for a prolonged action or suspension type dosage form.

The first stage of screening utilized microscopy as the primary means of initially eliminating salt candidates. Microscopic observations were made immediately and 48 hours after the automated salt formation and wash procedures to determine whether precipitation had occurred. A small amount of solid was placed on a microscope slide and observed under a polarizing light microscope to view crystallinity. Any reaction that either did not form a solid after 48 hours or was completely amorphous, as determined from polarized light microscopy, was eliminated. A 25 mg scale-up was done on the remaining salts and physicochemical parameters were determined according to the methods discussed below.

Powder X-ray Diffraction (PXRD)

X-ray powder diffraction patterns were collected using a SCINTAG XDS 2000 powder diffractometer [SCINTAG, Cupertino, CA, USA] with Co $K_{\alpha 1}$ radiation generated at 35 mA and 40 kV as shown in figure 4.9. Typical PXRD patterns for pharmaceutical products are usually collected using a copper (Cu) source rather than cobalt (Co). However, this machine was located in the geology department in which copper radiation tends to interfere with mineral PXRD patterns due to its lower wavelength [101]; therefore, cobalt is used instead. Some samples were ground under petroleum ether and placed on a flat quartz holder. Grinding under solvent in this manner gave more reproducible results, but was not required, as dry grinding in an agate mortar and pestle achieved adequate patterns for the initial screening. Due to the limited quantity of salt available to be tested, a pure quartz holder was required as the sample holder instead of the cheaper, more readily available acrylic holders. X-rays penetrate the sample a finite amount depending on x-ray intensity and absorbing power of the sample. The flat, pure quartz holder allows for minimum interference of the sample holder itself representing a “zero background” plate as well as helping to create a sample of “infinite” thickness [102]. Data was collected from 5-50° 2Θ at 0.02° intervals and 2°/minute using a germanium solid-state detector cooled under liquid nitrogen.

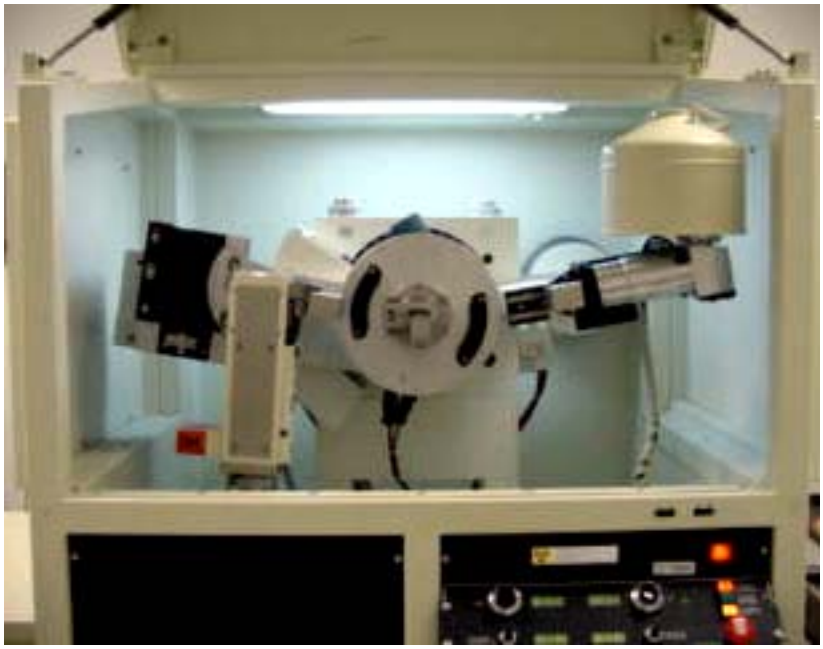

Figure 4.9. The SCINTAG XDS 2000 Powder Diffractometer Used to Collect X-Ray Powder Patterns

Differential Scanning Calorimetry (DSC)

A differential scanning calorimeter, DSC 7, [Perkin Elmer, CT, USA] was used to obtain melting and boiling points, identify any amorphous transitions, and determine any crystalline transitions that may occur in polymorphic substances. This type of thermal analysis is commonly used in the pharmaceutical industry due to its versatility, precision and low sample size requirements. The DSC was calibrated using Indium and Zinc reference standards before each use. Samples were prepared by sealing them in small volume sample pans, followed by piercing the top with a straight pin to allow vapor to escape. They were heated from 25° to 120°C at 10°C/min, cooled to 25°C at 30°C/min, heated again to 300°C at 10°C/min and cooled to 25°C at 30°C/min. Due to some difficulties with the sulfate salts, which will be discussed in the next chapter, the method was modified to only heat from 25° to 300° C at 10° C/min.

Melting Point Apparatus

A Mel-Temp melting point apparatus [Laboratory Devices, Cambridge, MA, USA] fitted with a 0-360°C mercury thermometer was used to help explain any unusual DSC results. This device, along with hot stage microscopy, is commonly employed to help identify polymorphs, solvates and hydrates in an initial salt screening. If dispersed in a drop of silicone oil, a pseudopolymorph may be recognized by the evolution of bubbles upon heating. A true polymorph will melt forming a second oily phase [70].

Samples were lightly packed into 1.5 X 90 mm capillary tubes and observed through the viewing glass as temperature was increased at a rate of

about 10-20°C/min. The magnification of the viewing glass was significantly less than that of a hot stage microscopy device making it difficult to see some of the transitions and to recognize potential polymorphs, solvates and hydrates.

Hygroscopic Analysis

A humidity chamber was constructed out of Plexiglas. A Cahn C-33 microbalance and a humidity/temperature probe was placed within the chamber to perform the hygroscopic analysis. Inlet and outlet pipes were placed at opposite corners of the chamber to allow air or steam circulation. A schematic of this setup is shown in figure 4.10. A BASIC program was written to automatically collect data from the balance and it is represented in figure 4.11. Data was saved in text files at user defined collection intervals. Other authors have used a Cahn digital recording balance fitted with a system capable of monitoring and even maintaining relative humidity conditions. Morris, et. al. constructed a glass, small volume moisture sorption-desorption apparatus utilizing saturated aqueous solutions of 3 different salts, $MgCl_2$, $Mg(NO_3)_2$, and NaCl to obtain relative humidities of 33, 52, and 75%, respectively [74]. The hygroscopic chamber made of Plexiglas contained such a large volume that using salt solutions to effect a humidity change would have been impractical since it would have taken an extremely long period of time to reach equilibrium. Therefore, steam was used to obtain these three humidity conditions with only a 5-10 minute equilibration time. Complete automation of the hygroscopic chamber is possible using computer controlled valves to input steam or dry air, turn on circulation, and monitor and maintain temperature and humidity. A visual BASIC program could be

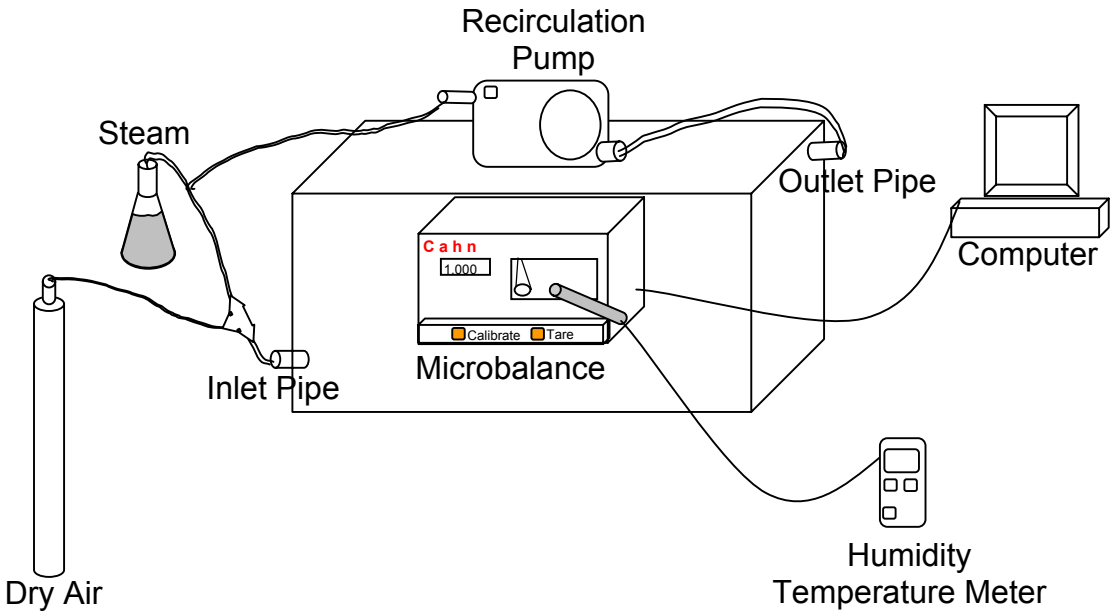

Figure 4.10. Schematic of the Controlled Humidity Chamber and Equipment Used to Perform the Hygroscopic Analysis

QBASIC Program Filename: BALANCE.BAS

```
10   REM C-33 Data Acquisition
15   DEFINT B, I, L, N, S-T
18   N=0: S=0: L=0: I=0: T=0
20   OPEN "COM 1:600, N, 8, 2" FOR RANDOM AS #1
30   CLS : TIMER ON
40   PRINT "PRESS W FOR CURRENT WEIGHT, T TO TARE, OR R TO RUN   DATA
     COLLECTION"
45   INPUT Z$
60   IF Z$ = "T" OR Z$ = "t" GOTO 80 ELSE GOTO 70
70   IF Z$ = "W" OR Z$ = "w" GOTO 100 ELSE GOTO 75
75   IF Z$ = "R" OR Z$ = "r" GOTO 100 ELSE GOTO 40
80   PRINT #1, "T": PRINT "BALANCE IS NOW TARED": GOTO 40
100  PRINT #1, "E"
110  LINE INPUT #1, W$
120  IF RIGHT$(W$, 1) = "U" THEN PRINT "READING IS UNSTABLE": GOTO 40
130  IF RIGHT$(W$, 1) = "O" THEN PRINT "OVER-RANGE": GOTO 40
140  L = LEN(W$)
150  B$ = LEFT$(W$, L-2)
160  B = VAL(B$)
170  N = N+1: PRINT "DATA"; N; "="; B$; "mg": IF Z$ = "W" OR Z$ = "w" GOTO 40
180  PRINT "HOW OFTEN DO YOU WANT DATA TAKEN: (IN SECONDS)";
190  INPUT S:
195  IF S<=0 THEN PRINT "MUST BE GREATER THAN 0 TO START" ELSE GOTO 200
198  GOTO 180
200  PRINT "ENTER FILE TO SAVE DATA TO: C:\";
205  INPUT FILE$
207   START! = TIMER
210  ON TIMER(S) GOSUB COLLECT
220  PRINT "PRESS RETURN KEY TO BEGIN, THEN ANY KEY TO TERMINATE DATA
     COLLECTION"
230  INPUT END$
240  END$ = INKEY$
250  IF END$ <> "" THEN GOTO 270 ELSE GOTO 240
270  CLOSE #1
280  END


COLLECT:
  OPEN FILE$ FOR APPEND AS #2: NOW$ = TIME$
  PRINT#2, NOW$; ELAPSED!; B$
  PRINT #1, "E": LINE INPUT #1, W$
  FINISH! = TIMER: ELAPSED! = FINISH! – START!
  L = LEN(W$): B$ = LEFT$(W$, L-2)
  NOW$ = TIME$: B = VAL(B$)
  N = N+1: PRINT "DATA"; N; "= "; B$; " mg, WITH STABILITY OF "; RIGHT$(W$, 1)
  CLOSE #2
  RETURN
```

Figure 4.11. A Quick BASIC Program Written to Interface Between a PC and a Cahn Microbalance to Allow Automatic Weight Data Collection at User Defined Collection Intervals and Duration

incorporated to automatically record and graph weight and humidity data so that the user could see changes in real time.

Samples were prepared by allowing them to equilibrate within a vacuum-sealed desiccator containing Drierite for at least 48 hours. They were then placed on the sample pan of the balance within the dry (~6% RH) chamber, which had previously been purged with dry air to obtain the low humidity starting condition. A collection interval of 60 seconds and a total duration of 170-200 minutes were used for each hygroscopic analysis session. Humidity and temperature data were manually collected from the humidity meter, but it is capable of computer connection through a RS-232 cable. All the weight gains were corrected by taking into account the empty pan weight gain.

After a second elimination and scale-up to 1-2 gram quantities, physico-chemical data for each of the remaining salts was collected. This third and final stage of screening included density, surface area, particle size and pH-solubility testing. After conducting these experiments, one final salt was chosen as optimum compared to the HCl salt and free base for a suspension or prolonged release dosage form. The experimental methods for each of these tests are described below.

Density Analysis

Bulk and tapped density data was collected in accordance with the USP [98], using a 5 mL glass graduated cylinder and 0.8 – 2.25 g of sample. For tapped density, manual tapping was done at a height of 14 $\pm$ 2 mm until no volume change occurred. In order to obtain an estimation of powder

compressibility and flow, the compressibility index and the Hausner ratio were calculated according to the formulas below [98]:

$$\text{Compressibility Index} = \frac{100\,(V_0 - V_f)}{V_0} \quad (1)$$

$$\text{Hausner Ratio} = \frac{V_0}{V_f} \quad (2)$$

where V_0 is the unsettled apparent volume and V_f is the final tapped volume. These values do not indicate true compressibility of the powders, but give an idea based on volume change of flowability and interparticulate interactions that may have an impact on manufacturability of the final product.

True density was obtained using a helium pycnometer, Accupyc 1330 [Micromeritics, Norcross, GA, USA] and data was collected in triplicate to obtain an average density for each salt. Calibration using a tungsten carbide ball calibration standard was performed before each initial run.

Surface Area Analysis

Surface area was obtained using a Flowsorb II 2300 [Micromeritics, Norcross, GA, USA] fitted with a dual channel mass flow controller model 5841 [Emerson, Hatfield, PA, USA] setup to deliver a gas mixture of 30% krypton and 70% helium. The machine was calibrated with krypton gas before each use. Desorption and adsorption values were recorded in triplicate for each salt. The average of the desorption values was taken to calculate the true surface area of the material since the machine more accurately integrates as gas is desorbed rather than adsorbed.

Particle Size Analysis

An ATM sonic sifter model L3P [ATM Corporation, Milwaukee, WI, USA] equipped with 4 sonic sieves and a fraction collector was used to obtain the particle size distribution in accordance with the USP Method I, a dry sieving method [98]. The size of the openings in the mesh and types of sieves used were 90 μm ATM standard sonic sieve, 63 μm ATM standard sonic sieve, 40 μm ATM precision sonic sieve, and 25 μm ATM precision sonic sieve [ATM Corporation, Milwaukee, WI, USA]. Each sieve along with the top assembly and bottom fines collector assembly were weighed on a balance before a 3 gram sample was added to the top sieve. Each sample underwent a 10 minute sift/pulse at amplitude 5-6 followed by a 5 minute sift. The sieves and top and bottom assemblies were reweighed to obtain weight fraction retained, and the sieve fractions were recovered for further testing. Each piece of the sieve assembly was carefully washed in a sonic bath containing mild detergent, rinsed with distilled water, and dried before the next analysis.

The calculation of various average diameters was performed after calculating cumulative % weight and mid-size diameters according to the following equations:

$$D_{av} = \Sigma wd/\Sigma w \quad (3) \qquad D_{v} = \sqrt[3]{\Sigma wd^3/\Sigma w} \quad (6)$$

$$D_{gc} = \text{antilog } \Sigma w \log d/\Sigma w \quad (4) \qquad D_{vs} = \Sigma wd^3/\Sigma wd^2 \quad (7)$$

$$D_{s} = \sqrt{\Sigma wd^2/\Sigma w} \quad (5) \qquad D_{w} = \Sigma wd^4/\Sigma wd^3 \quad (8)$$

where n is the weight retained in grams and d is the sieve size in μm. The average diameter (D_{av}) was reported.

pH-Solubility Analysis

A modified form of the phase solubility technique was used [103, 104]. A saturated solution of each salt was prepared by allowing excess solid to equilibrate in distilled, deionized water for 24 hours. Some authors suggested, depending on the salt, that 1-2 hours initial equilibration was sufficient. After preliminary experiments using the HCl salt, it was determined that 1-2 hours was not sufficient time for initial equilibration. This will be discussed more in the next chapter.

After 24 hours, the pH was recorded and a 10 μL sample was taken while being filtered through a 0.2 μm filter. HCl or NaOH was added to adjust pH. After two hours of constant agitation via stir bars, the pH was noted and another sample was taken. This process was continued at each pH value ranging from 1-12. The samples were properly diluted and analyzed for concentration using UV spectrophotometry at 246 nm (Biomate 5, Thermospectronic, Rochester, NY, USA) or fluorescence (DyNA Quant 200, Hoefer Pharmacia Biotech, San Francisco, CA, USA) [105].

CHAPTER 5

RESULTS AND DISCUSSION

Salt Screening

Immediately and 48 hours after washing with petroleum ether, microscopic observations were made of the wells of the two 96 well plates to detect the presence of solids. No solids were present in a number of cases leading to preliminary elimination of methane and ethane sulfonic acids. Propylene glycol is a viscous solvent and did not evaporate from any of the wells. Upon washing, it clung to reactants and products and facilitated in removing everything from those wells so that nothing remained. It was therefore, eliminated. All of the alcohols seemed to prevent crystallization or precipitation in a number of cases, and therefore they were eliminated before the first scale-up, leaving only four crystallizing solvents.

A summary table of the preliminary microscopic observations is shown in table 5.1 with double-banded boxes representing the conditions eliminated before the first scale-up. Although no solid was present, citric and tartaric acids were not initially eliminated because they had been dissolved in water. This possibly resulted in incomplete mixing with the acetone-dissolved Trazodone. Citric acid was dissolved in acetone for the scale-up run, but tartaric acid required a mixture of water and acetone for solubilization. Additionally, pamoic acid is insoluble in most organic acids. It was thought to have dissolved in DMF

Table 5.1. Summary Table of the Microscopic Observations of Trazodone Salts with Preliminary Eliminations Depicted as Double Banded Boxes

	Counterions						
Solvents	**HCl Acid**	**Acetic Acid**	**Phosphoric Acid**	**Sulfuric Acid**	**Methane Sulfonic Acid**	**Ethane Sulfonic Acid**	**p-Toluene Sulfonic Acid**
Ethanol	I: Nothing AW: Oil, no solid	I: Nothing AW: Oil, no solid	I: Little Solid AW: Wet MS: Xtal Clusters	I: Little Solid AW: Wet MS: Xtal Clusters	I: Nothing AW: Oil, no solid	I: Little Solid AW: Oil, no solid	I: Little Solid AW: Sticky MS: Xtal Shards
Methanol	I: Nothing AW: Oil, no solid	I: Nothing AW: Brown Solid MS: Fine Xtal Clusters	I: Nothing AW: Wet Solid MS: Xtal Sheets	I: Nothing AW: White Solid MS: Xtal Clusters	I: Nothing AW: Oil, no solid	I: Nothing AW: Oil, no solid	I: Nothing AW: Wet Gel MS: Needle Xtals
Chloroform	I: Oily Film AW: Oil, no solid	I: Nothing AW: Sticky, Orange MS: Xtal Shards	I: Solid AW: Wet, White MS: Xtal Clusters	I: Oily Film AW: Orange Solid MS: Xtal Clusters	I: Oily Film AW: Oil, no solid	I: Nothing AW: Oil, no solid	I: Solid AW: Flaky, White MS: Needle Xtals
Acetone	I: Solid AW: Wet MS: Plate Xtals	I: Nothing AW: Flaky, Brown MS: Xtal Shards	I: Solid AW: Flaky, White MS: Xtal Clusters	I: Solid AW: Flaky, White MS: Xtal Clusters	I: Nothing AW: Oil, no solid	I: Nothing AW: Oil, no solid	I: Solid AW: Sticky, White MS: Needle Xtals
Isopropanol	I: Nothing AW: Sticky, Brown MS: Xtal Clusters	I: Nothing AW: Oil, no solid	I: Solid AW: Flaky, White MS: Xtal Clusters	I: Nothing AW: Flaky, White MS: Xtal Clusters	I: Nothing AW: Oil, no solid	I: Nothing AW: Oil, no solid	I: Solid AW: White MS: Xtal Shards
THF	I: Solid AW: Crumbly, White MS: Xtal Clusters	I: Nothing AW: Sticky, Brown MS: Xtal Clusters	I: Solid AW: Flaky, White MS: Xtal Clusters	I: Oily Film AW: Flaky, White MS: Xtal Clusters	I: Nothing AW: Oil, no solid	I: Nothing AW: Oil, no solid	I: Solid AW: Sticky, White MS: Needle Xtals
Ethyl Acetate	I: Solid AW: Flaky, White MS: Xtal Clusters	I: Nothing AW: Flaky, Orange MS: Xtal Clusters	I: Solid AW: Flaky, White MS: Xtal Clusters	I: Oily Film AW: Flaky, White MS: Xtal Clusters	I: Oily Film AW: Oil, no solid	I: Nothing AW: Oil, no solid	I: Solid AW: Sticky, White MS: Xtal Clusters
Propylene Glycol	I: Little Solid AW: EMPTY	EMPTY	EMPTY	EMPTY	EMPTY	EMPTY	EMPTY

Notes: I is initial observations; AW is observations after washing with petroleum ether; MS is after microscopic observations; Xtal is abbreviation for crystal.
Double-banded boxes indicate conditions eliminated during preliminary run.

Table 5.1. Continued

Solvents	Counterions: Citric Acid	Propionic Acid	Tartaric Acid	n-Decanoic Acid	Pamoic Acid	Elaidic Acid (plate 2)
Ethanol	I: Nothing AW: Oil, no solid	I: Nothing AW: Oil, no solid	I: Nothing AW: Oil, no solid	I: Nothing AW: Oil, no solid	I: Little Solid AW: Yellow MS: Xtal Clusters	I: Solid AW: Flaky, White MS: Needle Xtals
Methanol	I: Nothing AW: Oil, no solid	I: Nothing AW: Gooey, Brown MS: Xtal Shards	I: Nothing AW: Oil, no solid	I: Nothing AW: Gooey, Orange MS: Needle Xtals	EMPTY	I: Solid AW: Sticky, White MS: Needle Xtals
Chloroform	I: Oily Film AW: Oil, no solid	I: Nothing AW: Flaky, Brown MS: Needle Xtals	I: Oily Film AW: Oil, no solid	I: Nothing AW: Flaky, Peach MS: Needle Xtals	I: Nothing AW: Oil, no solid	I: Solid AW: Sticky, White MS: Needle Xtals
Acetone	I: Nothing AW: Oil, no solid	I: Nothing AW: Flaky, Brown MS: Needle Xtals	I: Nothing AW: Oil, no solid	I: Nothing AW: Gooey, Peach MS: Needle Xtals	I: Nothing AW: Yellow Solid MS: Needle Xtals	I: Solid AW: Sticky, Orange MS: Needle Xtals
Isopropanol	I: Nothing AW: Oil, no solid	I: Nothing AW: Oil, no solid	I: Nothing AW: Oil, no solid	I: Nothing AW: Sticky, Peach MS: Needle Xtals	I: Nothing AW: Yellow Solid MS: Xtal Clusters	I: Solid AW: White MS: Needle Xtals
THF	I: Nothing AW: Oil, no solid	I: Nothing AW: Flaky, Peach MS: Needle Xtals	I: Nothing AW: Oil, no solid	I: Nothing AW: Sticky, Peach MS: Needle Xtals	I: Little Solid AW: White MS: Xtal Clusters	I: Solid AW: Flaky, Peach MS: Xtal Clusters
Ethyl Acetate	I: Oily Film AW: Oil, no solid	I: Nothing AW: Sticky, Orange MS: Fine Xtals	I: Oily Film AW: Oil, no solid	I: Nothing AW: Sticky, Orange MS: Needle Xtals	I: Nothing AW: Yellow Solid MS: Xtal Clusters	I: Solid AW: Flaky, White MS: Needle Xtals
Propylene Glycol	EMPTY	EMPTY	EMPTY	I: Little Solid AW: EMPTY	I: Nothing AW: Yellow Solid MS: Xtal Clusters	I: Solid AW: Wet Solid MS: Oil dissolved

Notes: I is initial observations; AW is observations after washing with petroleum ether; MS is after microscopic observations; Xtal is abbreviation for crystal.
Double-banded boxes indicate conditions eliminated during preliminary run

initially, but much settling out occurred. For the scale-up run, THF was used, which seemed to work much better in dissolving pamoic acid.

Polarized light microscopy was performed on the preliminary solids to determine crystallinity or amorphous content and to get an idea of crystal habit. In every case in which a solid was present, most if not all of the substance exhibited the ability to rotate the plane of polarized light creating magnificent color variations. This is indicative of birefringent crystalline materials [75]. There were a few cases in which a small portion of the solid material appeared amorphous with no color seen upon turning the polarized filter. Table 5.2 depicts the polarized light microscopy results for each solid obtained.

A scale-up was carried out on 11 counterions and 4 solvents to obtain 25 mg quantities. Among these, citric and tartaric acids still did not give solid precipitates regardless of the crystallizing solvent used; neither did acetic and propionic acids in acetone, and therefore, they were not involved in the solid-state characterization. Only 34 of the 44 scaled-up solids were further evaluated with the order of physicochemical analysis being PXRD, DSC, hygroscopicity, and melting point apparatus to maximize data collecting efficiency and preserve the most usable solid quantities for subsequent evaluations [73, 106-108]. The results of the physicochemical analyses are discussed below.

Table 5.2. Polarized Light Microscope Results of Solids Obtained from Reacting Counterions with Trazodone Free Base

	Chloroform	Acetone	Isopropanol	THF	Ethyl Acetate
HCl	NA		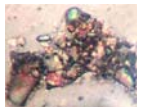		
Acetic			NA		
Phosphoric					
Sulfuric					
Propionic			NA		
p-Toluene Sulfonic					
Capric	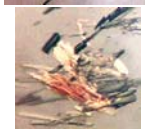		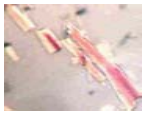		
Pamoic	NA			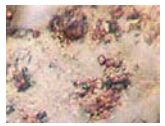	
Elaidic			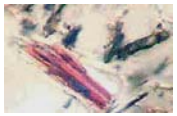	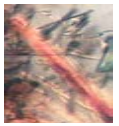	

Physicochemical Results After First Scale-Up

PXRD, DSC and Melting Point Apparatus

It is better to discuss the results from these analyses together as one helps explain the other. Each salt will be explained as a separate section to minimize confusion and provide organization of the results.

Hydrochloride Salt and Free Base

Several batches of hydrochloride salt were ordered from two different vendors. The first batch was the purest according to the DSC thermogram shown in figure 5.1 and the PXRD pattern compared to an already indexed trazodone HCl from the powder diffraction library shown in figure 5.2. This was the material used to compare to the other salts formed. The extraction to free base was verified by DSC and was previously shown in figure 4.4. Success in the automated salt formation method was determined by DSC and PXRD results shown in figures 5.3 and 5.4, respectively. The DSC thermogram for all four HCl salts formed from different crystallizing solvents indicate 12 hours was not quite long enough to complete the reaction from free base to salt form. The peak occurring at around 96°C corresponds to the free base, and it appears that the melting peaks of all HCl salts are depressed about 10°C compared to the bulk material due to the mixture of free base and salt. The powder patterns of all four salts also show characteristic peaks from both free base and hydrochloride salt indicating a mixture of products. For the second scale-up to gram quantities, a reaction time of 48 hours was used instead of 12 to allow complete conversion of reactants to salt products.

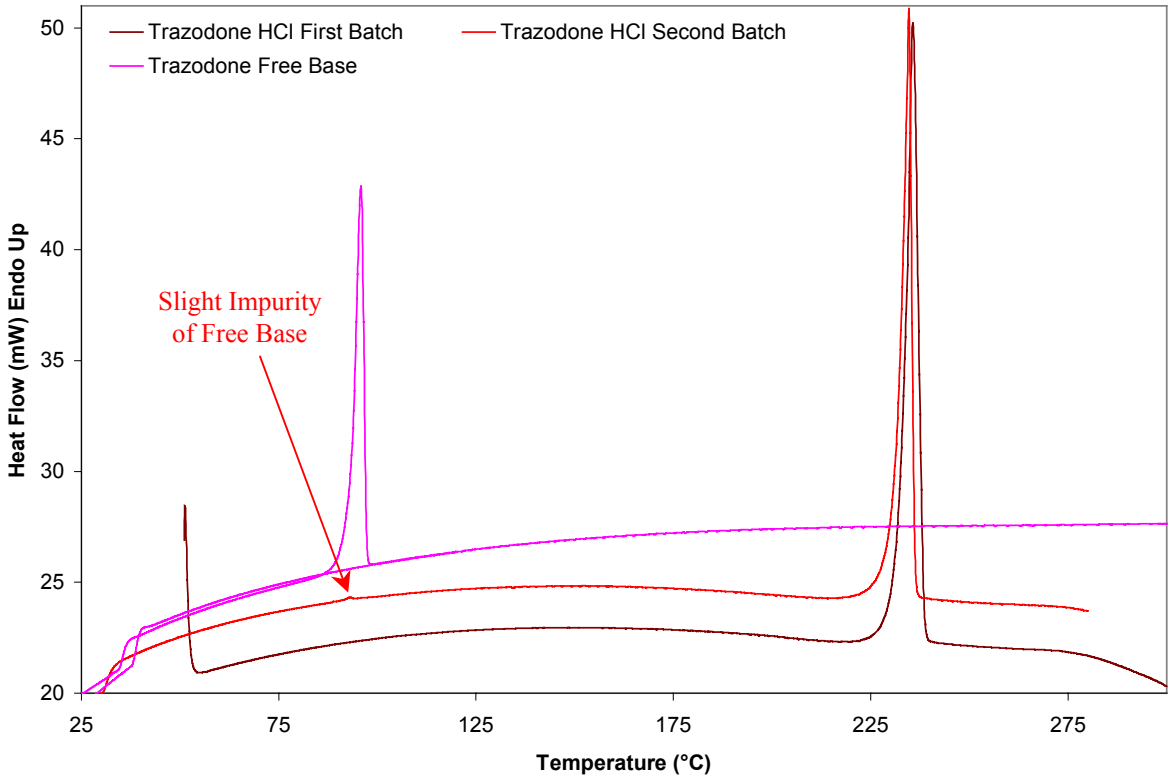

Figure 5.1. DSC Thermogram Comparing Different Batches of HCl Bulk Material from Two Different Vendors

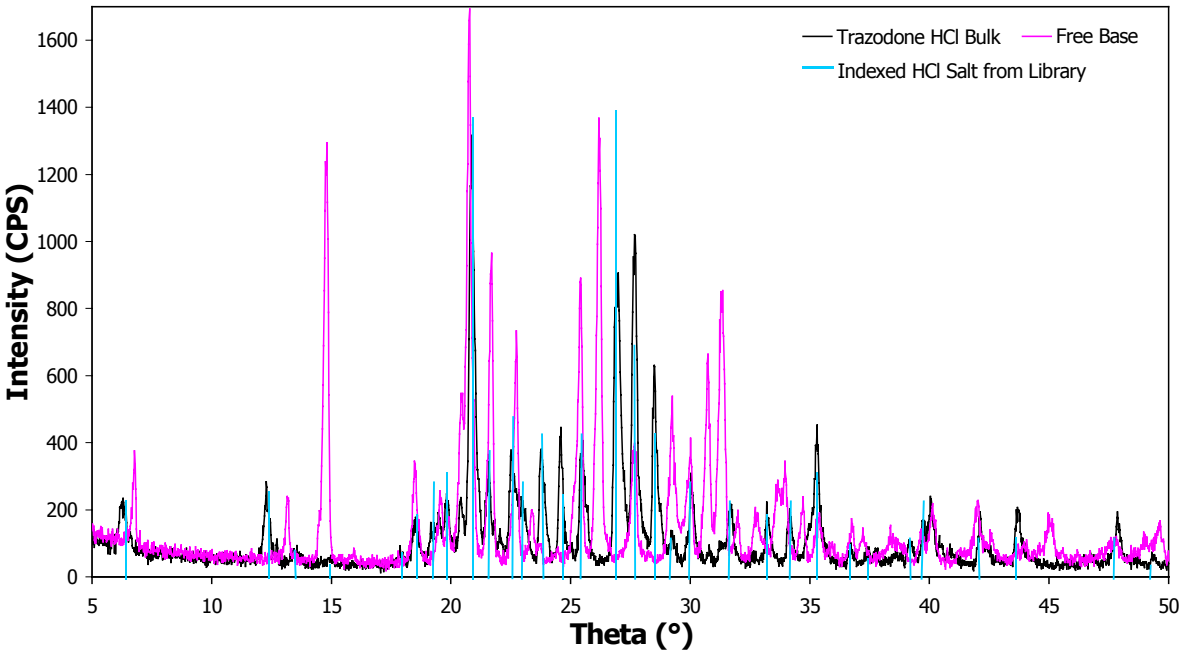

Figure 5.2. PXRD Pattern of the Purest Batch of Trazodone HCl Compared to Free Base and Previously Indexed Salt Found in the Powder Diffraction Library

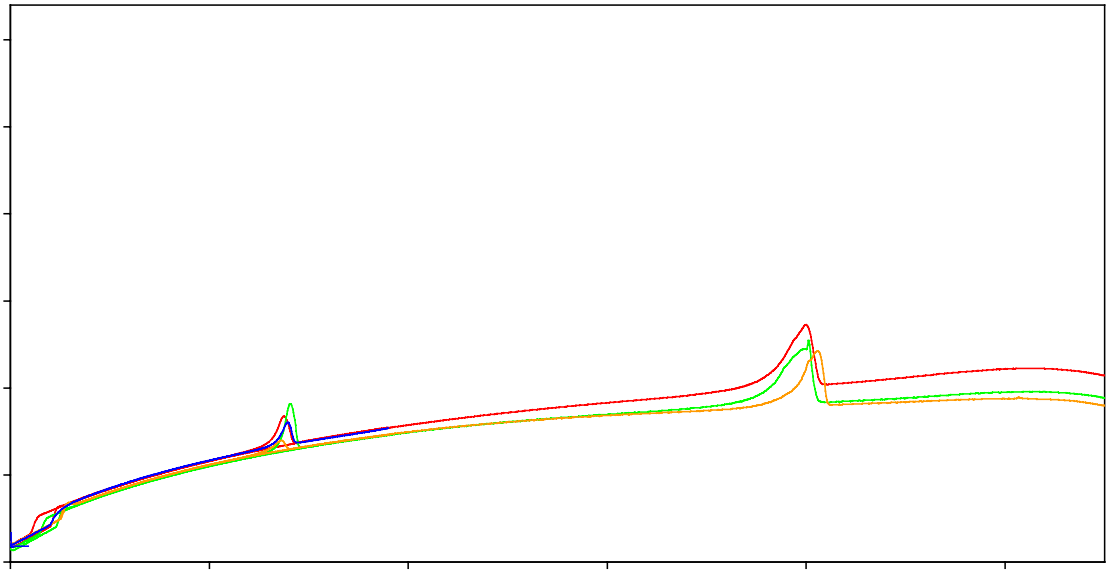

Pamoate Salts

The PXRD pattern of the freshly ordered pamoic acid matches up almost identically to the previously indexed substance found in the powder diffraction library. The DSC thermogram for pamoic acid does not indicate any transitions occurring throughout the temperature range tested, up to 300°C. This agrees with MSDS data from ACROS organics, which shows a melting point greater than 300°C and decomposition beginning around 280°C.

The PXRD patterns of the four pamoate salts, seen in figure 5.5, show a much more amorphous material, depicted by the curved baseline, than either the free base or the pamoic acid reactants. The intensity of the peaks is also much lower and the noise level is quite high making comparisons among the salts very difficult. The peak positions and intensities appear fairly consistent among the pamoate salts. However, some peaks especially in the chloroform crystallized salt are more intense and slightly shifted compared to the other salts. This does not necessarily mean a polymorph or pseudopolymorph is present, but could indicate some preferred orientation of the chloroform-crystallized salt. Preferred orientation occurs in cases in which samples may not be ground to a small enough crystallite size or in which the crystallites are of such a shape that they pack and lay in a certain direction causing more intense reflections at some theta angles than others.

The DSC thermograms in figure 5.6 of all four salts are nearly identical with no peak occurring at 96°C. This suggests that all four salts are probably the same substance and complete conversion of reactants occurred. After heating

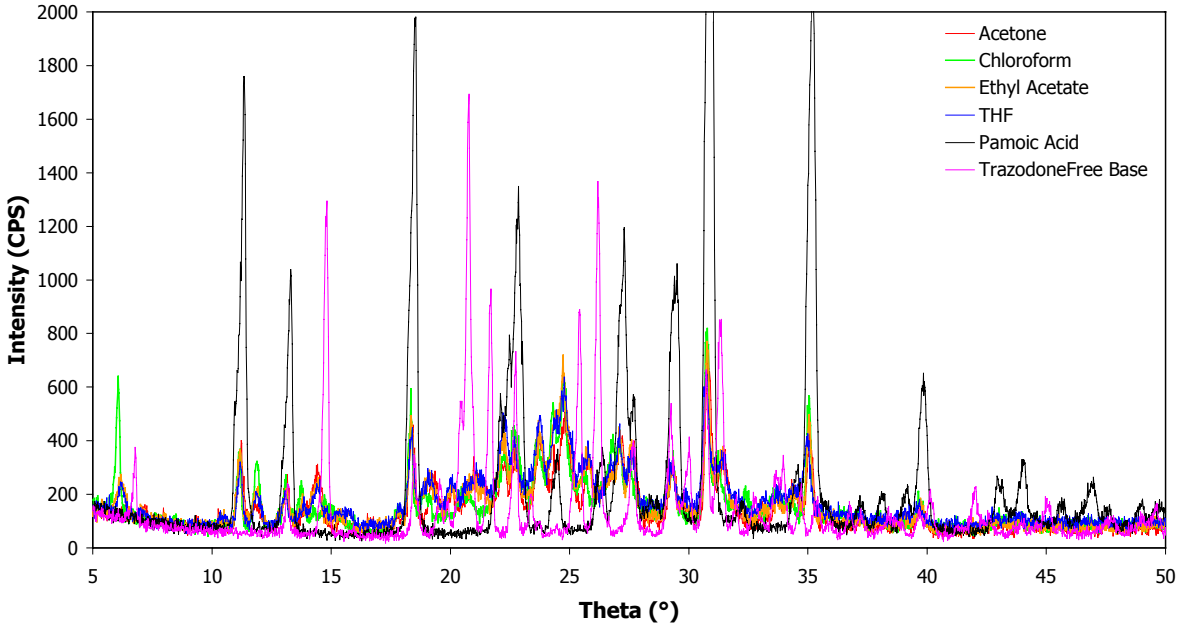

Figure 5.5. PXRD Patterns of Trazodone Pamoate Salts Compared to Reactants

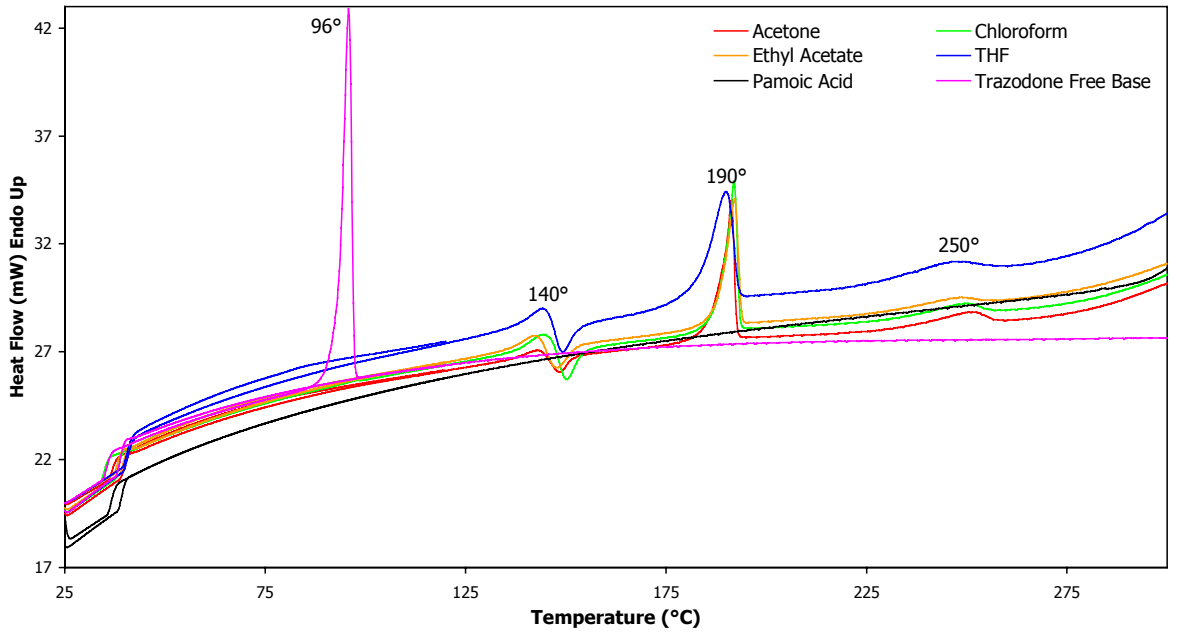

Figure 5.6. DSC Thermograms of Trazodone Pamoate Salts Compared to Reactants

all four salts using the melting point apparatus and viewing the transitions, 190°C is the melting point with boiling occurring at 250°C. The transition at 140°C is more mysterious. At first thought, a potential hydrate may exist since the transition occurs near the boiling point of water and at the same temperature for each salt. However, this material is quite lipophilic and nonhygroscopic. Also, much care was taken to prevent water incorporation into the reactants and products; they were stored in a vacuum-sealed desiccator containing fresh Drierite until analysis. From the melting point apparatus, nothing appeared to take place less than 140°C, but just over this temperature the crystals became more transparent. Since it is obvious from polarized light microscopy and PXRD that some of the material is amorphous, this transition at 140°C could be a glass transition temperature and transformation into a more crystalline product. A third explanation could be that a less stable, lower melting polymorph is present, melts at 140°C, recrystallizes into a more stable, higher melting form which then melts at 190°C. This type of transition has been noted in other pharmaceutical salts [109]; however, a melting and recrystallization should have been noted using the melting point apparatus if this was the case. More experimentation is needed before a final conclusion can be made regarding the pamoate salts. This will be discussed further in later sections of this chapter.

Tosylate Salts

The powder diffraction library did not have p-toluene sulfonic acid indexed so comparison of this reactant to known PXRD data could not be accomplished. However, the DSC thermogram shows a material with melting point of 103°C and

boiling point around 140°C which agrees well with the MSDS from fisher's website [110].

The DSC thermograms and PXRD patterns for the tosylate salts, shown in figure 5.7 and 5.8, respectively, depict a mixture of free base and salt evidenced by the DSC peak at 96°C and the additional free base peaks present in their powder patterns. The chloroform formed salt appears to be the only one that is pure without reactants present. This could be due to complete dissolution of both free base and p-toluene sulfonic acid in chloroform allowing for more complete mixing and consumption of all reactants. A second possibility is that slightly more free base than acid was present in the other three reactions preventing reaction completion. Whichever the case, the chloroform crystallized salt has a unique thermogram. All of the salts melt around 182°C, but the chloroform salt has a slightly higher melting point around 186°C and the acetone formed salt has a slightly lower melting point around 176°C. The acetone salt also appears to have the largest free base peak. This indicates that the amount of free base, an impurity in this case, present in the sample acts to depress the melting point of the salts. In addition, this impurity prevents the second and third transitions, which are believed to be recrystallization into a second polymorphic form followed by melting of this polymorph at 198°C. The chloroform-crystallized salt needs more investigation before a final conclusion can be made as to the nature of this occurrence. The second scale-up and results from additional experiments will be discussed in later sections of this chapter.

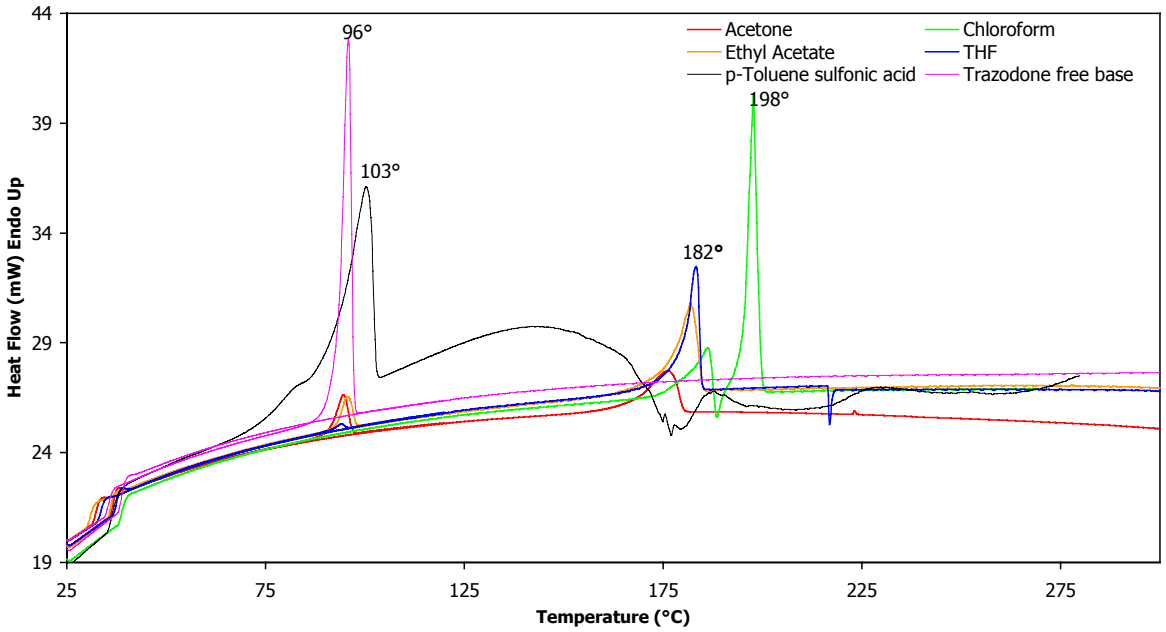

Figure 5.7. DSC Thermograms of Trazodone Tosylate Salts Compared to Reactants

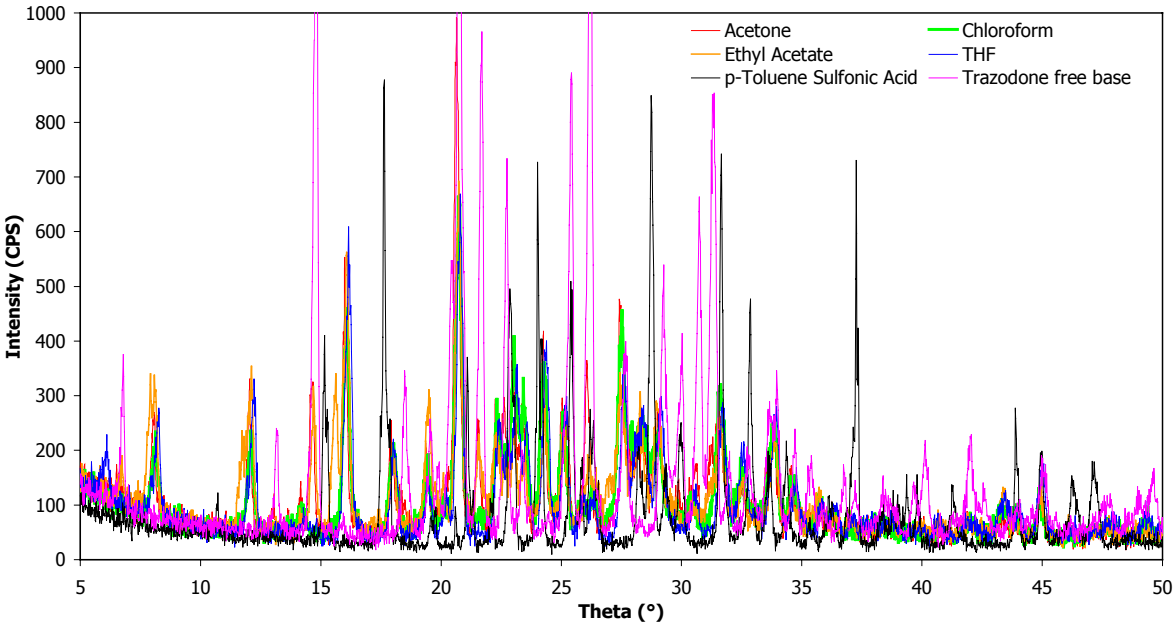

Figure 5.8. PXRD Patterns of Trazodone Tosylate Salts Compared to Reactants

Sulfate Salts

When the sulfate salts were first run on the DSC using the same heat/cool/heat method as used for the other salts, a problem was encountered. The DSC method was setup to heat to 120°C, cool to 25°C, and then heat back up to 300°C. The problem was that the sulfate salts were beginning to undergo a transition at 120°C and when the method stopped there and cooled, some of the substance that was beginning to melt or evaporate remained and showed up in the second heating step making the thermogram quite complex. Therefore, the DSC method was altered for the sulfate salts to just one heat step from 25-300°C. The DSC thermograms from both the initial heat/cool/heat method and the altered one step method are shown in figures 5.9 and 5.10, respectively. The PXRD patterns for all four Trazodone sulfate salts compared to free base are shown in figure 5.11. From the melting point apparatus, it is clear that all four salts melt at about 193-197°C and boil at 260-263°C. Similarities among these salts seem to occur in pairs, where the THF and chloroform crystallized salts are quite similar to each other, but different from the acetone and ethyl acetate crystallized salts according to both DSC and PXRD results. The THF salt looks as though it is most “pure” or at least most crystalline with the highest intensity PXRD peaks and a cleaner looking DSC thermogram. As in the case with the pamoate and tosylate salts, there is a mysterious transition occurring in the DSC thermogram around 117-122°C for each salt. Since the powder patterns exhibit a flat baseline with fairly high intensities, these salts probably have very little if any amorphous content. This rules out a glass transition temperature. For the

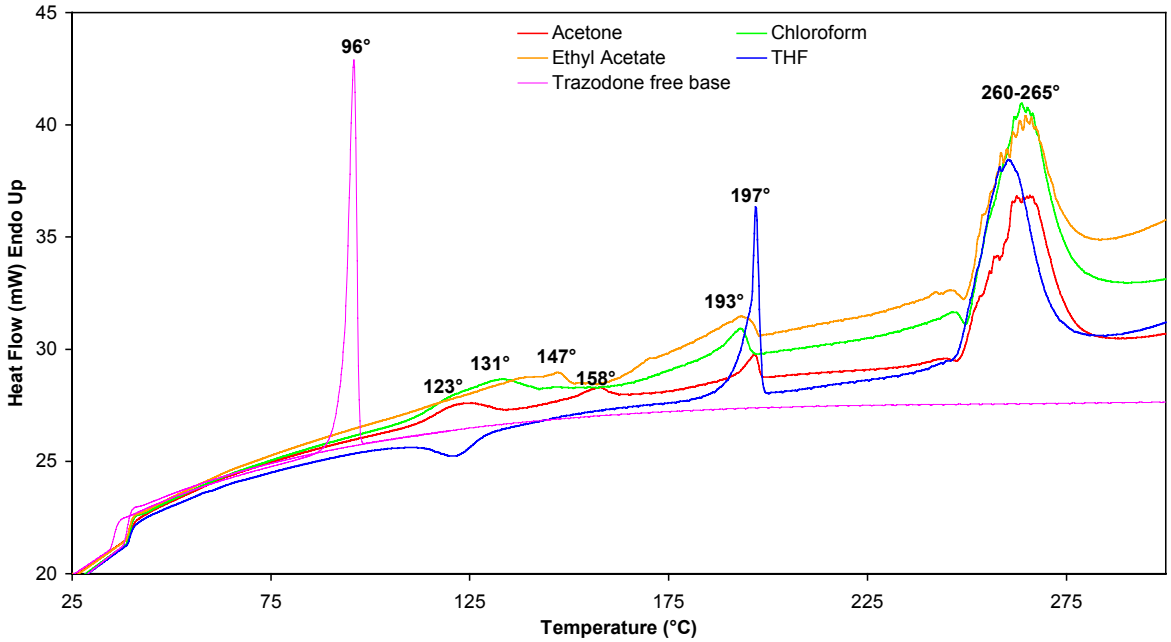

Figure 5.9. DSC Thermograms of Trazodone Sulfate Salts from the Initial Heat/Cool/Heat DSC Method

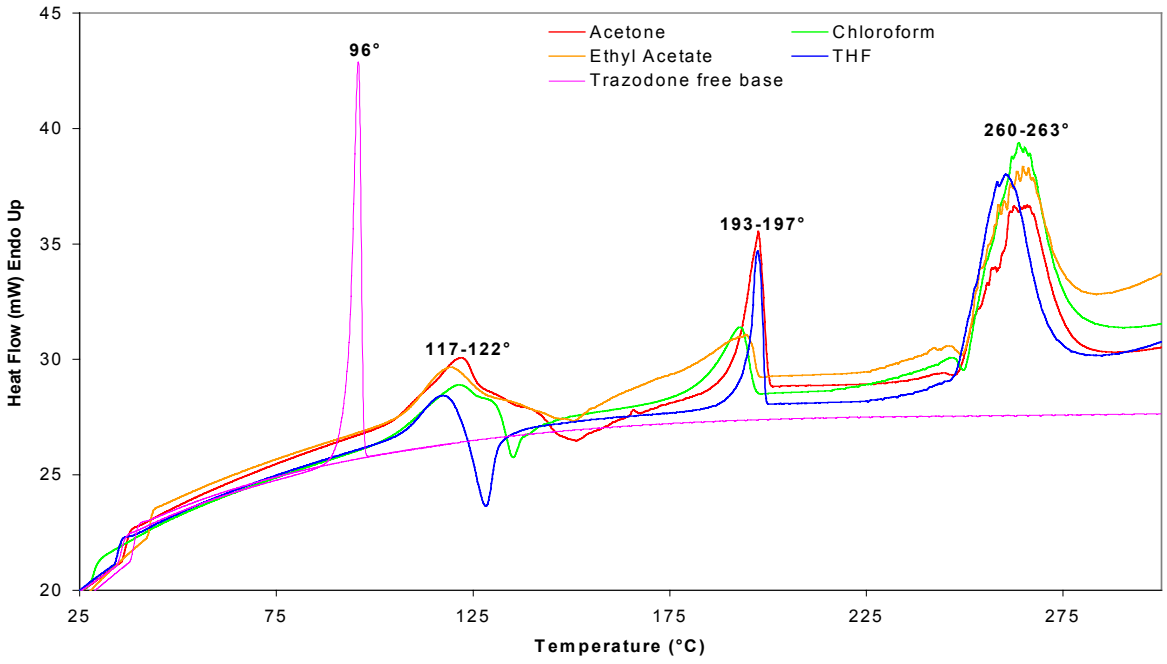

Figure 5.10. DSC Thermograms of Trazodone Sulfate Salts from the Altered One Step DSC Method

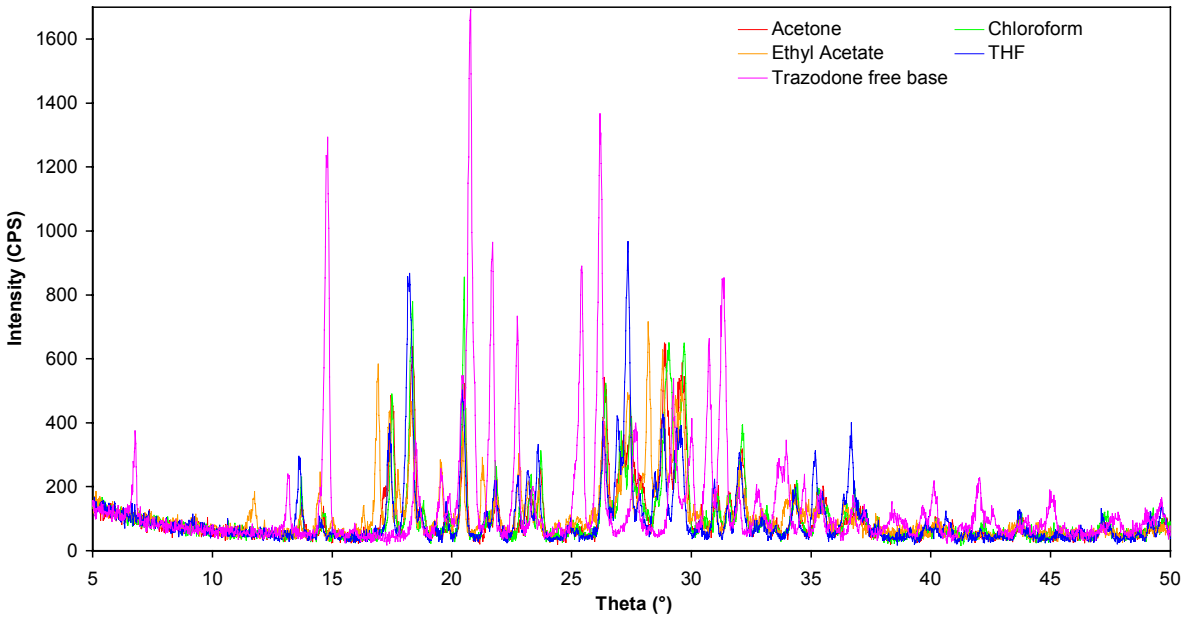

Figure 5.11. PXRD Patterns of Trazodone Sulfate Salts Compared to Free Base

acetone and ethyl acetate salts, the transition is quite broad and could potentially be boiling off of water from hydrate formation. This is truly a good possibility for all of the salts since sulfate salts of many drugs are typically hygroscopic. Presence of a solvate is another possibility especially in the ethyl acetate crystallized salt since it exhibits several different peaks in the powder pattern. A final possibility, especially in the THF crystallized salt, is the melting of one polymorphic form at 117°C, recrystallization of a second form, and melting of the second form at 197°C. Again, more experimentation is necessary to better explain this transition. Results from the second scale-up will be discussed in later sections of this chapter.

Phosphate Salts

The DSC thermograms and PXRD patterns of all the phosphate salts are shown in figures 5.12 and 5.13, respectively. The chloroform crystallized salt reaction did not go to completion since there was a large remainder of free base present in the sample as seen in the DSC and PXRD patterns. After utilizing the melting point apparatus, it is clear that a mixture of products resulted melting at different temperatures due to the polyprotic nature of phosphoric acid. Since this will require an extra, potentially difficult separation step in the manufacturing process, this salt was eliminated from further consideration.

Caprate and Elaidate Salts

The DSC thermograms and PXRD patterns for the caprate and elaidate salts are shown in figures 5.14, 5.15, 5.16, and 5.17, respectively compared to the reactants. DSC thermograms of physical mixtures of reactants are also

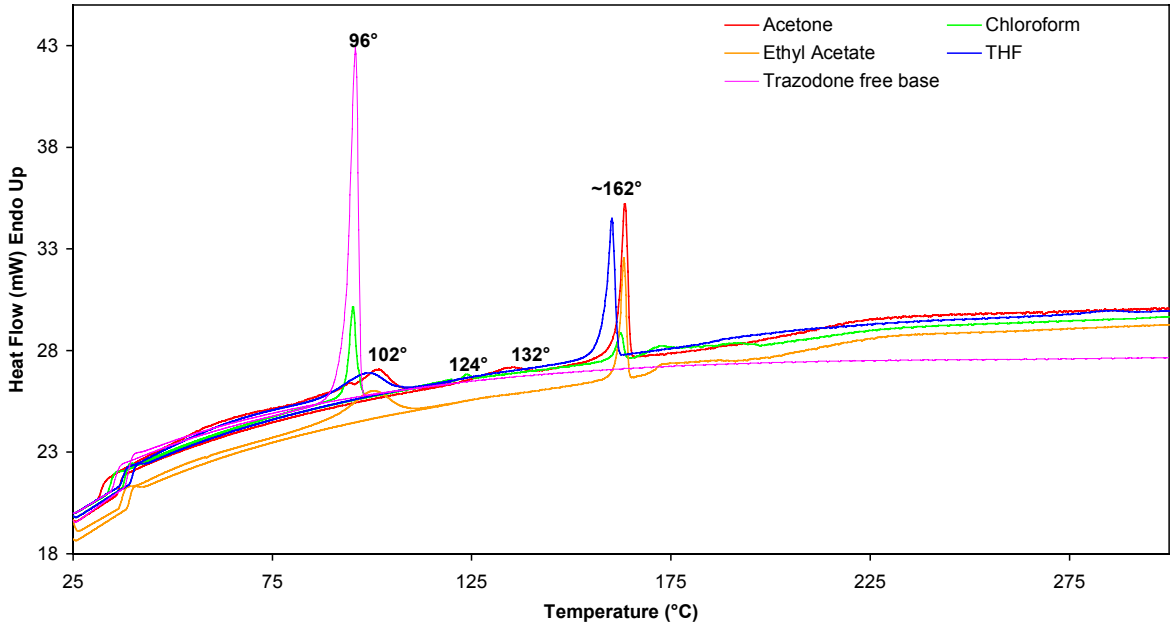

Figure 5.12. DSC Thermograms of Trazodone Phosphate Salts Compared to Free Base

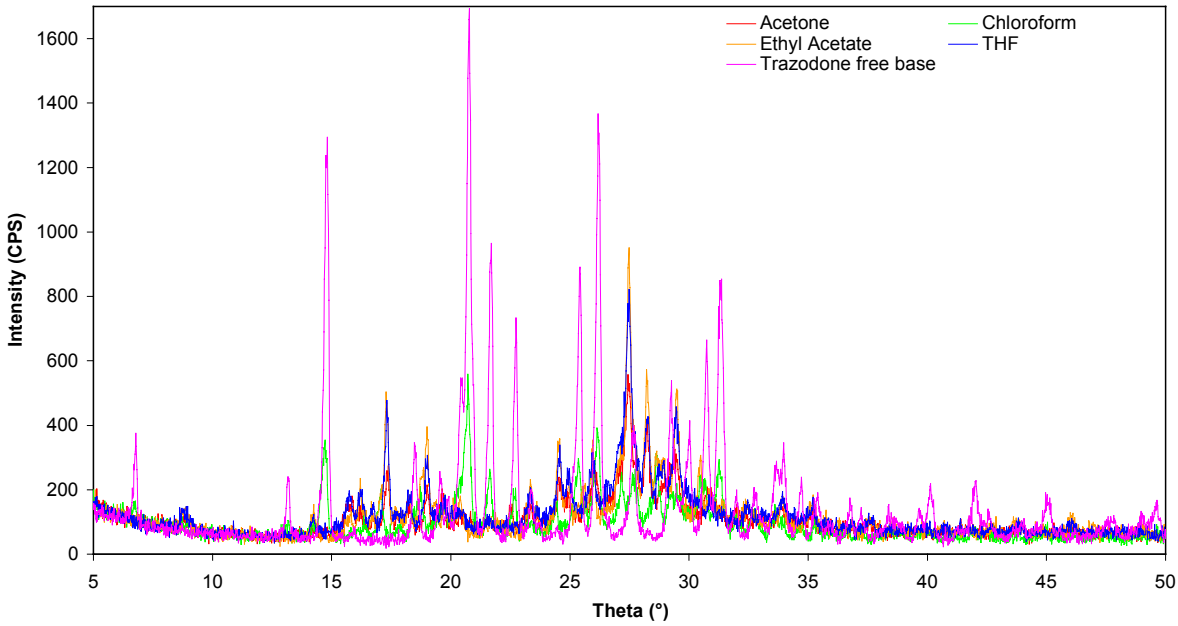

Figure 5.13. PXRD Patterns of Trazodone Phosphate Salts Compared to Free Base

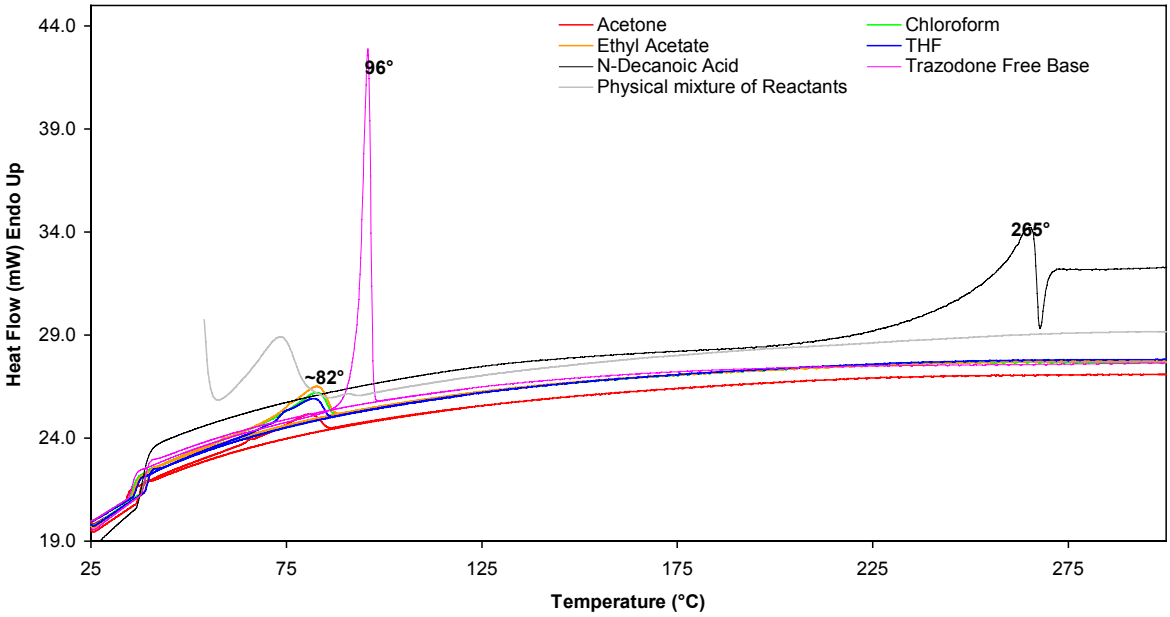

Figure 5.14. DSC Thermograms of Trazodone Caprate Salts Compared to Reactants and Physical Mixture

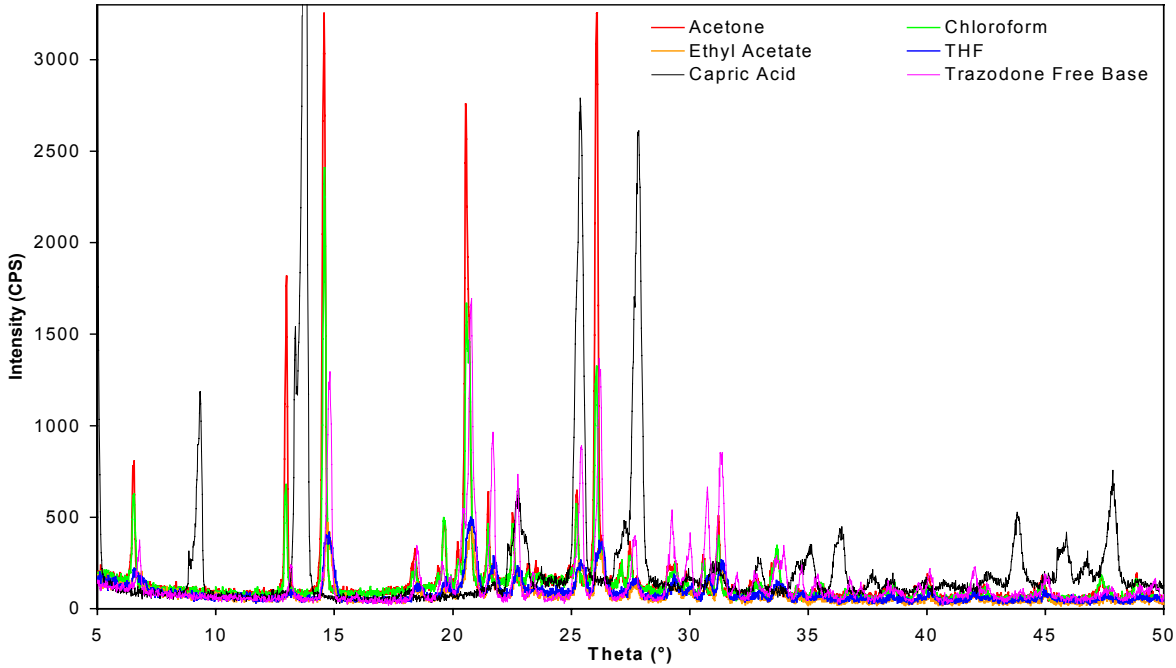

Figure 5.15. PXRD Patterns of Trazodone Caprate Salts Compared to Reactants

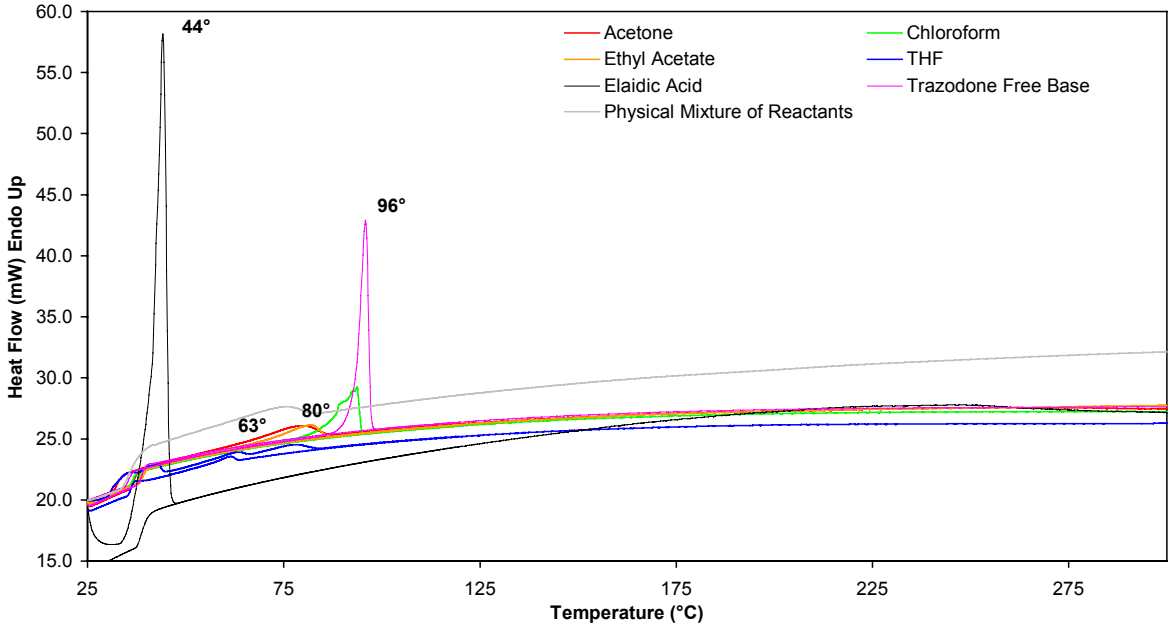

Figure 5.16. DSC Thermograms of Trazodone Elaidate Salts Compared to Reactants and Physical Mixture

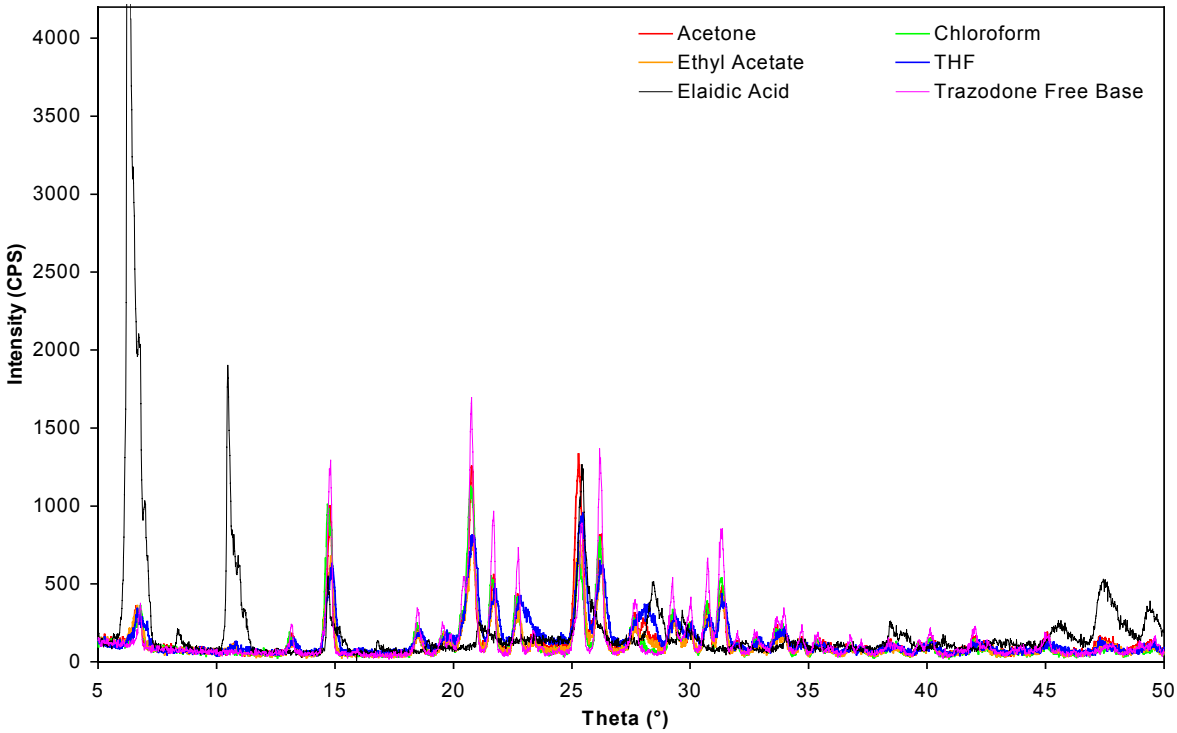

Figure 5.17. PXRD Patterns of Trazodone Elaidate Salts Compared to Reactants

shown to help interpret results. These two reactions are discussed together since both acids are solids and the same results were obtained regardless of solvent used. For all reactions involving these two acids, a mixture of reactants was obtained indicating no reaction took place in every case. Each of the DSC thermograms for the "salts" are nearly identical to the thermogram of the physical mixture of reactants. Additionally, the PXRD patterns for each "salt" contain characteristic peaks from both reactants. Since no reaction occurred for either of these acids, they were eliminated from further consideration.

Acetate and Propionate Salts

The DSC thermograms and PXRD patterns for the acetate and propionate salts are shown in figures 5.18, 5.19, 5.20, and 5.21, respectively. The reactions involving these two acids are discussed together since both acids are liquids and no reaction appears to have occurred in every case regardless of crystallizing solvent. This is obvious according to all the DSC thermograms, as only one peak is present occurring at the melting point of the free base, and all the PXRD patterns are identical to the pattern of the free base. Due to no successful reactions using these two acids, they were eliminated from further consideration.

Hygroscopic Analysis

In conjunction with the PXRD and DSC experiments, hygroscopic analysis was also performed on one salt from each counterion reaction. The choice of salt for this experiment was somewhat arbitrary. In two of the cases, with acetic and propionic acid, no solid resulted from using acetone as the crystallizing solvent. It was decided that ethyl acetate-crystallized salts should be tested for

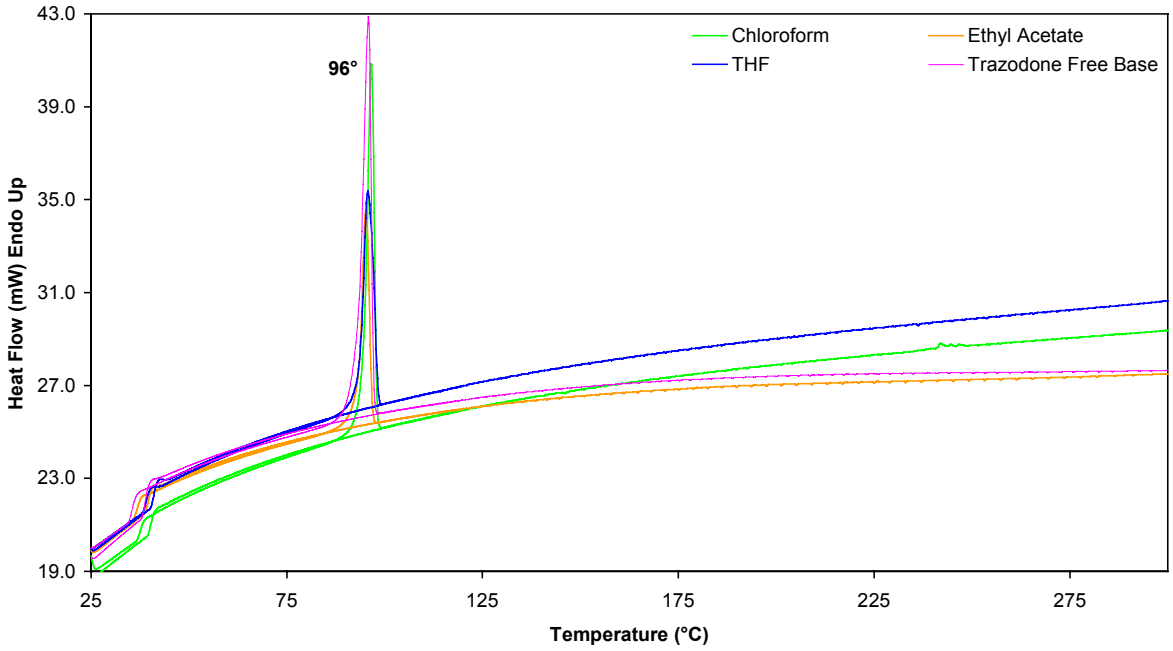

Figure 5.18. DSC Thermograms for Trazodone Acetate Salts Compared to Free Base

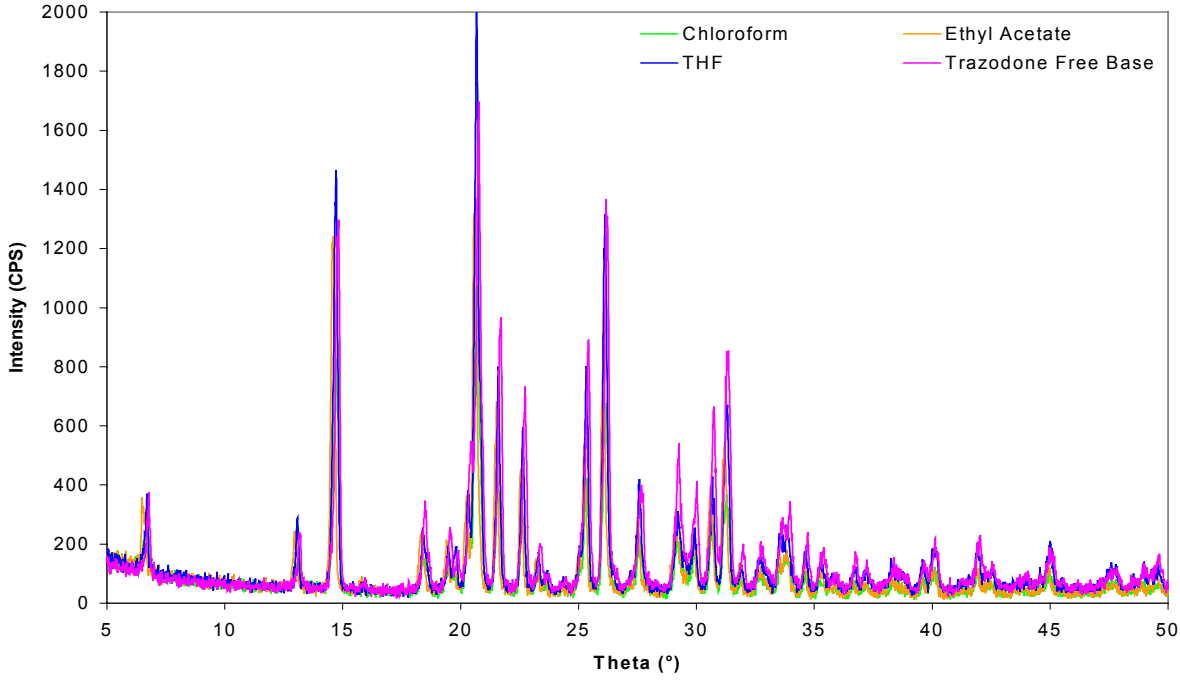

Figure 5.19. PXRD Patterns of Trazodone Acetate Salts Compared to Free Base

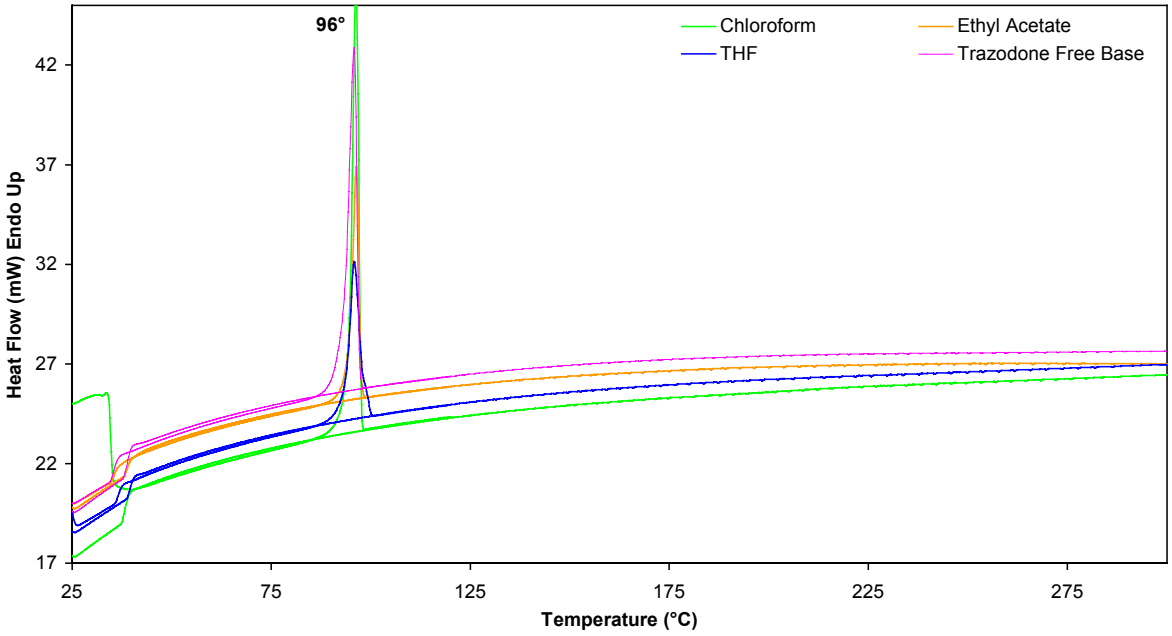

Figure 5.20. DSC Thermograms for Trazodone Propionate Salts Compared to Free Base

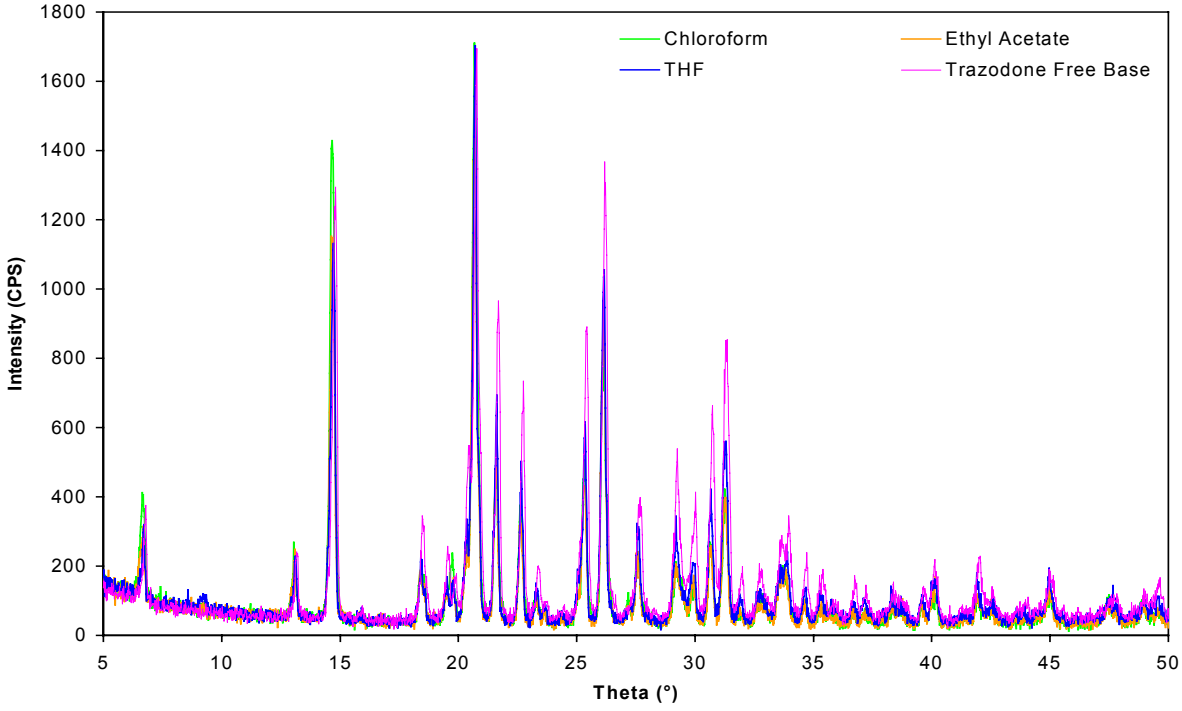

Figure 5.21. PXRD Patterns of Trazodone Propionate Salts Compared to Free Base

hygroscopicity to get an initial idea of stability and wettability. Before beginning this experiment, each salt was equilibrated at least 48 hours in a <4% relative humidity, vacuum-sealed desiccator containing fresh Drierite. The hygroscopic analysis sessions were quite work-intensive as the humidity and temperature had to be constantly monitored and adjusted, either through steam input, dry air input or circulation, to maintain each humidity condition. They each took approximately 6 hours to complete, and resealing of all joints and cord holes in the Plexiglas had to be done using vacuum grease after each experiment to allow for faster equilibration and less manual adjustments to maintain humidity conditions. This is why only one salt from each counterion was tested for hygroscopicity initially. It was decided that if a unique salt with properties different from the ethyl acetate crystallized salt was found, then that particular salt could be tested for hygroscopicity later, if necessary. The results of the moisture uptake at 33, 52, and 75% relative humidities for the ethyl acetate crystallized salts are shown in figure 5.22. The acetate salt was tested for hygroscopicity before DSC and PXRD analysis, whereas the propionate salt was not tested for hygroscopicity since DSC and PXRD analysis had determined it to be free base. Therefore, the hygroscopic profile of the acetate salt is actually that of the free base, and it is clear that the HCl salt is slightly more hygroscopic. The elaidate salt, which was determined to be a mixture of elaidic acid and free base had about the same hygroscopicity as the HCl salt, and the caprate salt, a mixture of n-decanoic or capric acid and free base, had a similar hygroscopicity as the pamoic acid. These substances are quite lipophilic and the low

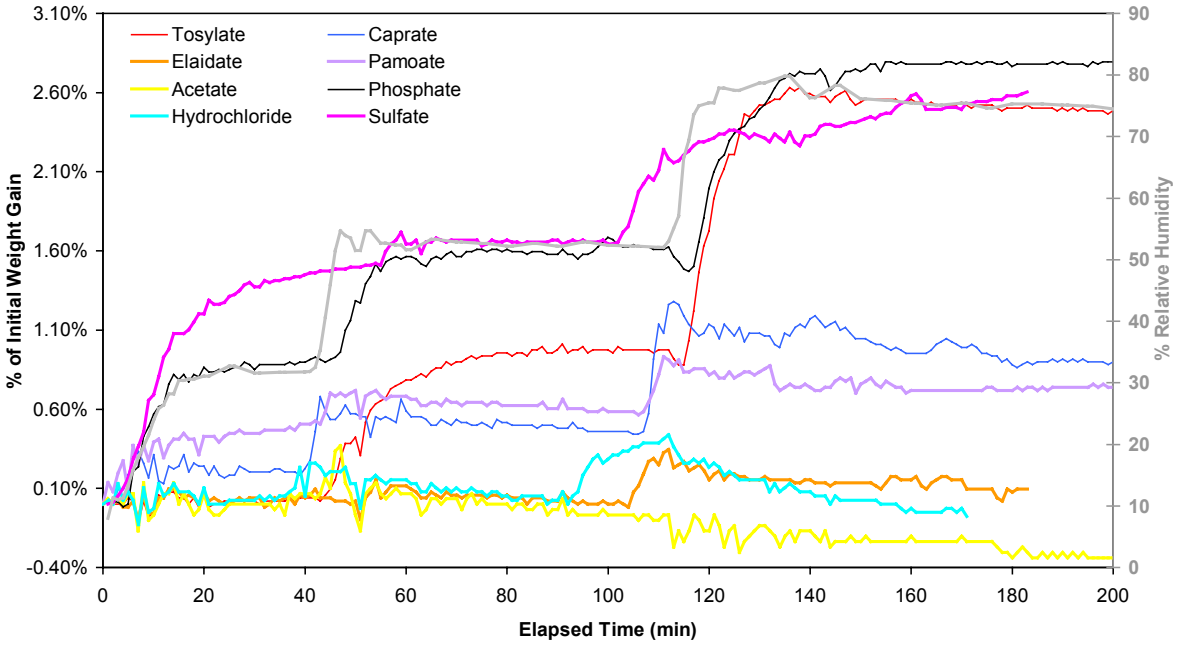

Figure 5.22. Corrected Hygroscopic Data of All Ethyl Acetate Crystallized Salts of Trazodone Equilibrated at 33%, 52%, and 75% Relative Humidities

hygroscopic value was expected. The sulfate, phosphate and tosylate salts had similar hygroscopicity at the 75% relative humidity condition up to about 2.6% weight gain compared to the initial weight of the salts. All of the salts were fairly nonhygroscopic with the phosphate and sulfate salts exhibiting the highest hygroscopicity.

Physicochemical Results After Second Scale-Up

As previously discussed, the elaidate, caprate, acetate, and propionate salts were eliminated due to no reaction taking place regardless of crystallizing solvent used, and the phosphate salt was eliminated due to a mixture of products. A final scale-up was performed to obtain gram quantities of the remaining salts: pamoate, tosylate, and sulfate. Since success in automated salt formation had been established, the bulk HCl salt was used for comparisons rather than extracting and resynthesizing the HCl salt. To allow sufficient time for the reactions to reach completion, the reaction time was increased from 12 hours to 48 hours. For tosylate and pamoate salts, chloroform was used as the crystallizing solvent due to an apparent purer product as seen in the DSC thermogram of the chloroform crystallized tosylate salt. All four pamoate salts, had the same thermogram and essentially the same PXRD pattern so that it made no difference which solvent was used in the scale-up. For sulfate salts, ethyl acetate (E) and THF (T) were used to make two different salt forms since there were apparent differences in both PXRD patterns and DSC thermograms.

Only these four Trazodone salts were used for the final preformulation characterization.

PXRD and DSC

From the initial PXRD and DSC experiments several unique thermal transitions were noted for each of these four scaled up salts. Therefore, after scale-up to gram quantities, about half of each salt was heated to just past the first thermal transition. This heated version of the salt was then tested against the initial and final batch as well as against the free base to help explain the nature of the transition. Each salt will be discussed below in separate sections.

Tosylate Salt

Figures 5.23 and 5.24 show the DSC thermograms and X-ray powder patterns, respectively, for the scaled-up tosylate salt compared to the heated salt, first batch, and free base. Since this salt was believed to exhibit a thermally induced polymorphic transition, it was expected that only the second melting peak would occur in the DSC thermogram of the heated salt and the PXRD patterns of the first and last batches of the tosylate salt compared to the heated salt would be different. This was indeed the case. Even though the first transition is quite high, around 186°C, the potential that a tightly bound hydrate exists is still present. One possible way to distinguish between a true polymorph of the tosylate salt and a hydrate or pseudopolymorph, is to perform a more in-depth PXRD study and determine the unit cell dimensions for each case. This will be talked about a little more in chapter 6.

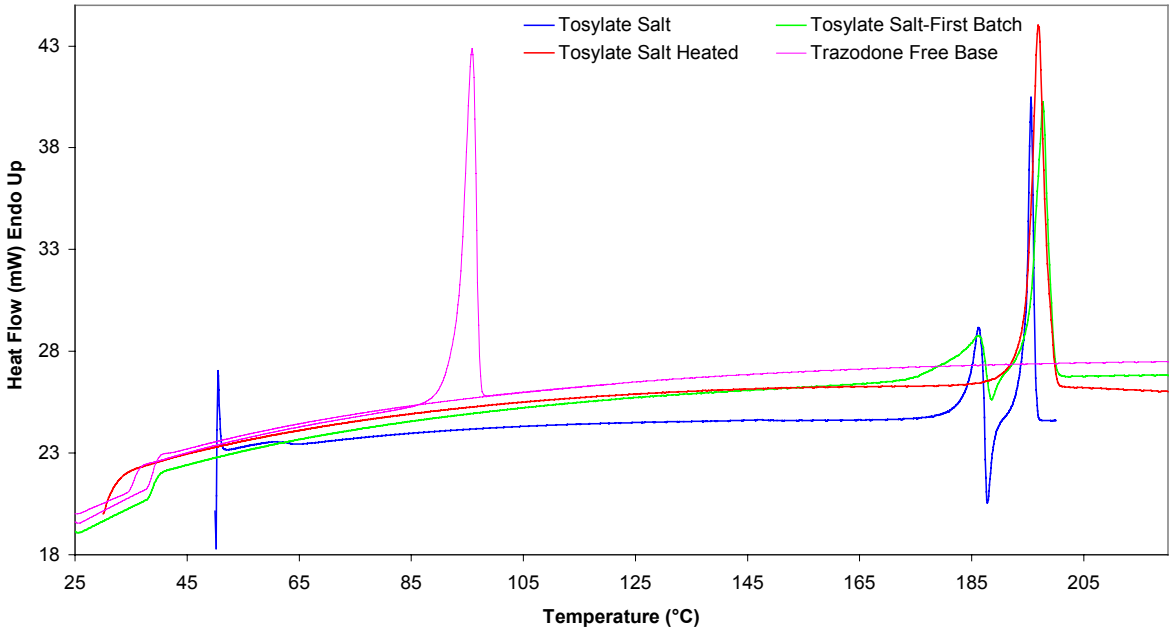

Figure 5.23. DSC Thermograms of Trazodone Tosylate Salt Compared to First Batch and Heated Salt

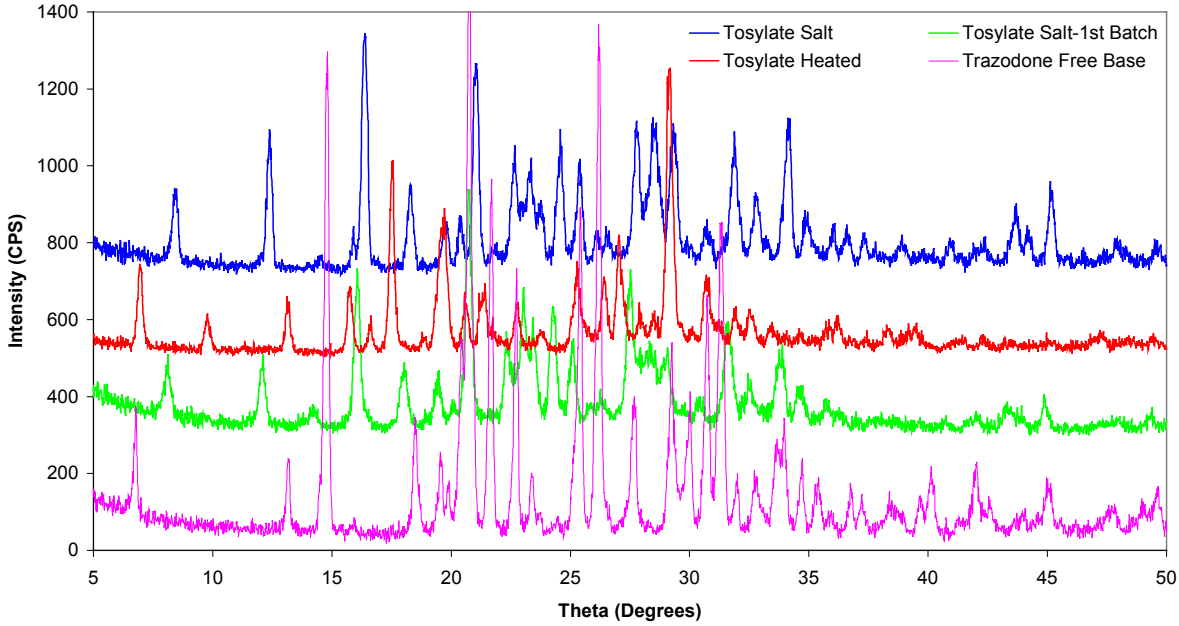

Figure 5.24. PXRD Patterns of Trazodone Tosylate Salt Compared to First Batch and Heated Salt

Pamoate Salt

Figures 5.25 and 5.26 show the DSC thermograms and PXRD patterns, respectively, for the scaled-up pamoate salt compared to the heated salt, first batch and free base. In this case, the transition was believed to be a glass transition temperature and transformation into a more crystalline material. The DSC thermogram from the first batch does not coincide exactly with the one from the scaled-up batch because the transition occurring at 140°C is not nearly as pronounced. The only changes made in the method of synthesis of this scaled-up batch, was to allow much more time for reaction to occur and a stir bar was added to the Erlenmeyer flask. The flask was left open to the air so that over the 48 hour period solvent could evaporate. It was noticed that after 48 hours, all solvent had evaporated and solid remained such that no wash with petroleum ether was performed. This may indicate that petroleum ether has something to do with this transition, possibly due to a solvate formation or changing the amorphous content of the salt.

The powder patterns of the first and last batch are also somewhat different as all the peaks of the latter appear shifted to the right about ½ to ¾ °. Since there was a long time period between measurements of the first batch and the scaled-up and heated batches, it is believed that a slight miscalibration of the x-ray diffractometer caused the peak shifts, which occurred on every scaled-up and heated salt. This was confirmed as a possibility by the geology department, specifically Dr. Paul Schroeder. If the peak shift is taken into consideration, the first batch and scaled-up batch of pamoate salts are nearly identical except that

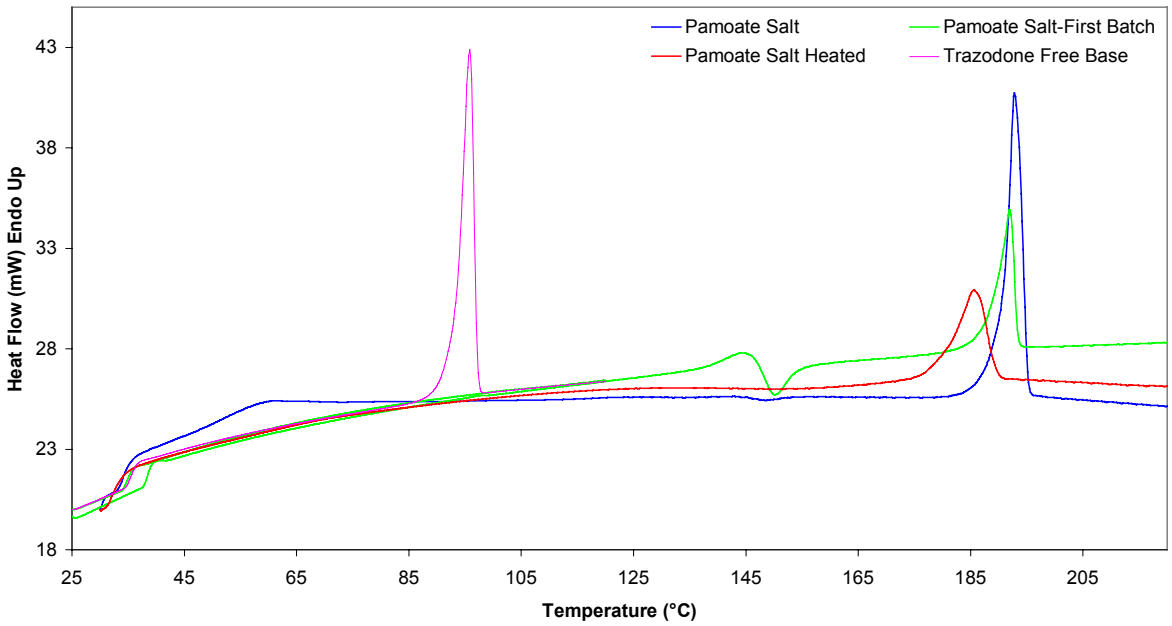

Figure 5.25. DSC Thermograms of Trazodone Pamoate Salt Compared to First Batch and Heated Salt

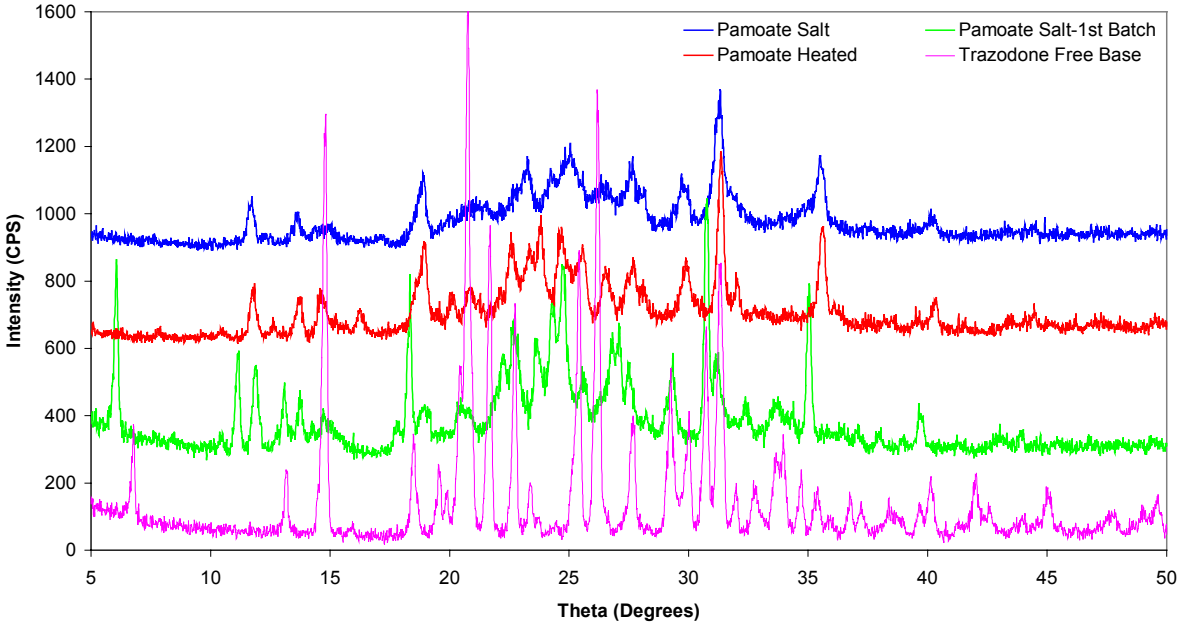

Figure 5.26. PXRD Patterns of Trazodone Pamoate Salt Compared to First Batch and Heated Salt

peak intensities of the scaled-up batch are depressed. The miscalibration of the machine may also have caused a reduction in the signal to noise ratio making comparisons difficult. If the DSC transition for the pamoate salt is a glass transition temperature due to amorphous content, heating past this transition should cause no change in the PXRD peak positions of the heated salt, only a possible increase in crystallinity should be observed. The heated salt did give an identical powder pattern with slightly higher peak intensities; but the DSC of the heated salt shows a wider melting peak and depression of the melting point. This could possibly indicate some degradation occurring due to heating the salt. Since there is very little evidence to support the presence of a pseudopolymorph or polymorph, the most likely explanation is that the unusual transition observed via DSC is an amorphous glass transition temperature and different amorphous contents were observed between the first and last batches.

Sulfate Salts

Figures 5.27, 5.28, 5.29, and 5.30 show the DSC thermograms and PXRD patterns, respectively, for the scaled-up sulfate (T) and sulfate (E) salts compared to the heated salt, first batch and free base and figure 5.31 is a combination graph of all PXRD patterns for both sulfate (T) and sulfate (E) salts. Similar to the pamoate salts, the second batch of sulfate salts is not exactly the same as the first batch. The transition at 120°C is only a peak in the sulfate (T) salt and is not even present in the sulfate (E) salt. This could be due to extra reaction/evaporation time eliminating solvent from the sulfate (E) salt. The same changes in synthesis method noted in the pamoate salts also occurred in the

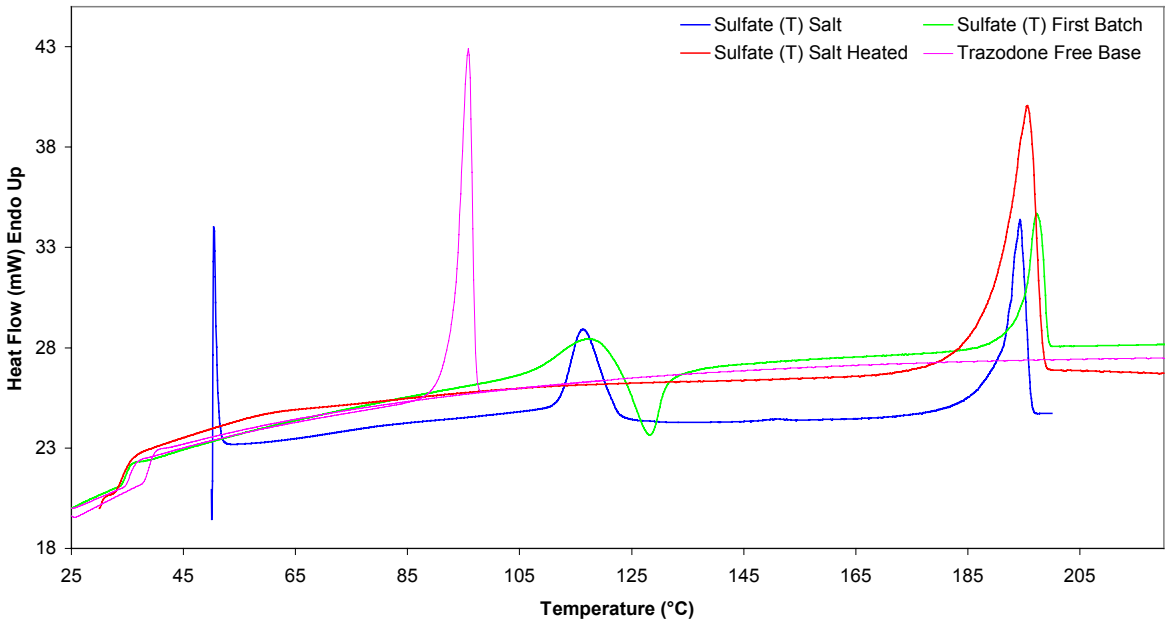

Figure 5.27. DSC Thermograms of Trazodone Sulfate (T) Salt Compared to First Batch and Heated Salt

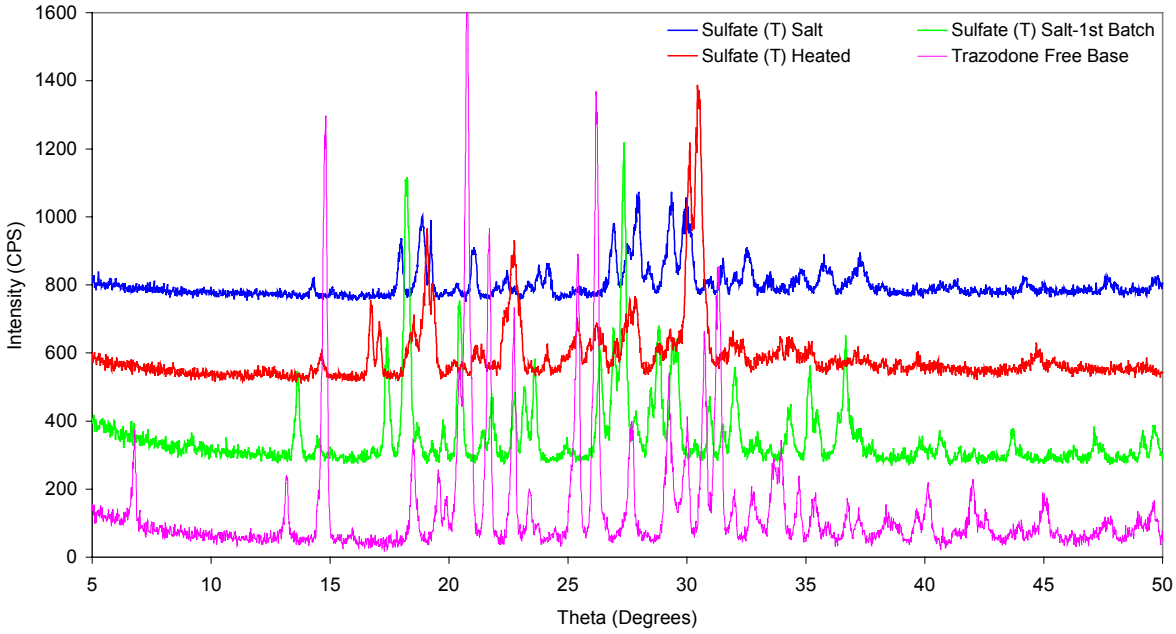

Figure 5.28. PXRD Patterns of Trazodone Sulfate (T) Salt Compared to First Batch and Heated Salt

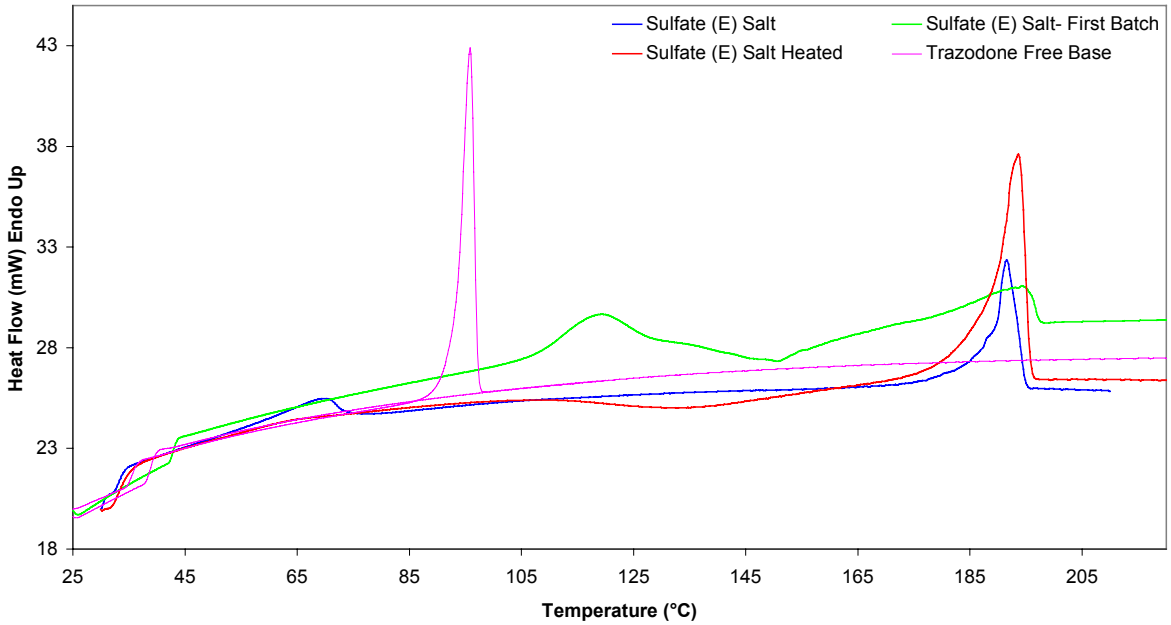

Figure 5.29. DSC Thermograms of Trazodone Sulfate (E) Salt Compared to First Batch and Heated Salt

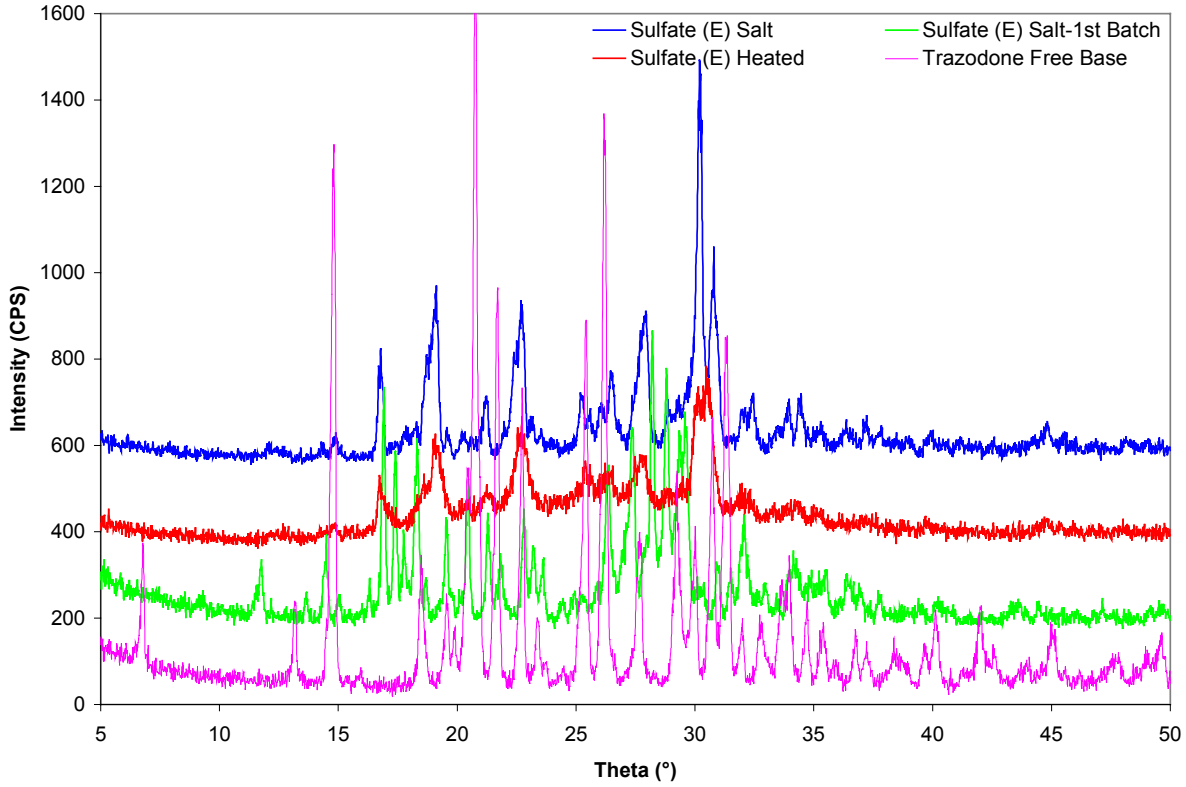

Figure 5.30. PXRD Patterns of Trazodone Sulfate (E) Salt Compared to First Batch and Heated Salt

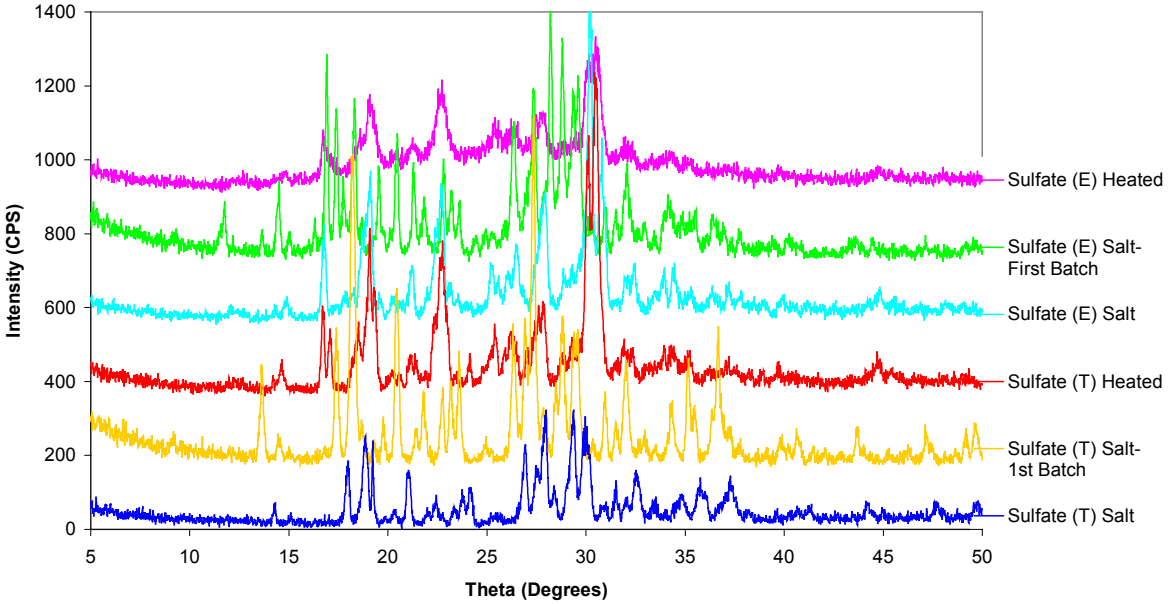

Figure 5.31. Comparison of PXRD patterns of All Sulfate Salts

sulfate salts. The PXRD pattern of the sulfate (E) salt is essentially the same as the first batch and the heated salt after taking into account the machine miscalibration. Again the peak intensities are lower. After heating, the DSC and PXRD results indicate apparent degradation of the salt. The PXRD patterns of the sulfate (T) salts show that the first batch appears to be the same as the second batch, but they are both different than the sulfate (E) salt until after they are heated. This indicates that a solvate is potentially present in the sulfate (T) salt, which disappears after heating. To determine if a solvate is indeed present, a more in-depth PXRD study should be done to calculate the unit cell dimensions for each case. This will be discussed in chapter 6.

Density, Surface Area, and Particle Size Analysis

The density, surface area and particle size data are all shown in table 5.3. All salts exhibited similar true densities of around 1.5 g/mL with bulk and tapped densities ranging from 0.2-0.6 g/mL. The surface area and compressibility index of the marketed HCl salt were significantly lower than the other four salts. This indicates that the HCl salt has slightly better flow properties with less interparticulate interactions, but the low surface area may make dissolution rate slightly slower than the new salts. The tosylate salt had the smallest average particle size of 32 μm and the highest compressibility index indicating poorer powder flow properties due to high interparticulate interactions; however the heated tosylate salt had the lowest compressibility index and Hausner ratio and the second highest surface area. This means it may have the best flowability

Table 5.3. Density, Surface Area and Particle Size Data for Trazodone Salts

Trazodone Salt	*Density (g/mL)*			*Compressibility*	*Hausner*	*Surface Area*	*Particle Size*
	Bulk	*Tapped*	*True*	*Index*	*Ratio*	*(m^2/g)* [a]	*(d_{avg}) (μm)*
Pamoate	0.199	0.339	1.507	41.25	1.70	2.54	70.32
Pamoate Heated	0.566	0.873	1.4359	35.21	1.54	0.68	54.58
Tosylate	0.208	0.428	1.448	51.43	2.06	1.02	32.93
Tosylate Heated	0.613	0.788	1.3736	22.22	1.29	2.29	64.68
Sulfate (THF)	0.388	0.598	1.545	35.14	1.54	0.79	74.01
Sulfate (THF) Heated	0.572	0.902	1.5251	36.62	1.58	0.80	54.02
Sulfate (E)	0.344	0.538	1.537	36.11	1.57	1.73	64.61
Sulfate (E) Heated	0.600	0.865	1.5218	30.67	1.44	0.71	53.16
Hydrochloride Bulk	0.431	0.594	1.358	27.40	1.38	0.24	69.31

Notes: [a]Data reported are the average of desorption values

and dissolution rate of any of the salts and further supports the possibility of a polymorph due to the large difference in physicochemical parameters.

The pamoate salt had the second largest average particle size of 70 μm with the largest surface area. The heated pamoate salt exhibited significantly lower surface area than the unheated version with smaller average particle size. A larger surface area would have been expected with smaller particles, but upon heating it was noticed that the particles fused and could have closed any pores that may have been present in the initial pamoate salt resulting in a smaller surface area. Another possibility is that agglomerates are present or the particle shape of the pamoate salt versus the heated pamoate salt would not allow it to pass through the sieve as easily.

The sulfate salts and their heated versions were very similar in nearly every physico-chemical property except surface area in which the sulfate (T) salt was 2.2 times lower than the sulfate (E) salt. Additionally, the heated salts had nearly the same surface area as the sulfate (T) salt, but not the sulfate (E) salt. This does not lend support to the idea of a potential solvate in the sulfate (T) salt case, but suggests that there may have been pores present in the initial sulfate (E) salt, which were fused upon heating causing a lower surface area even though particle size decreased slightly. Again it is possible that agglomerates are present or the particle shape of the sulfate salt versus the heated salt would not allow it to pass through the sieve as easily.

pH-Solubility Analysis

The pH-solubility profiles for the Trazodone salts are shown in figure 5.32. The free base gave a similar profile as the HCl salt below pH 5 because HCl acid was used to implement the pH change, thus causing formation of the HCl salt. Below pH 3, the solubility began to drop off due to common ion effects [111]. The free base showed a slightly higher solubility at higher pH's than the sulfate or HCl salts, but the pamoate salt showed the highest solubility at the higher pH's approaching 10 mg/mL at pH 10. The pamoate salt was the least soluble with a solubility value of only 0.077 g/mL at pH 5.8, which occurred upon adding distilled, deionized water to the solid powder. The sulfates were the most soluble salt with a solubility of 33-38 mg/mL at pH 1. Due to this extremely low initial pH value, which occurs upon addition of distilled, deionized water to solid powder, the sulfate salts would probably not be good candidates for oral tablets or capsules as they may cause damage to the GIT membrane upon dissolution due to a pH of around 1.0 upon dissolving in distilled water. The most interesting profile is the tosylate salt with a low solubility throughout the entire pH range. The solubility values range from 3 mg/mL at pH 1 to 0.2 mg/mL at pH 12. This could offer a significant benefit to the development of a prolonged release, prolonged action or suspension type of dosage form for this drug.

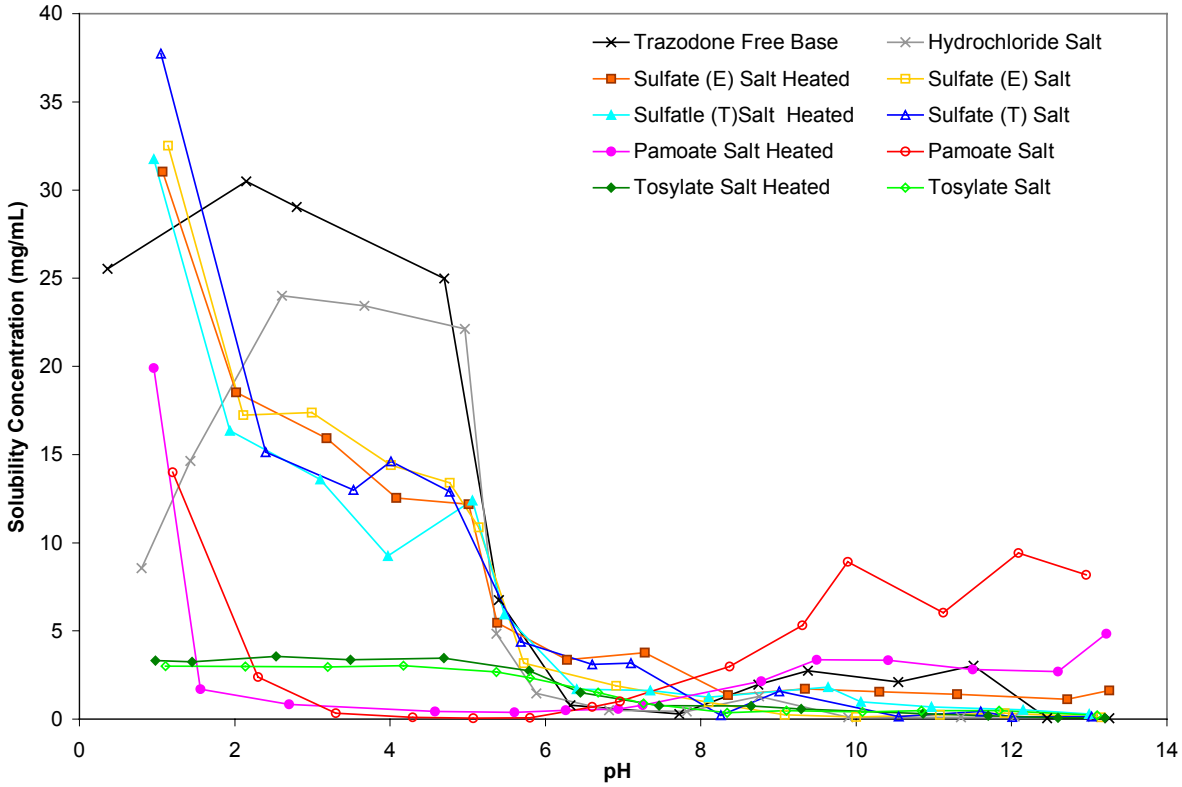

Figure 5.32. Comparison of pH-Solubility Profiles of Trazodone Salts

CHAPTER 6

SUMMARY, CONCLUSIONS, AND FUTURE EXPERIMENTS

Summary and Conclusions

Many pharmaceutical operations involve tedious and repetitive procedures, which potentially can be more efficiently performed using robotic equipment. Adoption of existing automation devices and methods widely used for drug discovery can provide a fast and accurate alternative. The Biomek 2000 workstation was originally designed for the high-throughput screening of new drug candidates synthesized through combinatorial chemistry. Its capabilities include automated liquid handling, moving labware around the workbench or onto a stacker carousel, and a plate reader for fluorescence and UV-Vis spectrophotometry. The operations of the Biomek 2000 workstation can be programmed to automatically perform pre-determined experimental steps, allowing precise and efficient operations. However, the use of such diversified robots for pharmaceutical preformulation development have not been widely executed. Implementation of such a machine may not only enhance the experimental efficiency, but will also significantly reduce experimental error, thereby helping to meet cGMP requirements. Automation of salt formation, scale-up and analysis procedures will save time and money, and it may lead to additional application opportunities never before imagined.

Many pharmaceutical preformulation programs are designed to obtain the maximum amount of information using the smallest quantity of drug product. They involve systematically analyzing and eliminating salt candidates in a multi-step process. With weakly basic drug candidates, the hydrochloride salt is usually the first choice due to ease of formation and straightforward recrystallization [73]; however, it may not be the optimum candidate in most cases. It is necessary to evaluate each salt according to the intended application, and this can be very time consuming and costly. In the present study, the Biomek 2000 workstation carried out a series of salt formation and screening procedures in an effort to search for a new Trazodone salt which has a low solubility at lower pH's. This kind of salt is beneficial for the development of prolonged action or suspension type dosage forms for Trazodone. Through the use of the Biomek 2000 workstation, 104 potential salts through the combination of 13 counterions and 8 crystallizing solvents were screened in a three-stage process. The first stage involved deciding which combinations of counterions and solvents gave solid crystalline drug products and how long the reaction should be run to consume all reactants. The solid drug products from this first stage were scaled up to 25 mg quantities for the second stage and analysed via DSC, PXRD, and hygroscopic stability to determine which conditions gave a new, pure drug salt versus mixtures of products or reactants. In the final stage of screening, only four remaining salts were scaled up to gram quantities and tested for particle size, pH-solubility, density, and surface area. From the comparison of

these four salts to the marketed hydrochloride salt and free base, one salt was chosen as the best for a prolonged action or suspension type dosage form.

Through the use of the Biomek 2000 workstation, a successful automated procedure was developed to form different salts of the model drug trazodone. Out of 104 salts formed in the preliminary run, 44 were scaled up for further analysis; however, only 34 were tested. DSC, PXRD and hygroscopic analyses were performed to determine if salt formation had occurred, if crystalline materials were present and to study the thermal properties of the substances. The results showed that out of the 34 salts tested, only 20 reactions successfully formed salts. Those were the hydrochloride control, tosylate, pamoate, phosphate, and sulfate salts. Most of the reactions did not go to completion so that reactants were present in the final products manifesting themselves in both XRD patterns and DSC thermograms. The phosphate salt formed a mixture of products due to its polyprotic nature and was also eliminated. The remaining pamoate, tosylate and sulfate salts were scaled up and subjected to physico-chemical profiling. Each of these salts was heated past the first DSC transition to determine if polymorphs or pseudopolymorphs were present. Similar physico-chemical parameters were observed in each of the salts and heated salts compared to free base and hydrochloride salt. Most significant was the pH-solubility profile of the tosylate salt and heated salt, both of which exhibited a low solubility throughout the entire pH range. This characteristic makes it an excellent candidate for a prolonged action or suspension type formulation. As an oral dosage form, it would be dissolution limited throughout the GI tract

potentially prolonging the action of the drug, which may also change the dosing regimen. This could significantly impact the patient compliance issue especially since this drug is shown to be superior in the elderly.

Future Experiments

This research has spawned some future experiments that may help resolve the few pieces of data that remain slightly mysterious. Apparently, it is the reaction of several professors that to solve a crystal structure whether through PXRD or single crystal x-ray analysis is a master's thesis worthy project. Therefore, several salts along with their heated counterparts could be used for this purpose. The tosylate salt and the apparent thermal induced polymorph would be excellent candidates for crystal structure determination and would help provide an answer for this research, which may be patentable. A second candidate for crystal structure determination or unit cell determination is the sulfate (T) salt and its heated version to answer whether or not a solvate is indeed present in this case. Formulation development of a suspension or other prolonged action dosage form could be done on the Trazodone tosylate salt or heated version and potentially patented and sold to a local generic company if successful. For automation purposes, the controlled humidity chamber could be fully automated with the right equipment, computer controlled valving, humidity and temperature monitoring devices, and a Visual BASIC program could be written to provide a more user-friendly interface capable of real-time data collection and graphing. Additionally, an automated dissolution setup could be

performed on the Biomek 2000 capable of continuous data collection on an unlimited number of samples through the use of the Fluostar Galaxy Plate Reader.

REFERENCES

1. Kataoka, K., *Targetable Polymeric Drugs*, in ***Controlled Drug Delivery: Challenges and Strategies***, K. Park, Editor. 1997, American Chemical Society. p. 49-71.
2. Ehrlich, P., ***Collected Studies on Immunity***. Vol. 2.8. 1906, New York: John Wiley.
3. Ghose, T., Cerini, M., Carter, M., et.al., *Immunoradioactive Agents Against Cancer.* ***Brit. Med. J.***, 1967. **1**(5532): p. 90.
4. Bale, W.F., Spar, J.L., Goodland, R.L., *Experimental Radiation Therapy of Tumors with I-31-Carrying Antibodies to Fibrin.* ***Cancer Res.***, 1960. **20**(10): p. 1488-1494.
5. Blaine, G., *The Uses of Plastics in Surgery.* ***Lancet***, 1946. **251**(OCT12): p. 525-528.
6. Griffith, L.G., *Polymeric Biomaterials.* ***Acta Mater.***, 2000. **48**(1): p. 263-277.
7. Ingraham, F.D., Alexander, E., Matson, D.D., *Synthetic Plastic Materials in Surgery.* ***New Engl. J. Med.***, 1947. **236**(10): p. 362-368.
8. Angelova, N., Hunkeler, D., *Rationalizing the Design of Polymeric Biomaterials.* ***Trends in Biotech.***, 1999. **17**(10): p. 409-421.
9. Alberts, B., Johnson, A., Lewis, J., Raff, M., Roberts, K., Walter, P., ***Molecular Biology of the Cell***. 4th ed. 2002, New York: Garland Science.

10. Washington, N., Washington, C., Wilson, C.G., ***Physiological Pharmaceutics: Barriers to Drug Absorption***. 2nd ed. 2001, New York: Taylor and Francis.

11. Hopkins, C.R., in ***Site-Specific Drug Delivery***, E. Tomlinson, Davis, S.S., Editor. 1986, John Wiley and Sons: Chinchester. p. 27-48.

12. Hillery, A.M., *Drug Delivery: The Basic Concepts*, in ***Drug Delivery and Targeting: For Pharmacists and Pharmaceutical Scientists***, A.M. Hillery, Lloyd, A.W., Swarbrick, J., Editor. 2001, Taylor and Francis: New York. p. 1-48.

13. DeDuve, C., DeBarsy, T., Poole, B., et.al., *Lysosomotropic Agents.* ***Biochem. Pharmacol.***, 1974. **23**(18): p. 2495.

14. Nishida, K., Mihara, K., Takino, T., et.al., *Hepatic Disposition Characteristics of Electrically Charged Macromolecules in Rat In Vivo and in the Perfused Liver.* ***Pharmaceut. Res.***, 1991. **8**(4): p. 437-444.

15. Maeda, H., Seymour, L.W., Miyamoto, Y., *Conjugates of Anti-Cancer Agents and Polymers--Advantages of Macromolecular Therapeutics In Vivo.* ***Bioconjugate Chem.***, 1992. **3**(5): p. 351-362.

16. Matsumura, Y., Maeda, H., *A New Concept for Macromolecular Therapeutics in Cancer Chemotherapy--Mechanism of Tumorotropic Accumulation of Proteins and the Anti-Tumor Agent SMANCS.* ***Cancer Res.***, 1986. **46**(12): p. 6387-6392.

17. Duncan, R., *Drug Polymer Conjugates--Potential for Improved Chemotherapy.* ***Anti-Cancer Drugs***, 1992. **3**(3): p. 175-210.

18. Duncan, R., Kopecek, J., *Soluble Synthetic Polymers as Potential Drug Carriers.* ***Adv. Polym. Sci.***, 1984. **57**: p. 51-101.

19. Kopecek, J., Bazilova, H., *Poly[N-(2-Hydroxypropyl) Methacrylamide] I. Radical Polymerization and Copolymerization.* ***European Polymer Journal***, 1973. **9**: p. 7-14.

20. Strohalm, J., Kopecek, J., *Poly[N-(2-Hydroxypropyl) Methacrylamide] IV. Heterogeneous Polymerization.* ***Die Angewandte Makromolekulare Chemie***, 1978. **70**(1978): p. 109-118.

21. Rejmanova, P., Obereigner, B., Kopecek, J., *Polymers Containing Enzymatically Degradable Bonds; Poly[N-(2-Hydroxypropyl) Methacrylamide] Chains Connected by Oligopeptide Sequences Cleavable by Chymotrypsin.* ***Makromol. Chem.***, 1981. **182**: p. 1899-1915.

22. Kopecek, J., Rejmanova, P., Strohalm, J., et.al., *U.S. Patent # 5037883: Synthetic Polymeric Drugs*. 1991: USA.

23. Kopecek, J., Rejmanova, P., Chytry, V., *Polymers Containing Enzymatically Degradable Bonds; Chymotrypsin Catalyzed Hydrolysis of p-Nitroanilides of Phenylalanine and Tyrosine Attached to Side-Chains of Copolymers of [N-(2-Hydroxypropyl) Methacrylamide].* ***Makromol. Chem.***, 1981. **182**: p. 799-809.

24. Kopecek, J., *Reactive Copolymers of N-(2-Hydroxypropyl) Methacrylamide with N-Methacryloylated Derivatives of L-Leucine and L-Phenylalanine.* ***Makromol. Chem.***, 1977. **178**: p. 2169-2183.

25. Drobnik, J., Kopecek, J., Labsky, J., et.al., *Enzymatic Cleavage of Side Chains of Synthetic Water-Soluble Polymers.* ***Makromol. Chem.***, 1976. **177**: p. 2833-2848.

26. Duncan, R., Cable, H.C., Lloyd, J.B., et.al., *Polymers Containing Enzymatically Degradable Bonds; Design of Oligopeptide Side-Chains in Poly[N-(2-Hydroxypropyl) Methacrylamide] Copolymers to Promote Efficient Degradation by Lysosomal Enzymes.* ***Makromol. Chem.***, 1983. **184**: p. 1997-2008.

27. Ashwell, G., Harford, J., *Carbohydrate Specific Receptors of the Liver.* ***Annu. Rev. Biochem.***, 1982. **51**: p. 531-554.

28. Lee, R.T., Lee, Y.C., *Preparation and Some Biochemical Properties of Neoglycoproteins Produced by Reductive Amination of Thioglycosides Containing an Omega-Aldehydoaglycon.* ***Biochemistry-U.S.***, 1980. **19**(1): p. 156-163.

29. Bodmer, J.L., Dean, R.T., *Carrier Potential of Glycoproteins.* ***Method Enzymol.***, 1985. **112**: p. 298-306.

30. Meijer, D.K.F., Molema, G., Jansen, R.W., et.al., in ***Trends in Drug Research***, H. Timmerman, Editor. 1990, Elsevier: Amsterdam. p. 303-332.

31. Choi, N.S., Heller, J., *U.S. Patent #4180646 Novel Orthoester Polymers and Orthocarbonate Polymers*. 1979, Alza Corporation: USA.

32. Klaveness, J., Strande, P, Wiggen, U.N., *U.S. Patent # 5534250: Polymers Containing Diester Units*. 1996: USA.

33. Merkli, A., Heller, J., Tabatabay, C., Gurny, R., *Purity and Stability Assessment of a Semi-Solid Poly(Ortho Ester) Used in Drug Delivery Systems.* ***Biomaterials***, 1996. **17**: p. 897-902.

34. Merkli, A., Heller, J., Tabatabay, C., Gurny, R., *Semi-Solid Hydrophobic Bioerodible Poly(Ortho Ester) for Potential Application in Glaucoma Filtering Surgery.* ***J. Controlled Rel.***, 1994. **29**(1994): p. 105-112.

35. Merkli, A., Heller, J., Tabatabay, C., Gurny, R., *Synthesis and Characterization of a New Biodegradable Semi-Solid Poly(Ortho Ester) for Drug Delivery Systems.* ***J. Biomat. Sci. Polymer Edn***, 1993. **4**(5): p. 505-516.

36. Oie, S., *Bioerodable Polymers in Drug Delivery.* ***?***, ? **?**(?).

37. Duncan, R., Cable, H.C., Rejmanova, P., et.al., ***Biochem. Biophys. Acta***, 1984. **799**: p. 1.

38. Holdsworth, M., Heath, O.V.S., *An Apparatus for Recording Automatically the Course of Bulb Formation with Some Preliminary Observations on Bulb Development in the Onion.* ***Ann. Bot.-London***, 1946. **10**(39): p. 293-300.

39. Scarlett, J.A., Robertson, J.A., *An Automatic Apparatus for Testing Refractories Under Tensile and Compressive Loads at High Temperatures.* ***J. Am. Ceram. Soc.***, 1951. **34**(11): p. 348-353.

40. King, G.W., Blanton, E.H., *Automatic Recording of IR Spectra on Punched Cards.* ***Anal. Chem.***, 1952. **24**(7): p. 1227.

41. Lees, K.A., Tootill, J.P.R, *Microbiological Assay on Large Plates. 3. High-Throughput, Low Precision Assays.* ***Analyst***, 1955. **80**(952): p. 531-535.

42. Anon, *High-Throughput Surface Grinding with In-Process Control.* ***Mach. Prod. Eng.***, 1974. **124**(3203): p. 464-465.

43. Jones, G.A.C., Owen, G., *Design Aspects of a Scanning Electron Beam Microfabrication Instrument having 10 X 10 mm Field Coverage, Normal Substrate Incidence and High-Throughput.* ***J. Vac. Sci. Technol.***, 1978. **15**(3): p. 896-900.

44. Berry, V.V., *Sequential Isocratic Step LC--A High-Throughput, Problem Solving Approach with Sensitive Near-Universal Detection for Wide Polarity Mixtures.* ***J. Chromatogr.***, 1980. **199**(Oct.): p. 219-238.

45. Burch, R.M., Kyle, D.J., *Mass Receptor Screening for New Drugs.* ***Pharmaceut. Res.***, 1991. **8**(2): p. 141-147.

46. Alanine, A., et al., *Lead generation - Enhancing the Success of Drug Discovery by Investing in the Hit to Lead Process.* ***Combinatorial Chemistry & High Throughput Screening***, 2003. **6**(1): p. 51-66.

47. Atterwill, C.K. and M.G. Wing, *In vitro Preclinical Lead Optimization Technologies (PLOTs) in Pharmaceutical Development.* ***Tox. Lett.***, 2002. **127**(1-3): p. 143-151.

48. Avdeef, A. and B. Testa, *Physicochemical Profiling in Drug Research: A Brief Survey of the State-of-the-Art of Experimental Techniques.* ***Cellular and Molecular Life Sciences***, 2002. **59**(10): p. 1681-1689.

49. Bell, P.A., *SNPstream (R) UHT: Ultra-High Throughput SNP Genotyping for Pharmacogenomics and Drug Discovery (vol 32, pg S70, 2001).* ***Biotechniques***, 2003. **34**(3): p. 496-496.

50. Bleicher, K.H., et al., *Hit and Lead Generation: Beyond High-Throughput Screening.* ***Nature Reviews Drug Discovery***, 2003. **2**(5): p. 369-378.

51. Kerns, E.H., *High-Throughput Physicochemical Profiling for Drug Discovery.* ***J. Pharm. Sci.***, 2001. **90**(11): p. 1838-1858.

52. Caporale, L.H., *Chemical Ecology: A View from the Pharmaceutical Industry.* ***Proc. Natl. Acad. Sci. USA***, 1995. **92**: p. 75-82.

53. Hobden, A.N., Harris, T.J.R., *The Impact of Biotechnology and Molecular Biology on the Pharmaceutical Industry.* ***Proc. Royal Soc. Edinburgh***, 1992. **99B**(1/2): p. 37-45.

54. Edwards, P.J., *Purification Strategies for Combinatorial and Parallel Chemistry.* ***Combinatorial Chemistry & High Throughput Screening***, 2003. **6**(1): p. 11-27.

55. Pan, Y.J., H. Zhang, and Y.Z. Chen, *New Approach for Screening Anti-Tumor Compounds.* ***Chinese Science Bulletin***, 2003. **48**(7): p. 630-633.

56. Snyder, L.R., Dolan, J.W., Tanaka, N., *Fully Automated, High-Throughput Analysis of Therapeutic Drugs in Serum by HPLC--New Approach to Sample Pretreatment.* ***Clin. Chem.***, 1979. **25**(6): p. 1117.

57. Sadowitz, J.P., *Expediting the Formulation Development Process with the Aid of Automated Dissolution in Analytical Research and Development.* ***J. Automat. Meth. Manag. Chem.***, 2001. **23**(6): p. 173-177.

58. Avdeef, A., *High-Throughput Measurements of Solubility Profiles*, in ***Pharmacokinetic Optimization in Drug Research; Biological, Physicochemical, and Computational Strategies.***, B. Testa, van de Waterbeemd, H., Folkers, G., et.al., Editor. 2001, Verlag Helvitica Chimica Acta: Zurich, Switzerland. p. 305-326.

59. Lipinski, C.A., Lombardo, F., Dominy, B.W., et. al., *Experimental and Computational Approaches to Estimate Solubility and Permeability in a Drug Discovery and Development Setting.* ***Adv. Drug Deliv. Rev.***, 1997. **23**: p. 3-25.

60. Lipinski, C.A., *Computational and Experimental Approaches to Avoiding Solubility and Oral Absorption Problems in Early Discovery*, in ***Designing Drugs with Optimal in Vivo Activity After Oral Administration***, R. Borchardt, Editor. 2000, Drew University Residential School on Medicinal Chemistry: Madison, NJ.

61. Bevan, C., Lloyd, R.S., *A High-Throughput Screening Method for the Determination of Aqueous Drug Solubility Using Laser Nephelometry in Microtiter Plates.* ***Anal. Chem.***, 2000. **72**: p. 1781-1787.

62. Bevan, C., Lloyd, R.S., *High-Throughput Aqueous Drug Solubility by Laser Nephelometry.*, in ***Pharmacokinetic Optimization in Drug Research; Biological, Physicochemical, and Computational Strategies***, B. Testa, van de Waterbeemd, H., Folkers, G., et.al., Editor. 2000, Verlag Helvetical Chimica Acta: Zurich, Switzerland.

63. Kansy, M., Senner, F., Gubernator, K., *Physicochemical High-Throughput Screening: Parallel Artificial Membrane Permeation Assay in the Description of Passive Absorption Processes.* ***J. Med. Chem.***, 1998. **41**: p. 1007-1010.

64. Valko, K., Bevan, C., Reynolds, D., *Chromatographic Hydrophobicity Index by Fast-Gradient RP-HPLC: A High-Throughput Alternative to Log P/ Log D.* ***Anal. Chem.***, 1997. **69**: p. 2022-2029.

65. Valko, K., Du, C.M., Bevan, C., et. al., *Rapid Method for the Estimation of Octanol/Water Partition Coefficient (Log Poct) from Gradient RP-HPLC Retention and a Hydrogen Bond Acidity Term.* ***Curr. Med. Chem.***, 2001. **8**: p. 1137-1146.

66. Poole, S.K., Durham, D., Kibbey, C., *Rapid Method for Estimating the Octanol-Water Partition Coefficient (Log Pow) by Microemulsion Electrokinetic Chromatography.* ***J. Chromatogr. B.***, 2000. **745**: p. 117-126.

67. Hill, A., Bevan, C., Reynolds, D. *UK QSAR and ChemoInformatics Group Meeting*. 1999. UK.

68. Carstensen, J.T., ***Pharmaceutical Preformulation***. 1998, Lancaster, PA: Technomic Publishing Co., Inc.

69. Gould, P.L., *Salt Selection for Basic Drugs.* ***Int. J. Pharm.***, 1986. **33**(1986): p. 201-217.

70. Wells, J.I., ***Pharmaceutical Preformulation:The Physicochemical Properties of Drug Substances***. 1988, New York: Ellis Horwood Limited. 221.

71. Bastin, R.J., Bowker, M.J., Slater, B.J., *Salt Selection and Optimization Procedures for Pharmaceutical New Chemical Entities.* ***Org. Proc. Res. Develop.***, 2000. **4**(5): p. 427-435.

72. Kaplan, S.A., ***Drug Metab. Rev.***, 1972. **1**: p. 15.

73. Bowker, M., *A Procedure for Salt Selection and Optimization*, in ***Handbook of Pharmaceutical Salts: Properties, Selection and Use***, P.H. Stahl and C.G. Wermuth, Editors. 2002, Wiley-VCH: Zurich. p. 161-220.

74. Morris, K.R., Fakes, M.G., Thakur, A.B., et.al., *An Integrated Approach to the Selection of Optimal Salt Form for a New Drug Candidate.* ***Int. J. Pharm.***, 1994. **105**(1994): p. 209-217.

75. Bernstein, J., ***Polymorphism in Molecular Crystals***. *International Union of Crystallography: Monographs on Crystallography*. Vol. 14. 2002, New York: Oxford University Press. 410.

76. Lehmann, O., *Uber Die Dimorphie Des Hydrochinons Und Des Paranitrophenols.* ***Z. Kristallogr.***, 1877. **1**: p. 43-48.

77. Lehmann, O., *Ueber Physikalische Isomerie.* ***Z. Kristallogr.***, 1877. **1**: p. 97-131.

78. Ostwald, W.F., *Studien Uber Die Bildung and Umwandlung Fester Korper. Studies on the Formation and Transformation of Solid Materials.* ***Z. Phys. Chem.***, 1897. **22**: p. 289-330.

79. Threlfall, T.L., *Analysis of Organic Polymorphs. A Review.* ***The Analyst***, 1995. **120**: p. 2435-2460.

80. McCrone, W.C., *Polymorphism*, in ***Physics and Chemistry of the Organic Solid State***, M.M.L. D. Fox, A. Weissberger, Editor. 1965, Wiley Interscience: New York. p. 725-767.

81. Buerger, M.J., Bloom, M.C., *Crystal Polymorphism.* ***Z. Kristallogr.***, 1937. **96**: p. 182-200.

82. Sirota, N.N., *Certain Problems of Polymorphism (I).* ***Cryst. Res. Technol.***, 1982. **17**: p. 661-691.

83. Sandow, N., http://www.rxlist.com/cgi/generic/traz_cp.htm. 2003, RxList LLC.

84. Dobashi, A., *Trazodone Hydrochloride;* http://www.ps.toyaku.ac.jp/dobashi/database/animation/t_group/trazodone_hydrochloride.html. 2003.

85. http://www.healthyplace.com/medications/trazodone.htm. 2002, Healthyplace, Inc.

86. http://www.nursespdr.com. 2002.

87. http://www.nlm.nih.gov/medlineplus. 2002.

88. http://www.rxlist.com. 2002.

89. http://www.merck.com. 2002.

90. http://www.aricept.com/productinfo.htm. 2002.

91. http://www.chemextra.com. 2002.

92. http://www.clevelandclinic.org/health. 2002.

93. http://www.stadol-nasal-spray.com/pages/facts.html. 2002.

94. http://www.aidsinfonyc.org. 2002.

95. http://www.chemsoc.org. 2002.

96. *Products / Prescription Products: Molipaxin CR tablets.* ***The Pharmaceutical Journal Online***, 2001. **266**(7146): p. 631.

97. Haria, M., Fitton, A., and McTavish D., *Trazodone. A Review of Its Pharmacology, Therapeutic Use in Depression and Therapeutic Potential in Other Disorders.* ***Drugs Aging***, 1994. **4**(4): p. 331-355.

98. Various, ***The United States Pharmacopeia (USP 24) and the National Formulary (NF 19)***. Vol. 24. 2000, Rockville, MD: The United States Pharmacopeial Convention, Inc. 1913-1992.

99. http://www.pharmj.com/editorial/20010505/products/products.html. 2002.

100. *Brain Breifings: Serotonin and Judgement*. 1997, Society for Neuroscience.

101. Glusker, J.P., Lewis, M., Rossi, M., ***Crystal Structure Analysis for Chemists and Biologists***. *Methods in Stereochemical Analysis*, ed. A.P. Marchand. Vol. 9. 1994, New York: VCH Publishers, Inc. 854.

102. ***Structure Determination from Powder Diffraction Data***. *International Union of Crystallography Monographs on Crystallography*, ed. W.I.F.

David, Shankland, K., McCusker, L.B., et.al. Vol. 13. 2002, Oxford: Oxford Science Publications. 337.

103. Dittert, L.W., Higuchi, T., and Reese, D.R., *Phase Solubility Techniques in Studying the Formation of Complex Salts of Triamterene.* ***J. Pharm. Sci.***, 1964. **53**: p. 1325-1328.

104. Serajuddin, A.T.M. and D. Mufson, *pH-Solubility Profiles of Organic-Bases and Their Hydrochloride Salts.* ***Pharmaceut. Res.***, 1985(2): p. 65-68.

105. El-Gindy, A., El-Zeany, B., Awad, T., et.al., *Spectrophotometric, Spectrofluorimetric, and LC Determination of Trazodone Hydrochloride.* ***J. Pharm. Biomed. Anal.***, 2001. **26**: p. 211-217.

106. Giron, D.a.G., D.J.W., *Evaluation of Solid State Properties of Salts*, in ***Handbook of Pharmaceutical Salts: Properties, Selection and Use***, P.H. Stahl and C.G. Wermuth, Editors. 2002, Wiley-VCH: Zurich. p. 41-80.

107. Serajuddin, A.T.M.a.P., M., *Salt Selection Strategies*, in ***Handbook of Pharmaceutical Salts: Properties, Selection and Use***, P.H. Stahl and C.G. Wermuth, Editors. 2002, Wiley-VCH: Zurich. p. 135-160.

108. Stahl, P.H. and C.G. Wermuth, *Introduction*, in ***Handbook of Pharmaceutical Salts: Properties, Selection and Use***, P.H. Stahl and C.G. Wermuth, Editors. 2002, Wiley-VCH: Zurich. p. 1-17.

109. Guillory, J.K., *Generation of Polymorphs, Hydrates, Solvates and Amorphous Solids*, in ***Polymorphism in Pharmaceutical Solids***, H.G. Brittain, Editor. 1999, Marcel Dekker: New York. p. 183-226.

110. http://fscimage.fishersci.com/msds/68765.htm, *Material Safety Data Sheet for p-Toluene Sulfonic Acid Monohydrate*. 2002.

111. Ledwidge, M.T. and O.I. Corrigan, *Effects of Surface Active Characteristics and Solid State Forms on the pH Solubility Profiles of Drug-Salt Systems.* ***International Journal of Pharmaceutics***, 1998. **174**(1-2): p. 187-200.

APPENDIX A: CELLULAR STRUCTURE, FUNCTION, AND MEMBRANE TRANSPORT

Numerous scientific disciplines have contributed significantly to the study of cellular drug delivery. From activity and toxicity screening of potential active ingredients to elucidating the biological mechanisms of site-specific interactions, the science of cellular drug delivery is a complex, integral part of the treatment and prevention of life-threatening illnesses. Every year, new information is made available from many different research areas allowing for continuous improvement through technological advancements. In order to continue along this route, a multi-disciplinary background is necessary to understand the process of drug delivery at the cellular level. The purpose of this chapter is to present basic principles of cellular biology and their importance in cellular drug delivery. Section 1 deals with the fundamentals of cellular structure and intracellular compartments. Membrane structure, transport inside the cell, passive transport through the membranes and other membrane properties are discussed in section 2 as well as how these membranes serve as a major barrier to the drug delivery process. Lastly, section 3 describes receptor proteins, how they function, where they are located on a cellular level, how they act as transporters to deliver drugs to the cell and their role in multi-drug resistance.

The effectiveness of a drug therapy is dictated by several factors including the rate and extent of the drug molecule's penetration into and permeation through the body tissues and cells to reach a site of action. Many barriers prevent the drug from reaching this site of action. They can be grouped according to size including the organism itself on a 1-2 m scale, an organ

representing the 1-100 mm scale, tissue in the 1-100 μm size, and the extracellular and intracellular space of only 1-100 nm (1). To understand the processes governing a single cell and its makeup is the fundamental objective of this chapter.

1. Internal Organization and General Function

Although there are many different types of cells, every cell has some common components necessary to carry out life processes. In general, the chemical make-up of cells and their internal compartments or organelles are similar (2). From a drug delivery point of view, the cell or a group of cells is in some way the "site of action", whether the therapy is to destroy cancer cells or produce antibodies through vaccination. There are several traits that an ideal drug carrier should possess in order to deliver the drug to this site of action. First, carriers should target the area or group of cells specific to their action while avoiding interactions with non-target cells. They should release therapeutically relevant amounts of bioactive substances at that site for a required duration and frequency. They should also be readily excretable or degradable without causing undesirable biochemical or immune reactions in the body (3). There are a number of cellular compartments common to most eukaryotic cells that a drug carrier may encounter in pursuing its therapeutic goal. A schematic of a typical cell and its compartments is shown in figure A.1, and table A.1 summarizes how each cellular compartment can act as a drug delivery barrier.

Table A.1. Internal cellular organelles can act as barriers to drug delivery

Compartment	Drug Delivery Barriers
Plasma Membrane	Membrane transport protein specificity Lipid bilayer penetration
Cytoplasm	Slow macromolecular transport Diffusion rate limited
Nucleus	Double lipid bilayer penetration Pore complex size and specificity Nucleus membrane receptor protein specificity
Endoplasmic Reticulum	Metabolic Enzymes
Golgi Apparatus	Metabolic Enzymes
Lysosomes	Presence of hydrolytic enzymes Low pH microenvironment
Mitochondria	Double lipid bilayer penetration
Peroxisomes	Presence of catalases Presence of membrane bound oxidative enzymes
Cytoskeleton	Microtubules restrict internal traffic

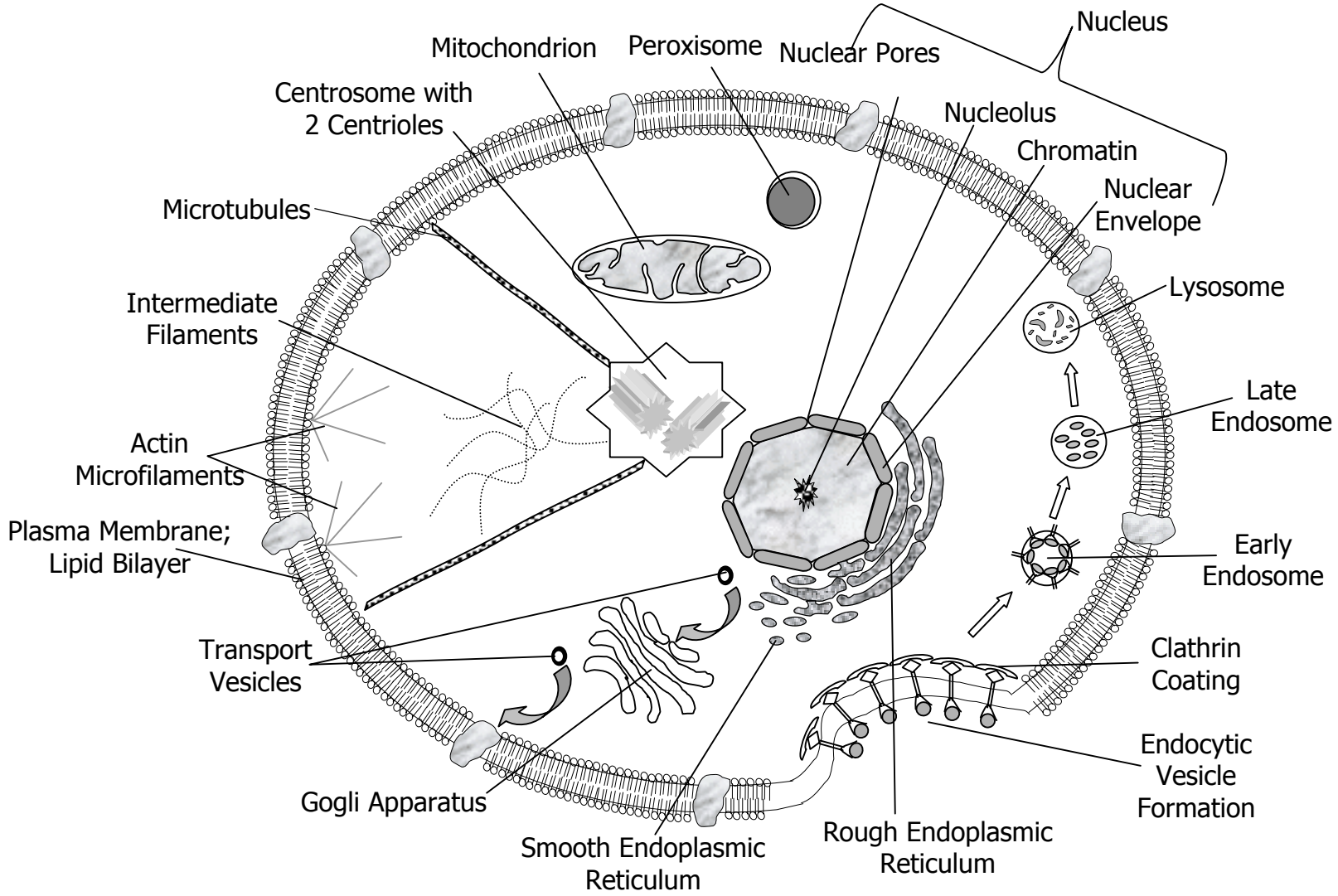

Figure A.1. Schematic of a typical eukaryotic cell including all internal compartments and endocytic vesicle formation and transformation to lysosomes

1.1. The Plasma Membrane

The plasma membrane forms the boundary around the cell and allows it to maintain chemical coordination. The membrane itself is formed from a series of phospholipids that are non-covalently linked together by hydrophobic interactions to form the bilayer around the cell. Imbedded within the membrane are proteins that function to transport molecules from one side to the other. Only specific types of molecules can be recognized, internalized or transported by these proteins making passage into the cell difficult for non-compatible molecules. There are other means of transporting molecules into the cell including fluid-phase pinocytosis, phagocytosis, receptor-mediated endocytosis, membrane fusion, passive diffusion, and channel or pore transport, which will be discussed in section 2.1.2.

1.2. The Cytoplasm

After drug molecules cross the plasma membrane, they may encounter the cytoplasm depending on the mechanism of uptake. The cytoplasm consists of the cytosol and the organelles or compartments of the cytoplasm. These compartments include the nucleus, mitochondria, peroxisomes, endoplasmic reticulum, golgi apparatus, lysosomes, endosomes and cytoskeletal elements. The cytosol makes up about 54% of the total cell volume and provides the semi-liquid media where proteins are synthesized and degraded and where most intermediate metabolism occurs. The main transport mechanism through the cytosol is diffusion. Macromolecules such as enzymes or high molecular weight

drug molecules diffuse slowly in the cytosol due to constant interactions with various cellular organelles. On the other hand, smaller molecules diffuse relatively efficiently (4-5).

1.3. The Nucleus

The nucleus is located in the cytoplasm and is bound by the nuclear envelope consisting of a double lipid bilayer membrane. These two bilayers are about 20-40 nm apart and form a significant barrier limiting molecular penetration into the nucleus. The main passage into the nucleus is through pores of about 60-100 nm in diameter formed in the bilayers. This passage is regulated by pore complexes composed of about 50 different proteins called nucleoporins, which are arranged in an octagonal shape. There are approximately 3000-4000 pore complexes in a nuclear envelope of the typical mammalian cell transporting many function-essential substances. Within the pore complexes are open aqueous channels that permit small molecules of <5,000 Daltons to diffuse readily while sufficiently preventing passage of macromolecules of 60,000 Daltons or greater. Macromolecules rely on specific receptor proteins to carry them into or out of the nucleus (2, 5-6). If a macromolecule is unrecognized by nuclear receptor proteins, it is prevented from entering the nucleus, making it difficult to use macromolecular targeting carriers. To overcome this impasse, researchers have developed macromolecular carriers, which can be used to target drugs specifically to the nucleus. They are made of N-[2-(hydroxypropyl) methacrylamide] (HPMA) copolymers, containing targeting sites for cell

specificity, and degradable drug units. As the carrier enters the cell—probably through endocytosis—and is carried to the lysosomal compartment, the drug unit is cleaved from the polymer backbone by lysosomal enzymes. The free drug molecule then enters the cytoplasm and rapidly diffuses into the nucleus to carry out its effect (7). Other research groups have utilized modular recombinant transporters (MRTs) to target cellular nuclei and deliver photosensitizer agents for anti-cancer therapy. These MRT constructs are made up of several components including alpha-melanocyte-stimulating hormone, Simian virus (SV40) large T-antigen nuclear localization signal and a translocation domain of the diphtheria toxin, allowing selective drug targeting to melanocyte nuclei (8).

The nucleus is one of the most important components of the cell as it contains the cell's genetic information encoded through deoxyribonucleic acid or DNA. Inside the nucleus, DNA is packaged into chromosomes by associating with proteins called histones to form chromatin. There are a variety of functional enzymes, strands of messenger ribonucleic acid (mRNA) and transfer ribonucleic acid (tRNA), and ribosomal components within the nucleus that are constantly constructed and transported into the cytosol. The ribosomal components (ribosomal RNA or rRNA) are synthesized and assembled in the subunit of the nucleus called the nucleolus, which has a spherical structure composed of 5-10% RNA, protein and DNA (5-6). Continuous exchange of components across the nuclear membrane is necessary for proper cellular function and can occur through specific transporters in the nuclear pore complex called importins and exportins (9). This nucleocytoplasmic transport pathway could be exploited as a

potential mechanism to deliver drugs to the nucleus. Many diseases may be more effectively treated with direct delivery of genetic material into the nucleus to treat or kill target cells. Potential delivery systems, both viral and non-viral vectors, to deliver genes to the nucleus are reviewed in chapters 5 and 6.

1.4. The Endoplasmic Reticulum (ER)

Interspersed throughout the intracellular space and continuous with the outer nuclear membrane is the endoplasmic reticulum. It accounts for more than half of the total membrane systems in the cell. It is a network of flattened sacs with bound ribosomes (the rough ER) and branching tubules (the smooth ER), each with different structures and functions. Inside the ER is the lumen or ER cisternal space, which is separated from the cytosol by the ER membrane. The rough ER is responsible for the synthesis and modification of membrane proteins and phospholipids as well as the synthesis of secretory proteins such as insulin. One of the main functions of the smooth ER is to bud off transport vesicles containing the newly synthesized proteins and lipids. In specialized cells, such as hepatocytes, the smooth ER is the site of drug and lipid metabolism and a site for the storage of calcium ions. The enzymes in the smooth ER are broad acting such that encountering more than one drug of the same type will cause proliferation of the smooth ER, increasing metabolism and potentially leading to drug tolerance (2, 5).

1.5. The Golgi Apparatus

After being released from the smooth ER, many transport vesicles travel to the golgi apparatus. The vesicle fuses with the golgi membrane releasing the contents into the golgi apparatus. Here the proteins and lipids are modified for specific functions and stored before being repackaged into other vesicles bound for a specific part of the cell or the cell surface. The golgi apparatus is also the manufacturing site for certain macromolecules, such as glycosaminoglycans and some carbohydrates. It is similar in structure to the rough ER, containing a series of flattened sacs or cisternae stacked upon each other. It is a polar membrane with cis and trans sides, and thus can receive and export transport vesicles, respectively, at opposite membranes.

1.6. Lysosomes

Lysosomes are membrane bound organelles whose specific function is digestion or chemical breakdown of various substances. They function to recycle some macromolecules produced in the cell by breaking them down into the constituent monomers. Lysosomes contain about 40 different hydrolytic enzymes and all of them are acid hydrolases. The internal pH of the lysosome is maintained at about 5 providing a more effective hydrolyzing environment. The lack of proper lysosomal enzymes can result in cellular damage due to accumulation of undigested toxic substances. For example, Pompe's disease is a disorder due to indigestion of glycogen in the liver, and Tay-Sach's disease sufferers are missing a lipid-digesting enzyme in the brain causing impairment (2,

5). Many of these kinds of diseases are treatable with the delivery of specific enzymes into the lysosomal compartment or genetic material into the cell allowing production of the necessary lysosomal enzymes.

Delivery of drug molecules to cells is often a challenge since most endocytosed drug molecules eventually suffer degradation in the lysosomal compartment. Some researchers have developed a method to circumvent lysosomal degradation using pH-responsive polymers capable of lysing the endosome and releasing the endocytosed drug molecules into the cytoplasm. These polymers are based on α-alkyl acrylic acids such as poly(2-ethylacrylic acid) which upon exposure to pH 6.3 or below undergo a conformational change disrupting the lipid bilayer of the endosome. The main mechanism of action is that the polymer permeabilizes phosphatidlycholine membranes, disrupting the lamellar structure of the bilayer and causing lysis (10). This type of technology can be useful in delivery of biomolecules to the cytoplasm, however little is known as to the potential toxic effects of releasing the endosomal components into the cell's cytoplasm.

1.7. The Mitochondria and Peroxisomes

The mitochondria within cells function to extract energy from sugars and fats to synthesize ATP. They are contained by a double lipid bilayer with an internal membrane that has a large surface area due to complex infoldings called cristae. In the heart of the mitochondria enclosed by the inner membrane is the mitochondrial matrix where many of the proteins and enzymes reside. The

mitochondria contain their own DNA, mitochondrial DNA, which is different from nuclear DNA, and their own ribosomes, which synthesize the proteins and enzymes necessary for specific functions. In a typical mammalian cell, there may be thousands of these 1-10 μm long mitochondria making up about 20-22% of the total cytoplasmic volume (2, 5-6).

Peroxisomes are also metabolic centers. They are bound by only a single lipid bilayer and produce hydrogen peroxide as a by-product from reactions of breaking down various substrates. They grow by incorporating cytosol-produced lipids and proteins into their membrane and split into two when they reach a certain size. Contained within the membrane of the peroxisomes are oxidative enzymes that act to break down fatty acids, sugars and macromolecules for use in other cellular processes. Another important function of the peroxisomes, especially in liver and kidney cells, is the detoxification of substances that enter the blood, such as alcohol.

1.8. The Cytoskeleton

The cytoskeleton provides the structural support necessary for the cell to maintain its shape. It consists of a network of fibers that extend throughout the cytoplasm. There are three main types of fibers of the cytoskeleton—the large microtubules, the intermediate filaments, and the actin filaments or microfilaments. Each serves a slightly different purpose within the cell.

The microtubules are small tube-like structures measuring 25 nm in diameter and 200 nm to 25 μm in length. They are made from the protein tubulin

and dictate the positions of various organelles while directing intracellular transport. The intermediate filaments have an intermediate diameter of 8-12 nm. They are constructed of a diverse family of proteins called keratins and may serve as the framework for the entire cytoskeleton. Some intermediate filaments line the inside of the nuclear envelope providing a strong support and barrier to protect DNA. Microfilaments are not hollow like microtubules. Instead they are solid rods composed of the globular protein actin. Actin filaments are flexible structures of 5-9 nm in diameter and tend to organize themselves in tight linear bundles. Their main purpose is to provide structural support so that the cell holds its shape.

2. Passive Transport into and through the Cell

The complexity of cells and their compartments pose tremendous challenges to drug delivery scientists. Nearly every component in and around the cell can be viewed as a barrier to drug delivery. Targeting specific pathways, receptor proteins, or various cellular transport mechanisms can help scientists overcome those barriers. In this section, the transport mechanisms occurring into and throughout the cell will be elucidated and several examples found in the literature will be given. Mostly passive transport will be talked about here; active transport and the proteins responsible for active transport are reserved for section 3.

2.1. Transport Across the Lipid Bilayer

The lipid bilayer or plasma membrane surrounding cells is composed of amphipathic molecules arranged in a dual layer configuration that is about 5 nm thick. Fatty lipid molecules make up 50% by weight of the membrane with the remainder being embedded proteins that serve to actively transport molecules across the membrane, catalyze membrane associated reactions, and provide many other functions. These lipid components act as formidable barriers to aqueous soluble substances. If a drug molecule approaches the cell surface attempting to gain entry, how does it cross the lipid bilayer and obtain access to the internal aqueous cytoplasm? There are several possible mechanisms described below.

2.1.1. Passive Diffusion

One of the main routes for both hydrophilic and hydrophobic drug molecules to enter the cytoplasm is through passive diffusion. The driving force for passive diffusion is a concentration gradient. The molecules move from an area of high concentration to an area of low concentration by random thermal motion. The factors that can affect the diffusion coefficient include solubility and molecular weight. Usually, small (<300 Daltons) molecules that are uncharged species and have a moderate oil/water partition coefficient such that they are somewhat hydrophobic can diffuse readily. If the partition coefficient is too high, the drug exhibits high lipophilicity and is unable to reach the membrane because it cannot dissolve in the aqueous extracellular compartment. On the other hand, if

the drug has a very low partition coefficient and hence is very hydrophilic, it cannot diffuse through the lipophilic membrane to reach the interior of the cell. As molecular weight increases, the rate of diffusion decreases. Larger macromolecules greater than 300 Daltons, such as many oligonucleotides and sucrose, are essentially excluded from the lipid bilayer with a diffusion half-life of 4-10 days (11). Nevertheless, large macromolecules may gain access into the cell by other means.

2.1.2. Endocytic Processes

Many large macromolecules, and even small particles, can be taken up by the cell through a process called cytosis, or endocytosis. The lipid bilayer forms a cavity or indentation due to an external stimulus, and through normal fluid motion and rearrangement of the membrane, an envelope, or endocytic vesicle forms engulfing the substance, including any surrounding extracellular fluid, in the cavity. Most cells undergo endocytosis on a regular basis and several different types of endocytosis exist based on the specificity and the size of the material engulfed (11-13). Several types of coating proteins are involved in the process to coat newly formed vesicles. For the internal compartments of the cell, there is a similar mechanism for vesicle formation with a major difference in the protein used to coat the cytosolic side of the membrane. One type of coating protein that has been identified in several types of endocytoses, including pinocytosis, trancytosis and potocytosis, is caveolae. This protein is unique because it uses part of the lipid bilayer that is very high in concentration of

cholesterol to form vesicles. Caveolae have been involved in the internalization of Simian virus (SV-40) and cholera toxin, and it is known that caveolae play a role in membrane fusion and intracellular trafficking of transport vesicles. Due to the high numbers of caveolae in pulmonary capillary epithelial cells, some researchers have investigated macromolecular delivery to the lungs specifically targeting caveolae membrane domains (14-15).

Pinocytosis is a process in which both small and large molecules dissolved in the extracellular fluid flow into the formed cavity and are pinched off as vesicles within the cell. Because pinocytosis deals with fluids it is also referred to as fluid-phase pinocytosis, and the vesicle internalized via fluid-phase pinocytosis is called an endosome. Much of the time, the dissolved drug molecule interacts with membrane protein receptors and is basically “caught” in the cavity through specific (receptor mediated pinocytosis) or non-specific (adsorptive pinocytosis) binding to the receptor when an endosome is formed (13). One fate of the endocytosed material is that its vesicle fuses with an organelle of the cell called an early endosome, which has an acidic environment. Some of the material, especially membrane components and receptor proteins, is then selectively recycled back to the membrane or exocytosed while the rest becomes a late endosome containing hydrolases and an even more acidic environment with a pH of around 5-6. The late endosomes move toward the interior of the cell and become lysosomes containing more digestive enzymes that act to degrade the contents previously endocytosed.

A less destructive endocytic process is transcytosis. Often, the endocytosed material is specifically diverted from the lysosomal route and sent to the plasma membrane, thereby being recycled through exocytosis, or more importantly in drug therapy, transferred to the other side of the cell. Proteins and peptides such as IgG, nerve growth factor, and epidermal growth factor are known to undergo pinocytosis and transcytosis through intestinal mucosa cells to reach the blood vessels on the other side. In some cases as with ricin, Shiga toxin, pertussis toxin and cholera toxin, the endocytosed protein toxin is transported to the golgi apparatus initially, instead of undergoing the normal transitions from endosomes to lysosomes. The toxins then, undergo retrograde transport to the ER (16). Elucidating these types of mechanisms provides insights not only into intracellular transport mechanisms but also on potential treatments for these toxins.

Another type of endocytosis involves the uptake of large substances such as drug particles, cells, bacteria or viruses. This is called phagocytosis and occurs in a series of steps similar to pinocytosis. Drug particles or other large substances adhere to the cell membrane. The binding usually occurs at a specific site that activates phagocytic mechanisms within the cell, similar to the process of when an antibody segment bound to a virus particle binds specifically to the Fc receptor on the surface of macrophages initiating uptake (2). The entire particle along with some extracellular fluid is ingested or engulfed by the membrane forming a detached vesicle or phagosome within the cell. The phagosome then fuses with a lysosome, and the particle and other phagocytosed

material is digested while the bilayer materials are recycled. Phagocytosis only occurs in specialized cells called professional phagocytes that exist in specific areas of the body, mainly the reticulo-endothelial system (RES). This includes the liver, bone marrow, and spleen macrophages and circulating blood monocytes. The phagocytes are tremendously important in regulating the body's immune system as they destroy foreign substances and remove particulate antigens. Their importance in drug therapy is limited to those drugs that are delivered in particulate carriers to the cell such as liposomes, erythrocytes, or microspheres. The therapy can be targeted with those drug molecules whose site of action is some region of the RES (13).

Receptor-mediated endocytosis is the most versatile type involving a high degree of recognition and specificity. Agonists binding to surface receptors activate the endocytic pathway causing invagination of the bilayer and vesicle formation. The receptors themselves are usually recycled back to the cell surface and the agonist either participates in metabolism or is taken back to the cell surface. The size of material that can be endocytosed via receptor-mediated endocytosis ranges from smaller than 100 Daltons to in excess of a million Daltons, such as a virus particle. Many drug delivery efforts focus on targeting various receptors on the cell surface so that particular biochemical pathways can be exploited. Agonists are typically developed to extend the duration of action via altered metabolic pathways in the lysosomal compartment, or to reduce side effects by specific binding to certain receptors on certain cells.

One interesting drug delivery application developed to exploit receptor-mediated endocytosis is to engineer specific receptors on the cell surface so that targeting can be more specific. This approach, investigated at the University of California, Berkley, involves feeding the cells with chemically modified sugars that can be metabolized and incorporated as the terminal sugar on membrane glycoproteins. The chemical modification adds an electrophilic group that dangles off the cell membrane. When nucloephilic-bound receptor molecules are presented to the cell surface, they bind instantly to the electrophile to provide the cell with newly inserted receptors. Specifically designed drug molecules or virus particles can bind to these receptors to initiate receptor-mediated endocytosis for targeted drug delivery (17-18).

2.1.3. Membrane Fusion

Membrane fusion occurs mostly intracellularly. However, similarities exist between membrane fusion occurring from extracellular space into the plasma membrane and from transport vesicles into the membranes of other internal organelles. Virus particles typically undergo membrane fusion to gain entry into host cells. The mechanism of action is not well known, but there are several hypotheses. Two of the most commonly accepted ones will be discussed briefly below.

One set of hypotheses are called “proximity models” where a cell and another bilayer surrounded entity come so close together that hydrophilic molecules are displaced and the two lipid bilayers fuse into one membrane

spilling the contents of the entity into the cellular cytoplasm (19). There are proteins that apparently catalyze all membrane fusions by anchoring the two membranes together to initiate the process. Inside the cell, these proteins are called soluble N-ethylmaleimide-sensitive factor attachment receptor (SNARE) (20) proteins and they function to fuse transport vesicles with a target organelle.

A second group of hypotheses are called “fusion pore models”, where the space between the two membranes is bridged by a protein or lipid pore complex (19, 21). Upon external activation, the pore complex undergoes a conformational change and an aqueous channel is formed linking the internal compartments of the two entities. The lipid layers then migrate inward opening up the channel until fusion is complete. This second hypothesis seems to explain many exocytic pathways that have been experimentally observed, and some authors suggest that this is the most likely theory (19, 21).

2.1.4. Pore Transport

The passive transport of solutes, small molecules or ions across the lipid bilayer can occur through aqueous pores or ion channels. Membrane transport proteins in the lipid bilayer form aqueous pores connecting the extracellular space with the cytosol. Due to the narrow channel in these pores, only small molecules and ions can effectively diffuse through, thereby protecting the cell from larger, potentially harmful substances. Some bacterial toxins manage to destroy cells by enlarging these pores to allow the entry of large harmful molecules (4). Aqueous pores may also be formed between two adjacent cells

joining their cytoplasms. This type of pore is called a gap junction and is typically much wider allowing larger molecule exchange between the cells. In either case, this route of cell entry is very fast, much more so than active transport through carrier proteins. The ion channels, which are specifically designed to transport inorganic ions across the lipid bilayer, can allow up to 100 million ions to pass per second.

One important difference between aqueous pores and ion channels is that aqueous pores remain open, but ion channels are gated and open and close in response to specific stimuli. There are several types of stimuli that can cause an ion gate to open. Voltage-gated channels open when a voltage change across the membrane occurs. Mechanical-gated channels open when a mechanical stress is applied or the membrane is stretched, and ligand-gated channels open when a specific ligand or receptor on the cell surface is bound. If the ligand is an extracellular mediator such as a neurotransmitter, it is a transmitter-gated channel. If the ligand is an intracellular mediator such as an ion or nucleotide, it is an ion-gated channel or nucleotide-gated channel, respectively. The main importance to cellular drug delivery is that there are many means to open an ion channel and these paths may be exploited to deliver drug molecules into cells. Under normal circumstances, however, ion channels allow only tiny ions to pass and may not be a feasible route to deliver any but the smallest drug. Similarly, aqueous pores may only be useful for delivering small molecule drugs into the cell unless a novel drug carrier can act to enlarge the pores or channels, as some bacteria and neurotoxins do, permitting entry of larger substances.

2.2. Intracellular Transport

Many of the barriers encountered at the plasma membrane also occur within the cell since lipid membranes surround most of the intracellular compartments. An overall schematic of general intracellular transport is shown in figure A.2.

As described earlier, movement of many substances through the cytosol occurs via diffusion. The rate of diffusion is inversely proportional to the size of the molecule. In addition, throughout this semi-liquid media even the diffusion of small molecules is slow compared to that in water. Small drug molecules entering the cytosol are often metabolized and then taken up into the ER, mitochondria or peroxisomes through transmembrane transport. Other substances, such as macromolecules or macromolecular assemblies are transported into the nucleus through gated channels or nuclear receptors, which only allow specific molecules to pass through. In most cases, large macromolecules in the cell have sorting signals that make them selective to certain organelles. If taken up into the mitochondria or peroxisomes, the substances are handled through the metabolic pathways to generate energy. If taken up into the ER, they become part of the biosynthetic secretory pathway in which they enter the golgi complex, become modified or metabolized and packaged. Eventually they are sent off as secretory vesicles bound for the cell surface or are diverted to lysosomes.

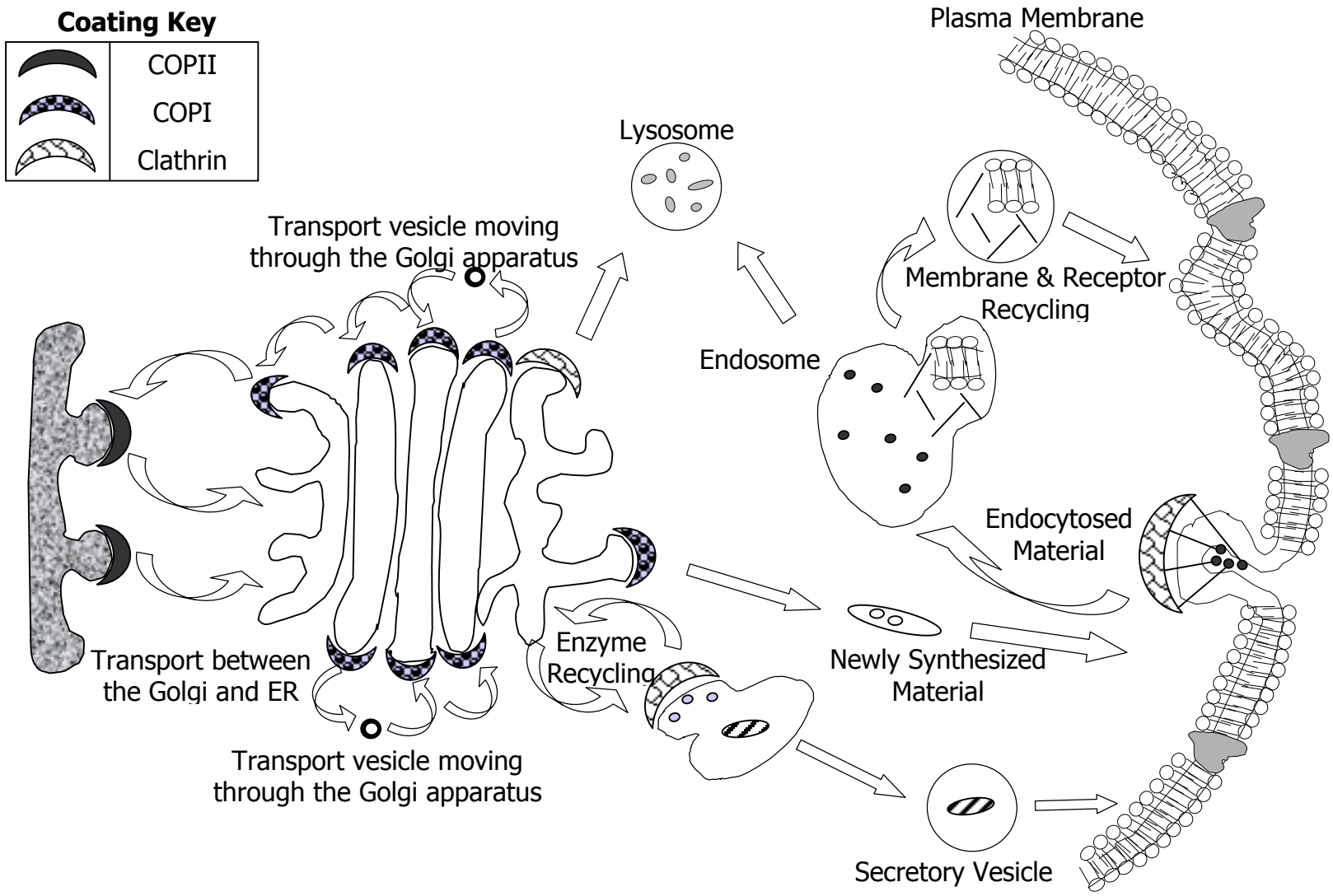

Figure A.2. General overview of the intracellular transport pathways occurring in most eukaryotic cells including recycling of receptor proteins and membranes

3. Receptor Proteins and Active Transport

Much research has been done to determine receptor protein structure and function and how these receptors initiate uptake mechanisms within cells. The research efforts continue so that every minute detail can be known as to how cells work. This knowledge can help us better understand specifically what causes diseases and what drugs or types of therapy can be used to cure or treat them by allowing us to target specific receptors on specific cells. In this section, receptor proteins and their function will be discussed with some specific examples given as to how proteins interact with drugs during cellular drug delivery.

3.1. Receptor Proteins

Proteins are composed of a specific sequence of amino acids. They are of great importance as enzymes in the cell, as receptors on the cell surface, and as biological motors and switches within the cell. But what makes some proteins function as receptors specific only to certain molecules and how do these certain molecules “fit” into the receptor so well? The answer lies in the numerous non-covalent interactions that play a major role in protein folding and receptor binding.

The long polypeptide chain of a protein, anywhere from 50-2000 amino acids long, is able to adopt many different conformations, limited mainly by steric interactions from the amino acid side chains. The sequential order of amino acids, where the polar versus non-polar groups are situated along the backbone,

determines the folded shape of the protein as corresponding hydrogen bonds, ionic bonds and van der Waals attractions hold specific sections together. The final conformation is usually the one in which the free energy of the system is at a minimum.

In order for a biological function to be carried out or activated, binding of a protein ligand or a drug to a protein receptor must occur. There are several different ways a ligand can bind to a particular protein receptor and most deal with only protein ligand or protein drug interactions at receptors. In the first case, the surface of one entity interacts with an extended string-like portion of another in a surface-string interaction. The second interaction, sometimes called a protein-protein interaction, occurs when two α-helices interact to form a coiled-coil structure. This type of interaction is often found in some gene-regulatory proteins and usually requires each entity to be a protein or large macromolecule with a coil structure. The third type of interaction is the most common one, generally stronger and more specific. It is the surface-surface interaction and it occurs when two protein surfaces are precisely matched up, such as the interaction between antibody and antigen. In most cases, the interaction is essential for the protein to function.

The binding of ligands or substrates to a receptor protein can initiate a protein conformational change. This plays a major role in cell signaling and enzyme regulation. For example, many antagonists or inhibitors bind to one site and prevent binding of other substances by causing the protein to shift conformations hiding other active sites. This property of having more than one,

differently shaped surface binding site is known as allostery and occurs in most receptor proteins. One site normally acts as a regulatory site for feedback mechanisms in the cell while the other is the active site. When one site is bound, the protein “switches” on or off depending on which site is activated, and a new conformation with different surface contours is adopted. These types of changes not only occur to regulate pathways in the cell or signal changes, but also to move subcellular units around in the cell or move the cell itself around, as seen in motor proteins. Allosteric proteins can also use the energy from ATP hydrolysis to accomplish active transport across cellular membranes. This mechanism of transport in addition to several examples will be discussed next.

3.2. Active Transport

There are several different kinds of active transport including ion transport through ion channels, electron pumps, and carrier mediated transport through transporter proteins. In order for each of them to work, binding of one or more substrates must occur. The process involves specificity at the binding site and the potential for saturation of the binding sites due to a high concentration of ligand. The transporters are capable of not only moving substances down a concentration or electrochemical gradient as in passive transport, but they can also pump substances against this gradient actively, which often occurs to get them inside the cell.

In general, carrier proteins bind drug molecules to bring them inside the cell without altering their chemistry. The process involves a reversible

conformational change of the bilayer-embedded carrier proteins in order to initially bind to the ligand outside the cell and subsequently release it inside the cell. In most cases of active transport, energy is required to pump the ligand against the concentration gradient. There are three mechanisms in which cells achieve active transport: coupled carriers, ATP-driven pumps, and light-driven pumps.

3.2.1. Coupled Carriers

There are three kinds of carrier-mediated transporters. Those only transporting one type of substance from one side of the plasma membrane to the other are called uniporters. The other two types are symporters and antiporters, which transport either two types of substances at the same time from one side to the other or two types of substances in opposite directions across the membrane, respectively. In the latter case, the coupled carriers often use the electrochemical gradient driving force of one of the substrates to transport the other. In many cells, Na^+ is the co-substrate providing the driving force into the cell. When Na^+ comes into the cell, an ATP driven pump embedded in the plasma membrane is activated to transport it out of the cell, thus maintaining a large electrochemical gradient for the influx of a particular substance. In other cases H^+ ions are the co-substrate as found in the uptake of enalapril, an angiotensin-converting enzyme (ACE) inhibitor, by small intestinal brush border membrane vesicles of rabbits (22). More information on transporters, their

superfamilies, and prodrug approaches to cellular drug delivery utilizing membrane transporters is discussed in chapter 8.

3.2.2. ATP-Driven Pumps and Light-Driven Pumps

Light-driven pumps are mainly found in bacterial cells and will not be discussed here in great detail. They use the energy from light to actively transport ligands against the electrochemical gradient.

ATP-driven pumps have an important role in cell regulation. The mechanisms that pump H^+ ions into lysosomes and other organelles where a low pH is required, act similarly to the motor proteins. One of the best understood pumps of this sort is the Ca^{2+} pump in muscle cells, which uses the energy of ATP hydrolysis to change conformations. This allows it to bind ions, bring them inside the cell, and release them while returning to the lower energy conformation. Another critical ATP pump in cell regulation is the Na^+-K^+ pump, or Na^+-K^+ ATPase as it is sometimes called. It is crucial not only to pH regulation but also in the regulation of cell volume, propagation of nerve impulses, and transport of essential nutrients.

3.3. Proteins Involved in Multi-Drug Resistance (MDR)

Finding a specific drug with high potency, delivered to the patient with a suitable and efficient formulation or drug carrier are not the only challenges facing drug delivery scientists. Often, therapy is hindered by multi-drug resistance, and the understanding of the mechanism as well as how to overcome

it becomes a tremendous task. There are many different resistance mechanisms that hinder the effective treatment of infectious and malignant diseases, but the resistance mechanism involving the ABC superfamily of transporter proteins has gained the most attention over recent years due to their role in some of the most common, widespread diseases such as malaria, leishmaniasis, and cancers (23). In many cases, drug influx into the cell is not enough to overcome drug efflux out the cell, resulting in the lack of drug accumulation inside the cell and unsuccessful therapy. Several transporters responsible for drug efflux are members of the ATP-binding cassette (ABC) superfamily. These proteins act as ATP-driven pumps and use the energy from ATP hydrolysis to actively transport substances across the plasma membrane. They include p-glycoproteins (P-gp), multi-drug resistance-associated proteins (MRP), and lung resistance-related proteins (LRP) (24-26). Many MDR cell lines have been found to exhibit excess numbers of these transport proteins thus causing a lack of drug accumulation within the cell due to extensive efflux. Additionally, the intracellular pH has been linked to MDR as found in drug-resistant mouse renal proximal tubule cells. Alkalinization of the endosomes and lysosomes by lysosomotropic agents have been found to stimulate the efflux of vinblastine, an anticancer drug (26).

Cancer is one of the most well studied illnesses in which MDR is a major problem. The reason many cancer chemotherapy regimens fail is multifactorial. Extracellular factors including bioavailability of the drug, drug metabolism, cell cycle stage and proliferation status as well as intracellular factors of drug influx and efflux involving these ATP-driven efflux pump proteins, DNA replication and

cellular repair mechanisms have all been identified as contributing significantly to MDR (24). One method to address MDR is to block efflux of drugs from the cell to increase retention. Several different types of drugs have been studied as effective efflux blockers and chemosensitizing agents. They include verapamil, phenothiazine calmodulin inhibitors, cyclosporins, and tamoxifene, and have generally been shown to be effective in overcoming resistance (24). The ABC superfamily and multi-drug resistance is discussed in more detail in chapters 8 and 9, and cancer and its treatment modalities are reviewed in chapters 11-12.

4. Conclusion

The complexity of even a single cell presenting formidable barriers to drug delivery both intracellularly and extracellularly can be overwhelming. By studying the mechanisms employed by viruses, bacteria and toxins in exerting their effect on cells, the drug delivery scientist can gain important insights on how to exploit these mechanisms to deliver drugs effectively to target cells or target organelles, overcome barriers associated with uptake either passive (endocytosis) or active (transport proteins), or conquer multi-drug resistance. A multidisciplinary background is necessary to understand the science of cellular drug delivery so that continuous improvements can be made striving to improve the quality of therapeutics.

Acknowledgement

The authors thank B. Neal Ware for critical reading of this manuscript.

REFERENCES

1. W.M. Saltzman, *Drug Delivery: Engineering Principles for Drug Therapy*, Oxford University Press, New York, 2001.
2. B. Alberts, A. Johnson, J. Lewis, M. Raff, K. Roberts, and P. Walter, *Molecular Biology of the Cell*, 4th ed., Garland Science, New York, 2002.
3. E. Tomlinson, "Pathophysiology and the Temporal and Spatial Aspects of Drug Delivery" in *Site-Specific Drug Delivery*, ed. E. Tomlinson & S.S. Davis, John Wiley & Sons, Chinchester, 1986, pp. 1-26.
4. D. Voet, and J.G. Voet, *Biochemistry*, 2nd ed., John Wiley & Sons, New York, 1995.
5. N.A. Campbell, J.B. Reese, L.G. Mitchell, *Biology*, 5th ed., Benjamin / Cummings, Menlo Park, CA, 1999.
6. P.W. Kuchel, G.B. Ralston, *Schaum's Outline of Theory and Problems of Biochemistry*, McGraw-Hill, New York, 1988.
7. K.D. Jensen, A. Nori, M. Tijerina, *et.al*., "Cytoplasmic delivery and nuclear targeting of synthetic macromolecules", *J. Control. Rel.*, 87(1-3):89-105, Feb.2003.
8. A.A. Rosenkranz, V.G. Lunin, O.V. Sergienko, *et.al*., "Targeted intracellular site-specific drug delivery: Photosensitizer targeting to melanoma cell nuclei", *Russ. J. Gen*., 39(2):198-206, Feb. 2003.

9. C. Dargemont, “Nuclear export of proteins: molecular mechanisms and functions”, *M S-Med. Sci.*, 18(12):1237-1244, Dec. 2002.
10. C.A. Lackey, “ N. Murthy, O.W. Press, *et.al*., “Hemolytic activity of pH-responsive polymer-streptavidin bioconjugates”, *Bioconj. Chem*., 10(3):401-405, May-June 1999.
11. N. Washington, C. Washington, C.G. Wilson, *Physiological Pharmaceutics: Barriers to Drug Absorption*, 2nd ed., Taylor and Francis, New York, 2001.
12. C.R. Hopkins, “Site-Specific Drug Delivery—Cellular Opportunities and Challenges” in *Site-Specific Drug Delivery*, ed. E. Tomlinson & S.S. Davis, John Wiley & Sons, Chinchester, 1986, pp. 27-48.
13. A.M. Hillery, “Drug Delivery: The Basic Concepts” in *Drug Delivery and Targeting: For Pharmacists and Pharmaceutical Scientists*, ed. A.M. Hillery, A.W. Lloyd, J. Swarbrick, Taylor and Francis, New York, 2001, pp. 1-48.
14. M. Gumbleton, A.J. Hollins, Y. Omidi, *et.al*., “Targeting caveolae for vesicular drug transport“, *J. Control. Rel*., 87(1-3):139-151, Feb. 2003.
15. D.P. McIntosh, X.Y. Tan, P. Oh, *et.al*., “Targeting endothelium and its dynamic caveolae for tissue-specific transcytosis in vivo: A pathway to overcome cell barriers to drug and gene delivery “, *P. Natl. Acad. Sci.* USA, 99:1196-2001, 2002.
16. K. Sandvig and B. van Deurs, “Membrane traffic exploited by protein toxins”, *Ann. Rev. Cell Dev. Bio.*, 18:1-24, 2002.

17. C. Bertozzi and M. Bednarski, “C-glycosyl compounds bind to receptors on the surface of escherichia-coli and can target proteins to the organism”, *Carb. Res.*, 223:243-253, Jan. 1992.
18. T.M. Handel, C. Bertozzi, and J.A. Hubbell, “Biopolymer engineering and design: beyond the genome - Editorial overview”, *Curr. Op. Chem. Bio.*, 5(6):675-676, Dec. 2001.
19. M. Lindau and W. Almers, “Structure and function of fusion pores in exocytosis and ectoplasmic membrane-fusion”, *Curr. Op. Cell Bio.*, 7(4):509-517, Aug. 1995.
20. M.M.K. Tsui, W.C.S. Tai, and D.K. Banfield, “Selective formation of Sed5p-containing SNARE complexes is mediated by combinatorial binding interactions”, *Mol. Bio. Cell*, 12 (2):521-538, Mar. 2001.
21. B.R. Lentz, V. Malinin, M.E. Haque, K. Evans, “Protein machines and lipid assemblies: current views of cell membrane fusion”, *Curr. Op. Struct. Bio.,*10:607-615, 2000.
22. S. Kitagawa, J. Takeda, and S. Sato, “Uptake of enalapril by rabbit small intestinal brush-border membrane vesicles”, *Bio. Pharm. Bull.*, 22 (7):762-764, July 1999.
23. S.P.C. Cole, and R.G. Deeley, “Multidrug resistance mediated by the ATP-binding cassette transporter protein MRP”, *BioEssays*, 20(11):931-940, Nov. 1998.
24. A. Krishan, C.M. Fitz, and I. Andritsch, “Drug retention, efflux, and resistance in tumor cells”, *Cytometry*, 29(4):279-285, Dec. 1997.

25. R. Sharma, Y.C. Awasthi, Y. Yang, *et.al.,* “Energy dependent transport of xenobiotics and its relevance to multidrug resistance”, *Curr. Cancer Drug Targets*, 3(2):89-107, April 2003.
26. Z. Ouar, R. Lacave, M. Bens, *et.al.,* “Mechanisms of altered sequestration and efflux of chemotherapeutic drugs by multidrug-resistant cells”, *Cell Bio. and Tox.*, 15(2):91-100, 1999.

APPENDIX B: AN AUTOMATED APPROACH TO SALT SELECTION AND PREFORMULATION DEVELOPMENT OF TRAZODONE

ABSTRACT

Purpose. To establish automated approach for salt selection and preformulation tests for a large number of Trazodone salts. **Methods.** Automated procedures were developed on a Biomek 2000 automation workstation with stacker and plate reader capabilities. Trazodone was dispensed into 96 well plates and an automated method was setup to form 104 Trazodone salts. Salts were observed under polarized light microscope to determine crystallinity. After stepwise eliminations, the remaining salts were scaled-up and subjected to DSC, PXRD and hygroscopic, pH-solubility, density, surface area and particle size analyses. **Results.** Oils formed in several cases resulting in preliminary elimination of mesyl and esyl salts and 4 crystallizing solvents. Crystallinity was observed in 34 of the 44 scaled-up Trazodone salts. PXRD, DSC, and hygroscopic analysis indicated a number of new salts that were comparable in physicochemical parameters to the marketed HCl salt. Among them, the tosylate salt showed its uniqueness for new applications. **Conclusions.** Automated procedures can be developed to increase the efficiency for pharmaceutical salt selection. The new tosylate salt gave a unique pH-solubility profile with low solubility over the entire pH range making it a better candidate for a suspension or prolonged action formulation compared to the other salts.

KEYWORDS: automation, high-throughput, preformulation, Trazodone.

INTRODUCTION

Automation and high throughput screening have become an important part of many drug development programs where time restrictions and product deadlines are critical and delays can cost as much as $1 million/day of revenue reduction in the first year (1). Most recent publications dealing with high-throughput have focused only on the drug discovery process (2-8). The need for automated, highly efficient steps in every part of a drug development program is being realized. This paper focuses on the automated approach to preformulation development with an emphasis on salt selection, using the model drug Trazodone.

Trazodone is currently marketed as the hydrochloride salt under several brand names. It is known as Desyrel, Trazon, and Trialodine in the U.S. with a former controlled release tablet marketed as Molipaxin CR in the U.K. (9-10). The chemical structure of Trazodone is shown in figure B.1 (11). It is indicated for the treatment of depression and for alleviation of the symptoms of agoraphobia, insomnia, essential tremor, repetitive screaming and some pain syndromes (12). The mechanism of action is not well understood, but in animals it works to increase the available serotonin levels in the brain by selectively inhibiting re-uptake at the brain synaptosomes (9, 13-14). Trazodone is chemically and pharmacologically unrelated to other currently marketed antidepressants. Several studies have shown it to be a superior antidepressant and anti-insomniac in the elderly with few side effects (14). To improve patient compliance in the

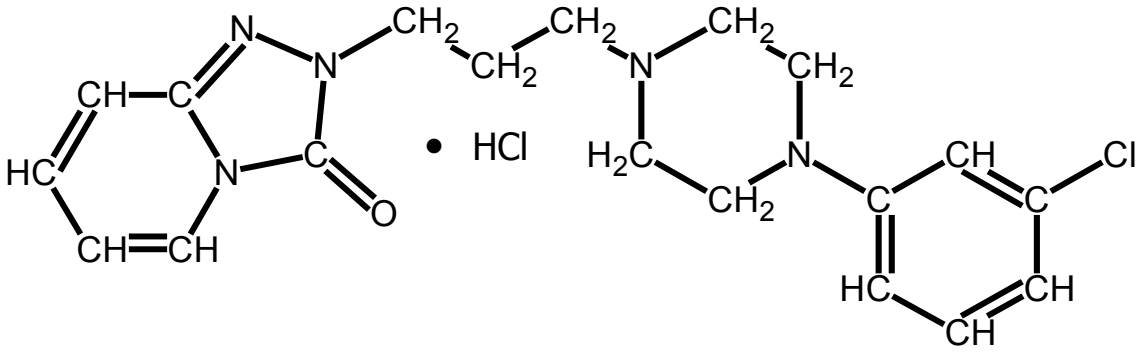

Figure B.1. Chemical Structure of Trazodone Hydrochloride

elderly, a prolonged action product or a suspension dosage form may be beneficial.

In the present study, we have implemented an automated procedure to efficiently screen a large number of pharmaceutical salts using the Biomek 2000 workstation (Beckman Instruments, Fullerton, CA. USA). The high-throughput procedure allows the screening of many different combinations of salts and crystallizing solvents with minimum time and effort on a small scale, thus minimizing drug usage. Therefore, we were able to efficiently screen various Trazodone salts while searching for a new salt form with lower aqueous solubility, especially at low pH, which can be used to formulate the prolonged action or suspension product. Preformulation characterization of various Trazodone salts was also performed.

MATERIALS AND METHODS

Materials

Trazodone hydrochloride, 98%, all acids and sodium hydroxide were obtained from Sigma-Aldrich (St. Louis, MO, USA). Ninety-six well deep well plates and robotic supplies were obtained from Beckman Coulter via VWR (South Plainfield, NJ, USA) and Beckman Instruments. All other chemicals were analytical grade and obtained from J.T. Baker (Phillipsburg, NJ, USA).

Extraction to Free Base

Trazodone hydrochloride was extracted to its free base form through a pH adjustment and liquid/liquid extraction procedure. Three grams of Trazodone

hydrochloride were dissolved in distilled water to slightly below saturation, and the solution was placed in a 125 mL separatory funnel. The pH was adjusted to about 13 using a saturated sodium hydroxide solution. Approximately 10-15 mL of chloroform was added to the separatory funnel, and the mixture was shaken to extract the free base into the chloroform layer. Extraction was repeated 10 times. The collected chloroform layers were washed with saturated sodium chloride solution to remove excess base, and then treated with anhydrous sodium sulfate to remove water. Solvent evaporation was performed using a Rotovapor until only a viscous yellow oil remained in the flask. Petroleum ether was used to salt-out the free base, giving an off-white precipitate. Around 95% yield was obtained and purity was indicated using DSC analysis against the supplied bulk Trazodone hydrochloride.

Automated Salt Formation

Automation of salt formation was performed using two 96 well deep well plates, 8 different crystallizing solvents and 13 different acids. A schematic of the automated salt formation setup on the Biomek 2000 workstation is shown in figure B.2. Trazodone free base was dissolved in acetone at a concentration of 50 mg/mL and placed in a 75 mL ½ module reservoir on the workbench of the Biomek 2000 workstation. For a 100 μL delivery per tip, 5 mg of free base were placed into each well, allowing for sufficient volume from each 250 μL pipette tip to reduce error and a minimum amount of Trazodone for the initial screening. Solutions of acids in acetone were prepared such that 15 μL of each acid solution gave a 1:1 molar ratio of acid to free base. The acids were placed in 19 mL ¼

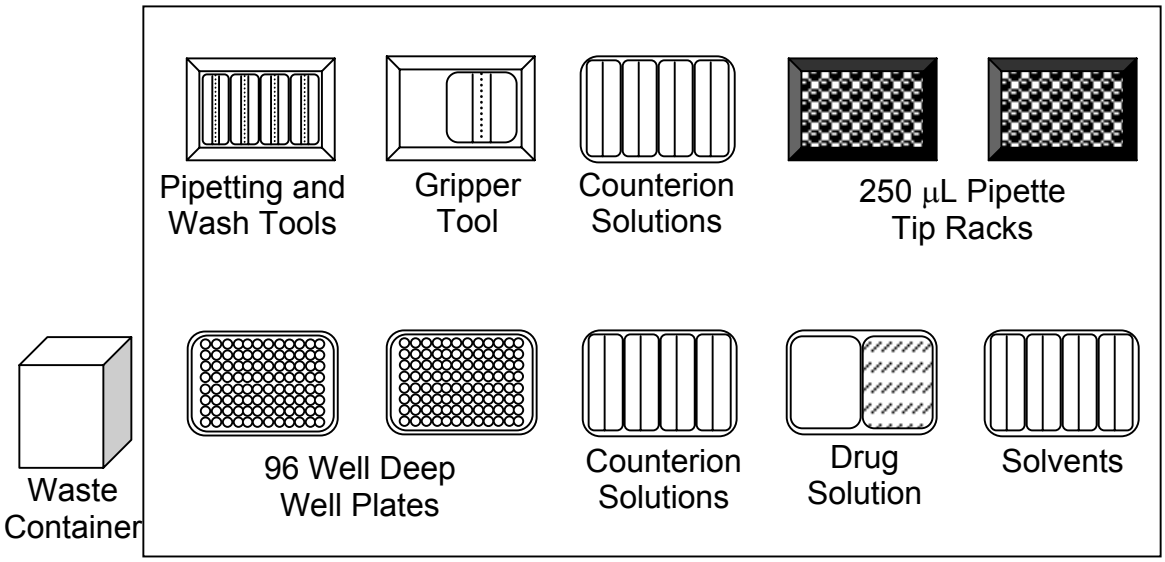

Figure B.2. Schematic of the Automated Salt Formation Setup on the Biomek 2000 Workbench

module reservoirs in the following order: hydrochloric acid (as a control), acetic acid, phosphoric acid, sulfuric acid, methane sulfonic acid, ethane sulfonic acid, p-toluene sulfonic acid, citric acid, propionic acid, tartaric acid, n-decanoic (capric) acid, pamoic acid, and elaidic (trans-oleic) acid. Initially, pamoic acid was dissolved in DMF, and citric and tartaric acids were dissolved in deionized water. Eight solvents were used, one for each row of the 96 well plate. Solvents were placed in 19 mL ¼ module reservoirs in the following order: ethanol, methanol, chloroform, acetone, isopropanol, tetrahydrofuran (THF), ethyl acetate (E), and propylene glycol.

The robotic method was setup to deliver 100 μL of the free base drug solution to every well of the first 96 well plate and the first column of the second. Subsequently, it delivered 200 μL of each solvent to the plate, one solvent for each row, and 15 μL of each acid solution, one acid for each of the 13 columns. Built into the method was a temporary halt so that the machine would stop all actions until the user clicked “Continue”. This pause was implemented to allow the reactions to occur while solvents evaporated and drug salts precipitated. The 96 well plates were allowed to sit at room temperature in a hood for 12 hours, and then placed back onto the workbench of the Biomek. The method was then continued. Each well was washed with petroleum ether to remove excess acids or solvents and to salt-out the final drug salt, if necessary.

Salt Screening Procedures

Microscopic observations were made immediately and 48 hours after the above process to determine whether precipitation had occurred. A small amount

of solid was placed on a microscope slide and observed under a polarized light microscope to view crystallinity. Any salt that either did not form a solid after 48 hours or was completely amorphous was eliminated. A 25 mg scale-up was done on the remaining salts involving 4 solvents: acetone, chloroform, ethyl acetate and THF; and 11 anions: citric, tartaric, p-toluene sulfonic, pamoic, n-decanoic, elaidic, hydrochloric, acetic, phosphoric, sulfuric, and propionic acids. Citric acid was dissolved in acetone at this time, but tartaric acid required an acetone/deionized water mixture. Pamoic acid was dissolved in THF.

Powder X-ray Diffraction (PXRD)

X-ray powder diffraction patterns were collected using a SCINTAG XDS 2000 powder diffractometer [SCINTAG, Cupertino, CA, USA] with Co $K_{\alpha 1}$ radiation generated at 35 mA and 40 kV. Samples were ground under petroleum ether and placed on a flat quartz holder. Data was collected from 5-50° 2Θ at 0.02° intervals and 2°/minute using a germanium solid-state detector cooled under liquid nitrogen.

Differential Scanning Calorimetry (DSC)

A differential scanning calorimeter, DSC 7, [Perkin Elmer, CT, USA] was used. It was initially calibrated using Indium and Zinc reference standards. Samples were prepared by sealing them in small volume sample pans, followed by piercing the top with a straight pin to allow vapor to escape. They were heated from 25° to 120°C at 10°C/min, cooled to 25°C at 30°C/min, heated again to 300°C at 10°C/min and cooled to 25°C at 30°C/min. Due to some difficulties

with the sulfate salts, the method was modified to only heat from 25° to 300° C at 10° C/min.

Melting Point Apparatus

A Mel-Temp melting point apparatus [Laboratory Devices, Cambridge, MA, USA] fitted with a 0-360°C mercury thermometer was used. Samples were lightly packed into 1.5 X 90 mm capillary tubes and observed through the viewing glass as temperature was increased at a rate of about 10-20°C/min.

Hygroscopic Analysis

A humidity chamber was constructed out of Plexiglas, and a Cahn microbalance along with a humidity/temperature probe was placed within the chamber to perform the hygroscopic analysis. Inlet and outlet pipes were placed on opposite corners of the chamber to allow air or steam circulation. A BASIC program was written to automatically collect data from the balance. Data was saved in a text file at user defined collection intervals. Samples were prepared by allowing them to equilibrate within a vacuum-sealed desiccator containing Drierite for at least 48 hours. They were then placed on the sample pan of the balance within the dry (~6% RH) chamber, which had previously been purged with dry air to obtain the low humidity starting condition. A collection interval of 60 seconds and a total duration of 170-200 minutes were used for each hygroscopic analysis session. Humidity and temperature data were manually collected from the humidity meter. All the weight gains were corrected after the empty pan weight gain was taken into account.

Density Analysis

After a second elimination and scale-up to 1-2 gram quantities, physico-chemical data for each of the remaining salts was collected. This included density, surface area, particle size and pH-solubility. The experimental methods for each of these tests are described below.

Bulk and tapped density data was collected in accordance with the USP (15), using a 5 mL glass graduated cylinder and 0.8 – 2.25 g of sample. For tapped density, manual tapping was done at a height of 14 $\pm$ 2 mm until no volume change occurred. In order to obtain an estimation of powder compressibility and flow, the compressibility index and the Hausner ratio were calculated according to the formulas below [98]:

$$\text{Compressibility Index} = \frac{100\,(V_0 - V_f)}{V_0} \quad (1)$$

$$\text{Hausner Ratio} = \frac{V_0}{V_f} \quad (2)$$

where V_0 is the unsettled apparent volume and V_f is the final tapped volume. True density was obtained using a helium pycnometer, Accupyc 1330 [Micromeritics, Norcross, GA, USA] and data was collected in triplicate to obtain an average density.

Surface Area Analysis

Surface area was obtained using a Flowsorb II 2300 [Micromeritics, Norcross, GA, USA] fitted with a dual channel mass flow controller model 5841 [Emerson, Hatfield, PA, USA] setup to deliver a gas mixture of 30% krypton and 70% helium. The machine was calibrated with krypton gas before each use.

Desorption and adsorption values were recorded in triplicate for each salt. The average of the desorption values was taken to calculate the surface area of the material since the machine more accurately integrates as gas is desorbed rather than adsorbed.

Particle Size Analysis

An ATM sonic sifter model L3P [ATM Corporation, Milwaukee, WI, USA] equipped with 4 sonic sieves and a fraction collector was used to obtain the particle size distribution in accordance with the USP Method I, a dry sieving method (15). The size of the openings in the mesh and types of sieves used were 90 μm ATM standard sonic sieve, 63 μm ATM standard sonic sieve, 40 μm ATM precision sonic sieve, and 25 μm ATM precision sonic sieve [ATM Corporation, Milwaukee, WI, USA]. Each sieve along with the top assembly and bottom fines collector assembly were weighed on a balance before a 3 gram sample was added to the top sieve. Each sample underwent a 10 minute sift/pulse at amplitude 5-6 followed by a 5 minute sift. The sieves and top and bottom assemblies were reweighed to obtain weight fraction retained, and the sieve fractions were recovered for further testing. Each piece of the sieve assembly was carefully washed in a sonic bath containing mild detergent and dried before the next analysis.

pH-Solubility Analysis

A modified form of the phase solubility technique was used (16-17). A saturated solution of each salt was prepared by allowing excess solid to equilibrate in distilled, deionized water for 24 hours. The pH was recorded and a

10 μL sample was taken after being filtered through a 0.2 μm filter. HCl or NaOH was added to adjust pH. After two hours of constant agitation via stir bars, the pH was noted and another sample was taken. This process was continued at each pH value ranging from 1-12. The samples were properly diluted and analyzed for concentration using UV spectrophotometry at 246 nm (Biomate 5, Thermospectronic, Rochester, NY, USA) or fluorescence (DyNA Quant 200, Hoefer Pharmacia Biotech, San Francisco, CA, USA) (18).

RESULTS

Salt Screening

Microscopic observations indicated no solid present in a number of cases leading to preliminary elimination of almost every well of the mesyl and esyl salts. A summary table of these observations is shown in table B.1 with double-banded boxes representing the conditions eliminated before the first scale-up. The citric acid and tartaric acid salts were not initially eliminated because they had been dissolved in water, which possibly resulted in incomplete mixing with the acetone-dissolved Trazodone. Citric acid was dissolved in acetone for the scale-up run, but tartaric acid was only slightly soluble in acetone and required a mixture of water and acetone for solubilization.

Polarized light microscopy was performed on the preliminary salts to determine crystallinity and amorphous character. In every case in which a solid was present, the substance exhibited the ability to rotate the plane of polarized light.

Table B.1. Summary table of the microscopic observations of Trazodone salts
(Preliminary Eliminations Depicted as Double Banded Boxes)

Solvents	Counterions						
	HCl Acid	**Acetic Acid**	**Phosphoric Acid**	**Sulfuric Acid**	**Methane Sulfonic Acid**	**Ethane Sulfonic Acid**	**p-Toluene Sulfonic Acid**
Ethanol	I: Nothing AW: Oil, no solid	I: Nothing AW: Oil, no solid	I: Little Solid AW: Wet MS: Xtal Clusters	I: Little Solid AW: Wet MS: Xtal Clusters	I: Nothing AW: Oil, no solid	I: Little Solid AW: Oil, no solid	I: Little Solid AW: Sticky MS: Xtal Shards
Methanol	I: Nothing AW: Oil, no solid	I: Nothing AW: Brown Solid MS: Fine Xtal Clusters	I: Nothing AW: Wet Solid MS: Xtal Sheets	I: Nothing AW: White Solid MS: Xtal Clusters	I: Nothing AW: Oil, no solid	I: Nothing AW: Oil, no solid	I: Nothing AW: Wet Gel MS: Needle Xtals
Chloroform	I: Oily Film AW: Oil, no solid	I: Nothing AW: Sticky, Orange MS: Xtal Shards	I: Solid AW: Wet, White MS: Xtal Clusters	I: Oily Film AW: Orange Solid MS: Xtal Clusters	I: Oily Film AW: Oil, no solid	I: Nothing AW: Oil, no solid	I: Solid AW: Flaky, White MS: Needle Xtals
Acetone	I: Solid AW: Wet MS: Plate Xtals	I: Nothing AW: Flaky, Brown MS: Xtal Shards	I: Solid AW: Flaky, White MS: Xtal Clusters	I: Solid AW: Flaky, White MS: Xtal Clusters	I: Nothing AW: Oil, no solid	I: Nothing AW: Oil, no solid	I: Solid AW: Sticky, White MS: Needle Xtals
Isopropanol	I: Nothing AW: Sticky, Brown MS: Xtal Clusters	I: Nothing AW: Oil, no solid	I: Solid AW: Flaky, White MS: Xtal Clusters	I: Nothing AW: Flaky, White MS: Xtal Clusters	I: Nothing AW: Oil, no solid	I: Nothing AW: Oil, no solid	I: Solid AW: White MS: Xtal Shards
THF	I: Solid AW: Crumbly, White MS: Xtal Clusters	I: Nothing AW: Sticky, Brown MS: Xtal Clusters	I: Solid AW: Flaky, White MS: Xtal Clusters	I: Oily Film AW: Flaky, White MS: Xtal Clusters	I: Nothing AW: Oil, no solid	I: Nothing AW: Oil, no solid	I: Solid AW: Sticky, White MS: Needle Xtals
Ethyl Acetate	I: Solid AW: Flaky, White MS: Xtal Clusters	I: Nothing AW: Flaky, Orange MS: Xtal Clusters	I: Solid AW: Flaky, White MS: Xtal Clusters	I: Oily Film AW: Flaky, White MS: Xtal Clusters	I: Oily Film AW: Oil, no solid	I: Nothing AW: Oil, no solid	I: Solid AW: Sticky, White MS: Xtal Clusters
Propylene Glycol	I: Little Solid AW: EMPTY	EMPTY	EMPTY	EMPTY	EMPTY	EMPTY	EMPTY

Notes: I is initial observations; AW is observations after washing with petroleum ether; MS is after microscopic observations; Xtal is abbreviation for crystal.
Double-banded boxes indicate conditions eliminated during preliminary run.

Table B.1. Continued

Solvents	Counterions: Citric Acid	Propionic Acid	Tartaric Acid	n-Decanoic Acid	Pamoic Acid	Elaidic Acid (plate 2)
Ethanol	I: Nothing AW: Oil, no solid	I: Nothing AW: Oil, no solid	I: Nothing AW: Oil, no solid	I: Nothing AW: Oil, no solid	I: Little Solid AW: Yellow MS: Xtal Clusters	I: Solid AW: Flaky, White MS: Needle Xtals
Methanol	I: Nothing AW: Oil, no solid	I: Nothing AW: Gooey, Brown MS: Xtal Shards	I: Nothing AW: Oil, no solid	I: Nothing AW: Gooey, Orange MS: Needle Xtals	EMPTY	I: Solid AW: Sticky, White MS: Needle Xtals
Chloroform	I: Oily Film AW: Oil, no solid	I: Nothing AW: Flaky, Brown MS: Needle Xtals	I: Oily Film AW: Oil, no solid	I: Nothing AW: Flaky, Peach MS: Needle Xtals	I: Nothing AW: Oil, no solid	I: Solid AW: Sticky, White MS: Needle Xtals
Acetone	I: Nothing AW: Oil, no solid	I: Nothing AW: Flaky, Brown MS: Needle Xtals	I: Nothing AW: Oil, no solid	I: Nothing AW: Gooey, Peach MS: Needle Xtals	I: Nothing AW: Yellow Solid MS: Needle Xtals	I: Solid AW: Sticky, Orange MS: Needle Xtals
Isopropanol	I: Nothing AW: Oil, no solid	I: Nothing AW: Oil, no solid	I: Nothing AW: Oil, no solid	I: Nothing AW: Sticky, Peach MS: Needle Xtals	I: Nothing AW: Yellow Solid MS: Xtal Clusters	I: Solid AW: White MS: Needle Xtals
THF	I: Nothing AW: Oil, no solid	I: Nothing AW: Flaky, Peach MS: Needle Xtals	I: Nothing AW: Oil, no solid	I: Nothing AW: Sticky, Peach MS: Needle Xtals	I: Little Solid AW: White MS: Xtal Clusters	I: Solid AW: Flaky, Peach MS: Xtal Clusters
Ethyl Acetate	I: Oily Film AW: Oil, no solid	I: Nothing AW: Sticky, Orange MS: Fine Xtals	I: Oily Film AW: Oil, no solid	I: Nothing AW: Sticky, Orange MS: Needle Xtals	I: Nothing AW: Yellow Solid MS: Xtal Clusters	I: Solid AW: Flaky, White MS: Needle Xtals
Propylene Glycol	EMPTY	EMPTY	EMPTY	I: Little Solid AW: EMPTY	I: Nothing AW: Yellow Solid MS: Xtal Clusters	I: Solid AW: Wet Solid MS: Oil dissolved

Notes: I is initial observations; AW is observations after washing with petroleum ether; MS is after microscopic observations; Xtal is abbreviation for crystal.
Double-banded boxes indicate conditions eliminated during preliminary run.

This is indicative of birefringent crystalline materials (19). There were a few cases in which a small portion of the solid material appeared amorphous.

A scale-up was carried out on the remaining 11 counterions and 4 solvents to obtain about 25 mg of each salt. Among these salts, the citrate and tartrate salts did not give solid precipitates regardless of the crystallizing solvent used, and therefore, they were not involved in the solid-state characterization. In addition, one acetate salt and one propionate salt, both using acetone as the crystallizing solvent, gave oils instead of solid precipitates. As a result, only 34 of the 44 scaled-up salts were further evaluated with the order of analysis being PXRD, DSC, hygroscopicity, and melting point apparatus to maximize data collecting efficiency and preserve usable drug salt quantities for subsequent evaluation (20-23).

DSC results of the acetate and propionate salts showed that none of the Trazodone free base reacted to form a salt. All thermograms gave peaks at 95-96°C corresponding to the melting point of the free base, and all PXRD patterns were identical to the pattern of the free base. In addition, DSC thermograms and PXRD patterns of the elaidate and caprate salts showed that a mixture of the reactants was present. The phosphate salt gave a mixture of products due to its polyprotic nature. This is undesirable as it will be difficult to separate the salts to obtain a pure product. Therefore all five of these salts were eliminated.

A final scale-up was performed to obtain gram quantities of the remaining four salts. To allow sufficient time for the reaction to reach completion, the reaction time was increased from 12 hours to 48 hours. For tosylate and

pamoate salts, chloroform was used as the crystallizing solvent in order to produce a purer product as found by DSC. For sulfate salts, ethyl acetate and THF were used to make two different salt forms. Only these four Trazodone salts were used for the final preformulation characterization.

Preformulation Characterization of Scaled-Up Salts

Trazodone hydrochloride from Sigma was used in the preformulation characterization tests to compare to the scaled-up Trazodone salts. Figures B.3 and B.4 show the DSC thermograms and X-ray powder patterns, respectively, for the scaled-up salts compared to Trazodone hydrochloride and free base. The pamoate, tosylate, and two sulfate salts had much higher melting points than the free base, but lower than Trazodone hydrochloride. The melting points of these four salts appeared around 186-195°C, which was about 40°C below that of the HCl salt.

Several interesting observations were noted. For the tosylate salt, an apparent salt melting peak was observed at 186°C. Immediately following the melting peak is an exothermic peak and another apparent salt melting peak. One possible explanation for this observation is that the tosylate salt undergoes a phase transition at 186.2°C, recrystallizes into a different polymorphic form, which then melts at 197.7°C. This type of transition has been noted in other pharmaceutical salts (24). For the pamoate salt, a small transition was found at 140°C. It appears that this is an amorphous glass transition temperature since a small portion of the pamoate salt appeared amorphous when it was viewed under polarized light microscope, and amorphous character was seen in the x-ray

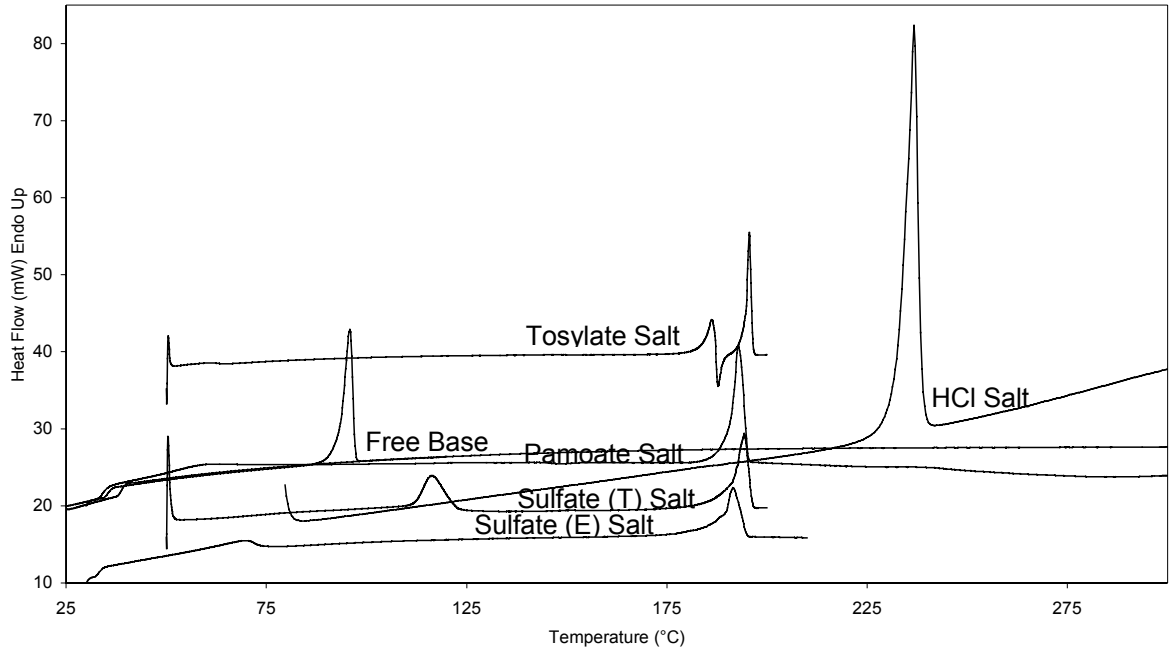

Figure B.3. DSC Thermograms of Scaled-Up Salts of Trazodone Compared to Free Base and Marketed HCl Salt

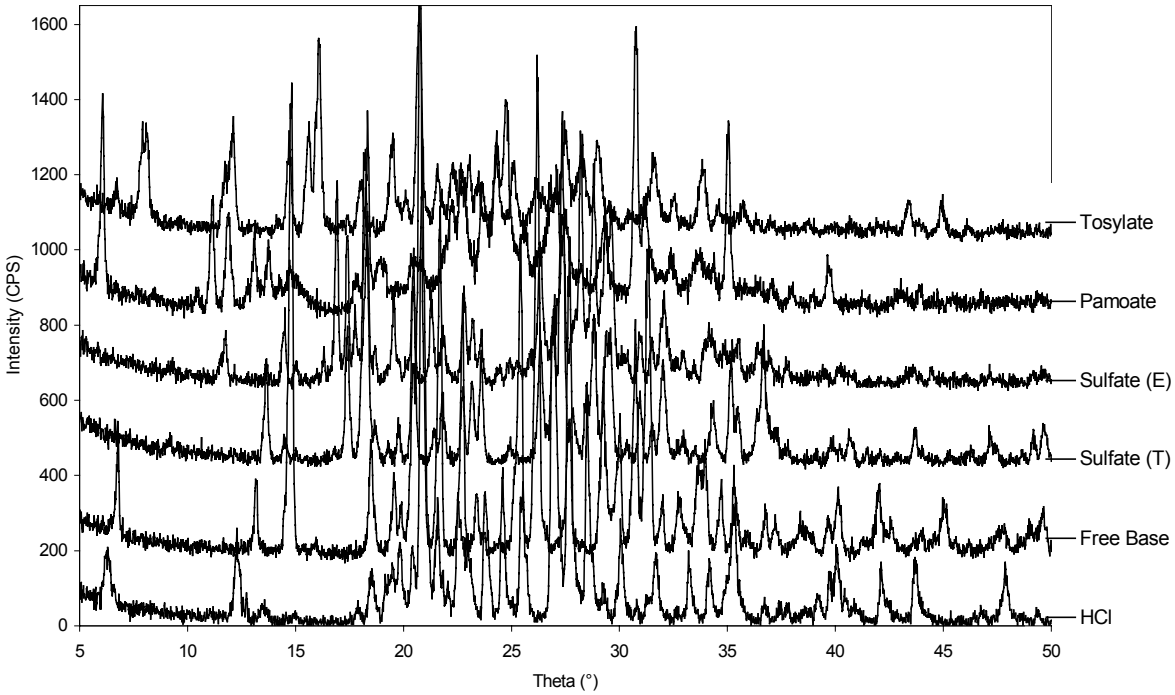

Figure B.4. X-ray Powder Patterns of Scaled-Up Salts of Trazodone Compared to Free Base and Marketed HCl Salt

powder pattern corresponding to an overall curved baseline throughout the theta angles measured. A similar transition was noted at 80°C and 120°C in the two sulfate salts crystallized using ethyl acetate and THF, respectively. However, little amorphous content was observed in either case, leading to the possible presence of solvates or hydrates. The temperatures at which these transitions occur were different in the two sulfate salts, potentially indicating boiling points of two different solvents. This can help explain the differences seen in the PXRD patterns and DSC thermograms. The excessive noise present in the PXRD patterns hides low intensity peaks and makes comparisons very difficult.

The hygroscopic results of the four salts compared to the HCl salt and free base were very similar and indicated that each salt had a low hygroscopicity with a maximum weight gain of 2.6%, 0.9% and 2.6% at up to 75% relative humidity for tosylate, pamoate and sulfate (E) salt, respectively. Lower hygroscopicity of the pamoate salt was expected since pamoic acid is considerably lipophilic. The other preformulation parameters measured for each salt are shown in table B.2. All salts exhibited similar true densities of about 1.5 g/mL with bulk and tapped densities ranging from 0.2-0.6 g/mL. The surface area and compressibility index of the marketed HCl salt were significantly lower than the other four salts. This indicates that the HCl salt has slightly better flow properties with less interparticulate interactions, but the low surface area may make dissolution rate slightly slower than the new salts. The tosylate salt had the smallest average particle size of 32 μm and the highest compressibility index indicating poorer powder flow properties due to high interparticulate interactions. The pamoate

Table B.2. Physico-chemical Properties of Trazodone Salts Compared to Marketed HCl Salt

Trazodone Salt	*Density (g/mL)*			*Compressibility*	*Hausner*	*Surface Area*	*Particle Size*	*Melting Point*	*Solubility*
	Bulk	*Tapped*	*True*	*Index*	*Ratio*	*(m^2/g)* [a]	*(d_{avg}) (μm)*	*(°C)*	*(pH ; g/mL)*
Pamoate	0.199	0.339	1.507	41.25	1.70	2.54	70.32	193	5.8 ; 0.077
Tosylate	0.208	0.428	1.448	51.43	2.06	1.02	32.93	186	5.37 ; 2.68
Sulfate (THF)	0.388	0.598	1.545	35.14	1.54	0.79	74.01	196	1.05 ; 37.73
Sulfate (E)	0.344	0.538	1.537	36.11	1.57	1.73	64.61	194	1.14 ; 32.52
Hydrochloride Bulk	0.431	0.594	1.358	27.40	1.38	0.24	69.31	237	4.96 ; 22.12

Notes: [a]Data reported are the average of desorption values

salt had the second largest average particle size of 70 μm with the largest surface area. The sulfate salts were very similar in nearly every physico-chemical property except surface area in which the sulfate (T) salt was 2.2 times lower than the sulfate (E) salt. A very low initial pH value of 1 was noted upon dissolution of the sulfate salts indicating that they would probably not be good candidates for oral tablets or capsules as they may cause damage to the GI membrane upon dissolution.

The pH-solubility profiles for these Trazodone salts are shown in figure B.5. The free base gave a similar profile as the HCl salt below pH 5 because HCl acid was used to implement the pH change, thus causing formation of the HCl salt. Below pH 3, the solubility began to drop off due to common ion effects (25). The free base showed a slightly higher solubility at higher pH's than the sulfate or HCl salts, but the pamoate salt showed the highest solubility at the higher pH's approaching 10 mg/mL at pH 10. However, the pamoate salt was the least soluble with a solubility value of only 0.077 g/mL at pH 5.8, which occurred upon adding distilled, deionized water to the solid powder. The sulfates were the most soluble salt with a solubility of 33-38 mg/mL at pH 1. The most interesting profile is the tosylate salt with a low solubility throughout the entire pH range. The solubility values range from 3 mg/mL at pH 1 to 0.2 mg/mL at pH 12.

DISCUSSION

Many pharmaceutical operations involve tedious and repetitive procedures, which potentially can be more efficiently performed using robotic

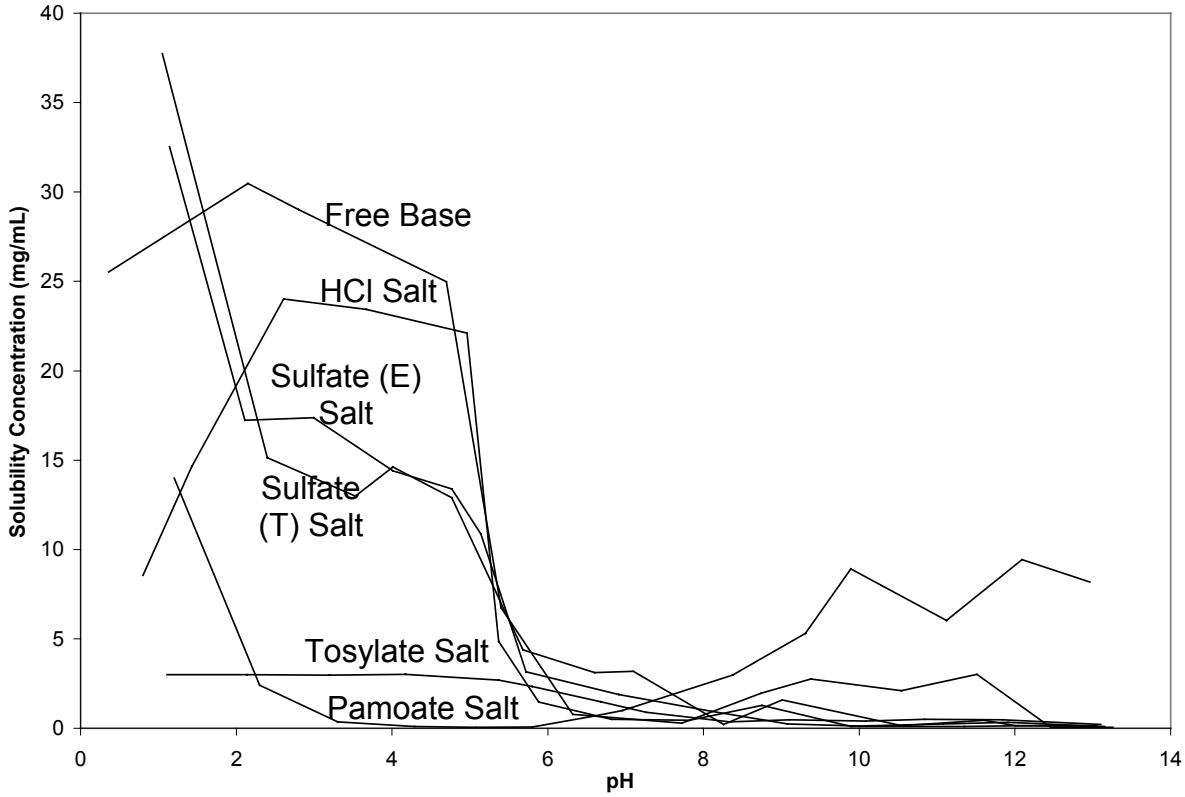

Figure B.5. pH-Solubility Plot of Trazodone Salts Compared to Free Base and Marketed HCl Salt

equipment. Adoption of existing automation devices and methods widely used for drug discovery can provide a fast and accurate alternative. The Biomek 2000 workstation was originally designed for the high-throughput screening of new drug candidates synthesized through combinatorial chemistry. Its capabilities include automated liquid handling, moving labware around the workbench or onto a stacker carousel, and a plate reader for fluorescence and UV-Vis spectrophotometry. The operations of the Biomek 2000 workstation can be programmed to automatically perform pre-determined experimental steps, allowing precise and efficient operations. However, the use of such diversified robots for pharmaceutical preformulation development has not been widely used. Implementation of such a machine may not only enhance experimental efficiency, but will also significantly reduce experimental error, meeting cGMP requirements. Automation of salt formation, scale-up and analysis procedures saves time and money, and it may lead to additional application opportunities, which are not feasible if performed manually.

Pharmaceutical salt selection programs are generally designed to obtain the maximum amount of information using the smallest quantity of drug product. They involve systematically analyzing and eliminating salt candidates in a multi-step process. With weakly basic drug candidates, the hydrochloride salt is usually the first choice due to ease of formation and straightforward recrystallization (20). However, it may not be the optimum candidate in most cases. It is necessary to evaluate each salt according to the intended application, and this can be very time consuming and costly. In the present

study, the Biomek 2000 workstation carried out a series of salt formation and screening procedures in an effort to search for a new Trazodone salt that has a low solubility at pH < 5. This salt will be beneficial in a prolonged action or suspension type dosage form for Trazodone. Through the use of the Biomek 2000 workstation, we were able to screen 104 potential salts through the combination of 13 counterions and 8 crystallizing solvents in a three-stage process. The first stage involved deciding which combinations of counterions and solvents gave solid crystalline drug products and how long the reaction should be run to consume all reactants. The solid drug products from this first stage were scaled up to 25 mg quantities for the second stage and analysed via DSC, PXRD, and hygroscopic stability to determine which conditions gave a new, pure drug salt versus mixtures of products or reactants. In the final stage of screening, only four remaining salts were scaled up to gram quantities and tested for particle size, pH-solubility, density, and surface area. From these four salts compared to the marketed hydrochloride salt and free base, one salt was chosen as the best for a prolonged action or suspension type dosage form.

Out of 104 salts formed in the preliminary run, 44 were scaled up for further analysis. However, only 34 formed solids and were tested with DSC, PXRD and hygroscopic analyses. The results showed that out of the 34 salts, only 20 reactions involving 5 different counterions and 4 solvents successfully formed salts. Those were the hydrochloride control, tosylate, pamoate, phosphate, and sulfate salts formed using acetone, chloroform, THF and ethyl acetate. Due to a mixture of products formed in the phosphate salt reaction, it

was eliminated from the final scale-up. The remaining pamoate, tosylate and sulfate salts were scaled up and subjected to physico-chemical profiling. The most significant finding was the pH-solubility profile of the tosylate salt, which exhibited a low solubility throughout the entire pH range. This characteristic makes it an excellent candidate to develop a prolonged action or suspension Trazodone product to improve patient compliance in the elderly.

ACKNOWLEDGEMENTS

We would like to acknowledge Neal Ware for his assistance in constructing the controlled humidity chamber, and Dr. Warren Beach, Dr. Jim Price, and Dr. Paul Schroeder for their support in drug extraction and analysis. Emily Ware was supported in part by the AFPE predoctoral fellowship.

REFERENCES

1. Kerns, E.H., *High-Throughput Physicochemical Profiling for Drug Discovery*. ***J. Pharm. Sci.***, 2001. 90(11): p. 1838-1858.
2. Avdeef, A. and B. Testa, *Physicochemical Profiling in Drug Research: A Brief Survey of the State-of-the-Art of Experimental Techniques*. ***Cellular and Molecular Life Sciences***, 2002. 59(10): p. 1681-1689.
3. Alanine, A., et al., *Lead generation - Enhancing the Success of Drug Discovery by Investing in the Hit to Lead Process*. ***Combinatorial Chemistry & High Throughput Screening***, 2003. 6(1): p. 51-66.
4. Atterwill, C.K. and M.G. Wing, *In Vitro Preclinical Lead Optimization Technologies (PLOTs) in Pharmaceutical Development*. ***Tox, Lett.***, 2002. 127(1-3): p. 143-151.
5. Wu, G., et al., *Assay Development and High-Throughput Screening of Capsases in Microfluidic Format*. ***Combinatorial Chemistry & High Throughput Screening***, 2003. 6(4): p. 303-312.
6. Ramirez, S., et al., *High-Throughput Flow Cytometry: Validation in Microvolume Bioassays*. ***Cytometry Part A***, 2003. 53A(1): p. 55-65.
7. Bleicher, K.H., et al., *Hit and Lead Generation: Beyond High-Throughput Screening*. ***Nature Reviews Drug Discovery***, 2003. 2(5): p. 369-378.
8. Muegge, I., *Selection Criteria for Drug-Lke Compounds*. ***Med. Res. Rev.***, 2003. 23(3): p. 302-321.

9. http://www.healthyplace.com/medications/trazodone.htm. 2002, Healthyplace, Inc.

10. Products / Prescription Products: *Molipaxin CR tablets*. ***The Pharmaceutical Journal Online***, 2001. 266(7146): p. 631.

11. Dobashi, A., *Trazodone Hydrochloride*; http://www.ps.toyaku.ac.jp/dobashi/database/animation/t_group/trazodone_hydrochloride.html. 2003.

12. http://www.psyweb.com/drughtm/trazod.html.

13. Sandow, N., http://www.rxlist.com/cgi/generic/traz_cp.htm. 2003, RxList LLC.

14. Haria, M., Fitton, A., and McTavish D., *Trazodone. A Review of Its Pharmacology, Therapeutic Use in Depression and Therapeutic Potential in Other Disorders*. ***Drugs Aging***, 1994. 4(4): p. 331-355.

15. Various, ***The United States Pharmacopeia (USP 24) and the National Formulary (NF 19)***. Vol. 24. 2000, Rockville, MD: The United States Pharmacopeial Convention, Inc. 1913-1992.

16. Dittert, L.W., Higuchi, T., and Reese, D.R., *Phase Solubility Techniques in Studying the Formation of Complex Salts of Triamterene*. ***J. Pharm. Sci***., 1964. 53: p. 1325-1328.

17. Serajuddin, A.T.M. and D. Mufson, *Ph-Solubility Profiles of Organic-Bases and Their Hydrochloride Salts*. ***Pharmaceut. Res***., 1985(2): p. 65-68.

18. El-Gindy, A., El-Zeany, B., Awad, T., et.al., *Spectrophotometric, Spectrofluorimetric, and LC Determination of Trazodone Hydrochloride*. ***J. Pharm. Biomed. Anal***. 2001. 26: p. 211-217.
19. Bernstein, J., ***Polymorphism in Molecular Crystals***. International Union of Crystallography: Monographs on Crystallography. Vol. 14. 2002, New York: Oxford University Press. 410.
20. Bowker, M., *A Procedure for Salt Selection and Optimization*, in ***Handbook of Pharmaceutical Salts: Properties, Selection and Use***, C.G. Wermuth, Editor. 2002, Wiley-VCH: Zurich. p. 161-220.
21. Giron, D.a.G., D.J.W., *Evaluation of Solid State Properties of Salts*, in ***Handbook of Pharmaceutical Salts: Properties, Selection and Use***, C.G. Wermuth, Editor. 2002, Wiley-VCH: Zurich. p. 41-80.
22. Serajuddin, A.T.M.a.P., M., *Salt Selection Strategies*, in ***Handbook of Pharmaceutical Salts: Properties, Selection and Use***, C.G. Wermuth, Editor. 2002, Wiley-VCH: Zurich. p. 135-160.
23. Stahl, P.H. and C.G. Wermuth, *Introduction*, in ***Handbook of Pharmaceutical Salts: Properties, Selection and Use***, C.G. Wermuth, Editor. 2002, Wiley-VCH: Zurich. p. 1-17.
24. Guillory, J.K., *Generation of Polymorphs, Hydrates, Solvates and Amorphous Solids*, in ***Polymorphism in Pharmaceutical Solids***, H.G. Brittain, Editor. 1999, Marcel Dekker: New York. p. 183-226.

25. Ledwidge, M.T. and O.I. Corrigan, *Effects of Surface Active Characteristics and Solid State Forms on the pH Solubility Profiles of Drug-Salt Systems*. ***International Journal of Pharmaceutics***, 1998. 174(1-2): p. 187-200.